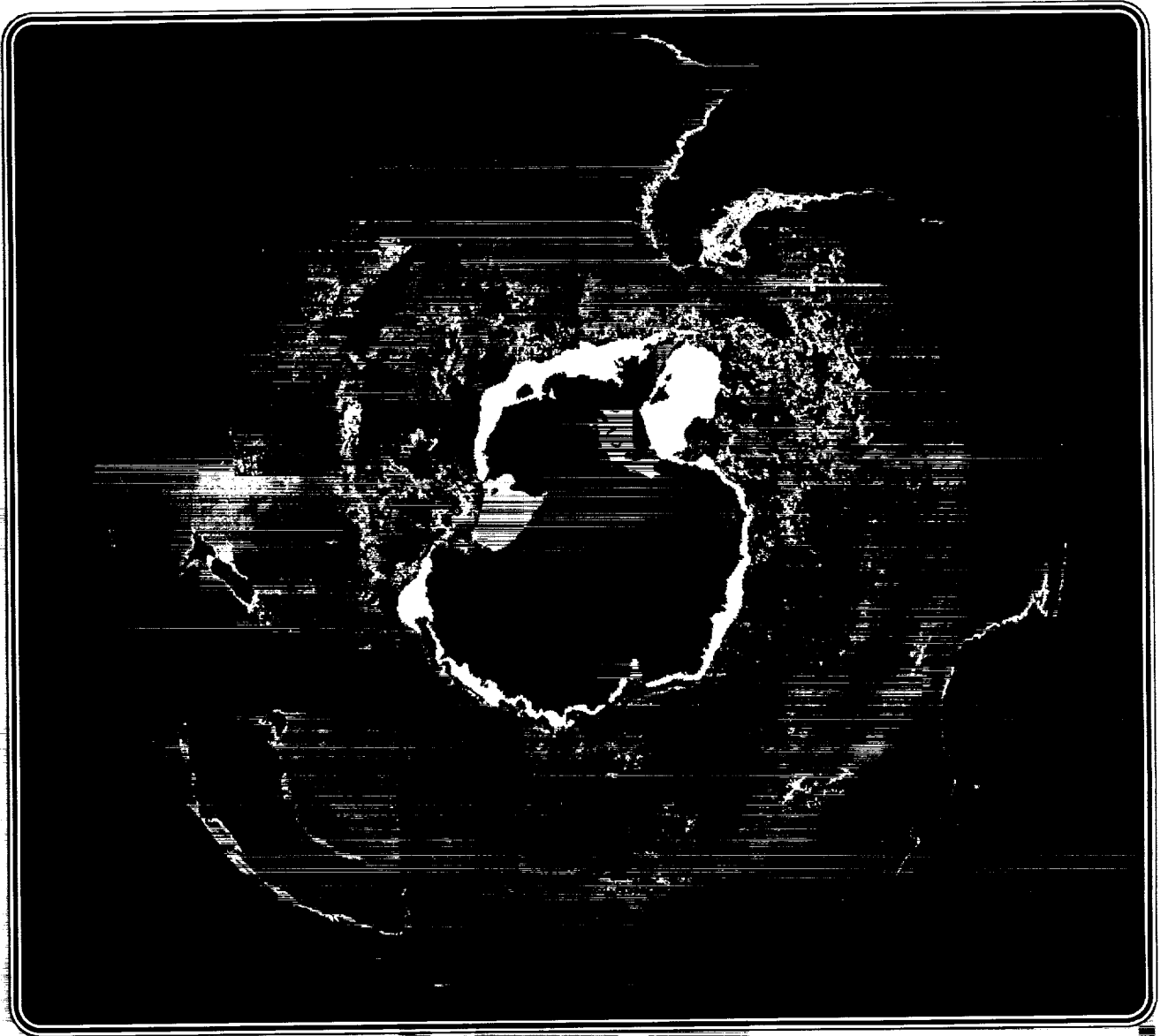


# POLAR RESEARCH FROM SATELLITES



— A review prepared by

**Robert H. Thomas**

(NASA-CR-188025) POLAR RESEARCH FROM  
SATELLITES (Joint Oceanographic Inst.)  
96 p

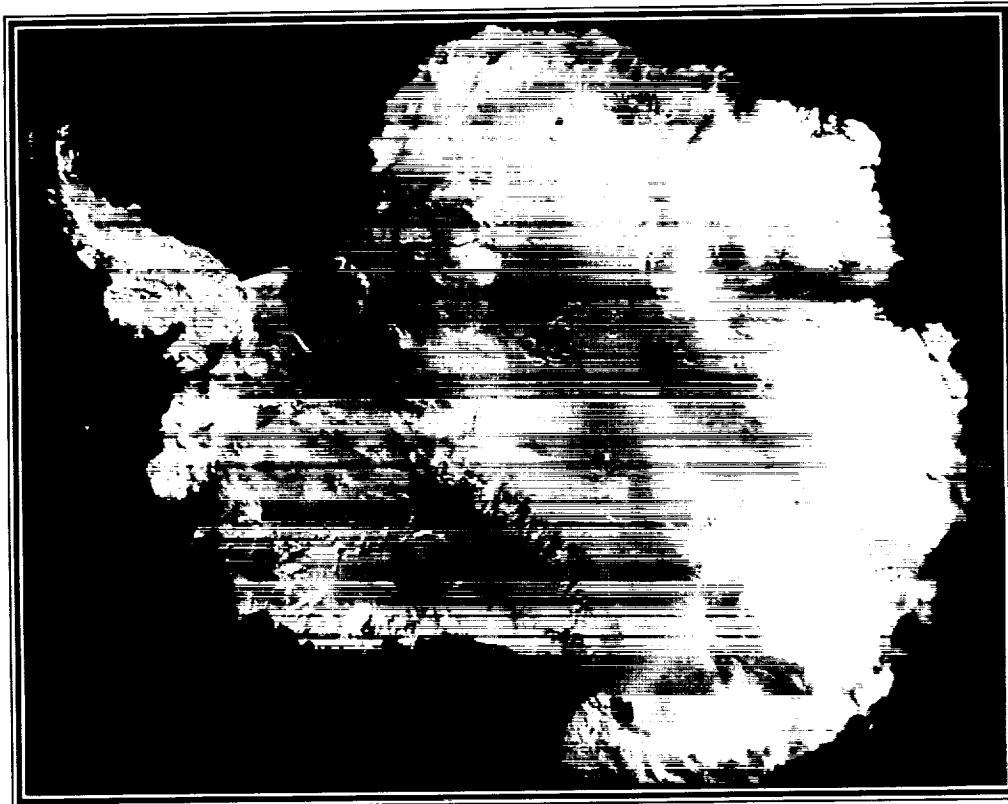
CSCL 04A

N91-21640

Unclas  
63/46 000011

Covers: **Ocean biological productivity around Antarctic (front cover) and in the Arctic (back cover).** The summer minimum sea-ice cover, shown in white, and phytoplankton pigment concentration derived from a composite of all the data acquired between 1978 and 1982 by NASA's Coastal Zone Color Scanner (CZCS) aboard Nimbus-7; pigment concentrations range from less than 0.1 mg/cubic meter of sea water (purple) to 30 mg/cubic meter (orange). [Images produced by G. Feldman, NASA/GSFC.]

# **Polar Research from Satellites**



**A review prepared by**

**Robert H. Thomas  
Joint Oceanographic Institutions, Inc.  
1755 Massachusetts Ave. NW  
Suite 800  
Washington, D.C. 20036-2102**

**Frontispiece: This satellite mosaic image of Antarctica was compiled from 1 km resolution AVHRR data obtained by NOAA weather satellites. [The image was produced by the National Remote Sensing Centre, United Kingdom.]**

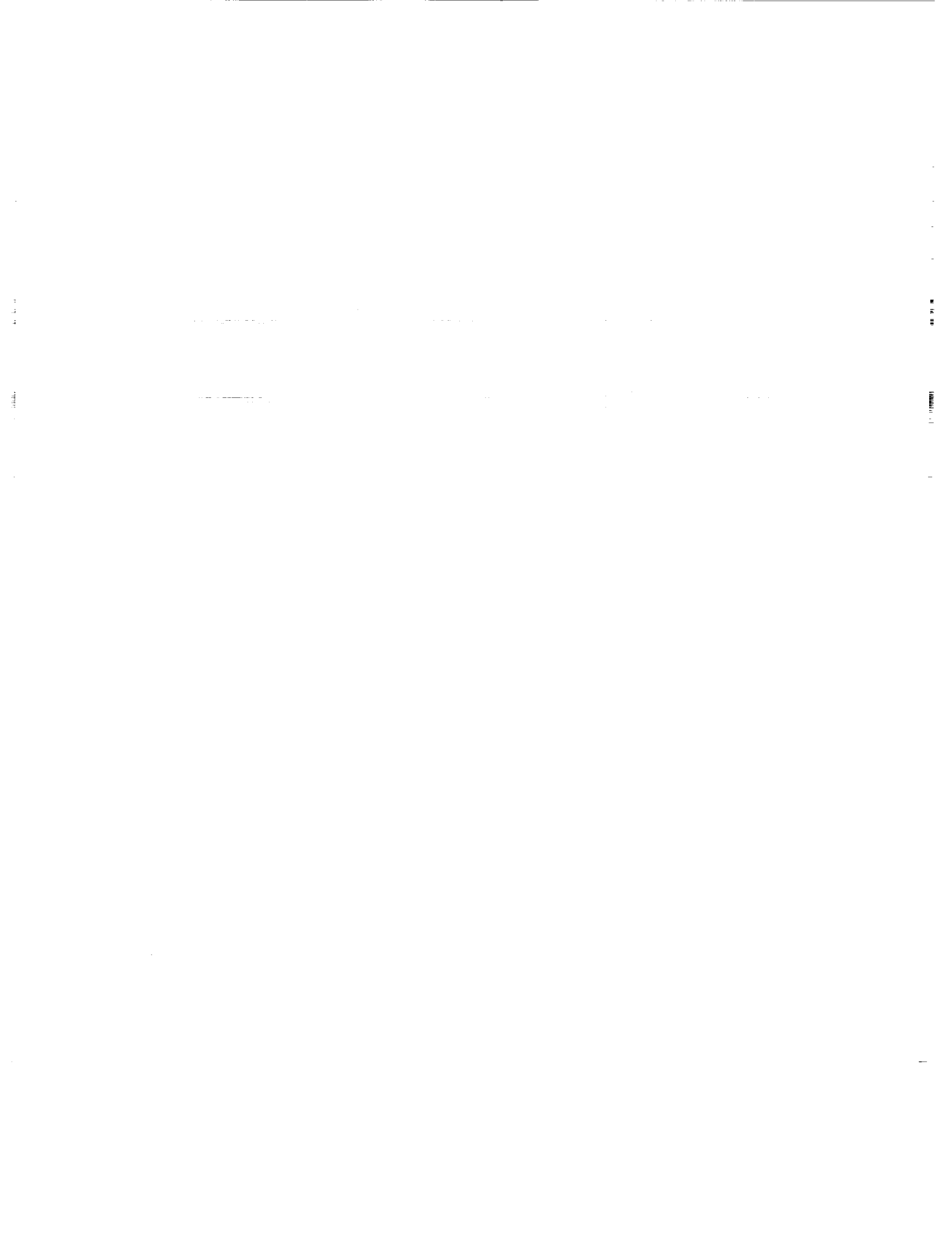


## Table of Contents

<b>1.</b>	<b>Introduction</b>	1
<b>2.</b>	<b>The Polar Regions and Climate Change</b>	6
2.1	Ocean/Atmosphere Heat Transfer	6
2.2	Trace Gases	9
2.3	Surface Albedo	12
2.4	Response to Climate Warming	14
<b>3.</b>	<b>The Satellite Instruments</b>	16
3.1	Basic Principles	16
3.1.1	Choice of Frequencies	17
3.1.2	Algorithms	18
3.1.3	Orbits	18
3.1.4	Remote-Sensing Techniques	~20
3.2	Passive Sensors	21
3.2.1	Microwave Radiometers	21
3.2.2	Medium-Resolution Visible and Infrared Sensors	27
3.2.2.1	Advanced Very High Resolution Radiometer (AVHRR)	28
3.2.2.2	Optical Line Scanner (OLS)	29
3.2.2.3	Earth Radiation Budget Experiment (ERBE)	29
3.2.2.4	Coastal Zone Color Scanner (CZCS)	32
3.2.3	High-Resolution Imagers	33
3.2.4	Atmospheric Sounding	36
3.3	Active Instruments	38
3.3.1	Synthetic Aperture Radar (SAR)	38
3.3.2	Radar Altimeter	45
3.3.3	Scatterometer	51
3.3.4	Lidar	52
<b>4.</b>	<b>The Next Decade</b>	54
4.1	The Role of the Polar Oceans and Their Sea-Ice Cover in the Transfer of Heat and Moisture between Ocean and Atmosphere, and the Redistribution of Heat from Low to High Latitudes	54
4.1.1	Required Satellite Sensors	54
4.1.2	Ancillary Measurements	55



4.2	The Role of the Polar Regions in the Global Carbon Balance	55
4.2.1	Required Sensors	55
4.2.2	Ancillary Measurements	55
4.3	The Response of the Polar Regions to Climate Change	55
4.3.1	Required Sensors	56
4.3.2	Ancillary Measurements	56
4.4	Modeling	57
<b>5.</b>	<b>Summary and Recommendations</b>	59
5.1	The Sensors	59
5.2	The Data	60
5.3	Algorithms	60
5.4	Calibration and Validation	61
5.5	Data Systems	62
5.6	Recommendations	62
	<b>References</b>	65
	<b>Appendix I: How to Get the Data</b>	71
	<b>Appendix II: Airborne Remote-Sensing Instruments</b>	78
	<b>Suggested Reading</b>	86
	<b>Acknowledgements</b>	89
	<b>Glossary</b>	90

2025 RELEASE UNDER E.O. 14176

## 1. Introduction

There is a growing need to improve our understanding of processes that occur at high latitudes. As we learn more about our planet, we become increasingly aware that a global perspective is needed to address issues that are important to people everywhere; issues such as ozone depletion in the stratosphere, acid rain, ocean pollution, and climate change. Fortunately, this growing awareness comes at a time when we also have the capability to acquire that global perspective from satellites.

Contrast between conditions at the equator and at the poles is the main driver of the large-scale atmospheric and oceanic circulation systems that redistribute heat, water, gases, and nutrients around the world and determine global climate, habitability, and biological productivity. Unique aspects of the polar regions that influence the climate machine include:

- the dramatic albedo change associated with the annual cycle of snow cover on land and sea ice on the ocean;
- the insulation between atmosphere and the ocean provided by the sea-ice cover;
- the effects of the melting and freezing of sea ice on ocean-density structure that controls the formation of the deep and bottom waters which cool and ventilate the deep oceans;

- the vast ice sheets in Greenland and Antarctica, containing enough water to raise sea level by some 70 meters;
- production of large amounts of methane from Arctic wetlands;
- exchange of carbon dioxide between the atmosphere and high-latitude waters, where the processes of deep-water formation offer a link with the deep ocean.

In addition, the effects of climate warming are expected to be amplified at high northern latitudes, where significantly enhanced warming is predicted. This offers the opportunity for early detection of warming by, for instance, measurement of surface air temperatures at many locations, systematic monitoring of seasonal sea-ice and snow (Figure 1), and observations of the extent and duration of summer melting on the terrestrial ice sheets. A particularly significant consequence of a warming climate is the reduction of permafrost cover in parts of the Arctic. Over longer periods, the effects of warming will feed back into the climate system through sustained changes in snow and sea-ice extent, in the condition of Arctic wetlands, and in global ocean circulation. Moreover, any major change in climate is bound to have some effect on the Greenland and Antarctic ice sheets, which contain more than 90% of the world's fresh water. At present, we do not know whether these ice sheets are growing larger or



Figure 1. Arctic snow and ice cover. The maximum extent of seasonal snow and sea ice (February/March) as derived from the Scanning Multichannel Microwave Radiometer (SMMR) which operated onboard NASA's Nimbus-7 satellite from 1978 to 1987. Sea ice is shown as white, and seasonal snow in three depth ranges: shallow snow (dark blue) from about 1 to 10 cm; moderately deep snow (medium blue) from about 11 to 33 cm; deep snow (light blue) greater than 33 cm. Permanent ice caps are shown in purple. [Image produced by G. Feldman, and the snow-cover and sea-ice information was provided by D. Hall and D. Cavalieri, all from NASA, Goddard Space Flight Center (GSFC).]

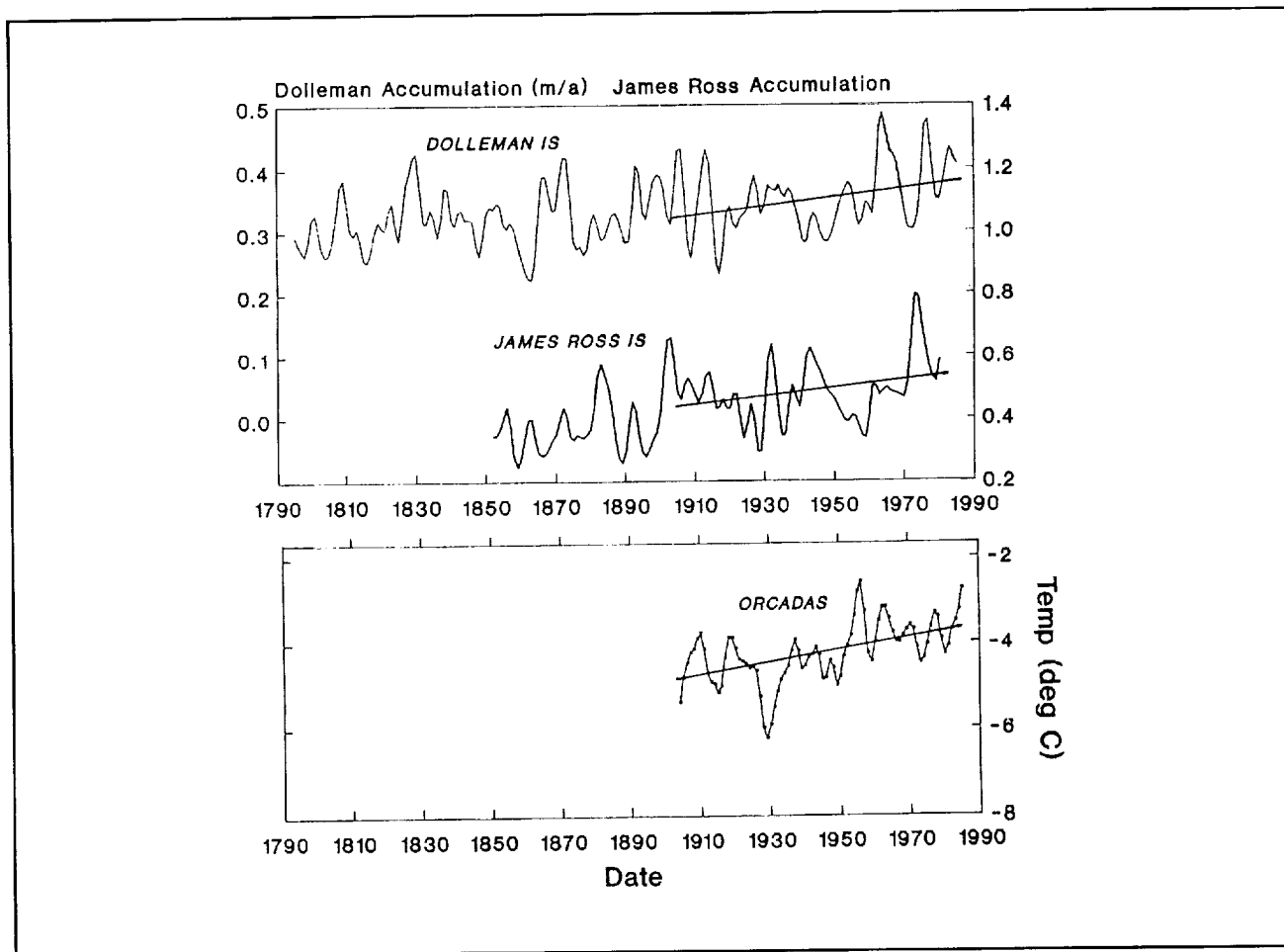


Figure 2. Temperature and accumulation rates in the Antarctic Peninsula. Surface temperatures from station measurements (lower plot), and snow-accumulation rates (upper plot) from ice-core analysis (composited from data presented by Peel, in press). These measurements reveal significant increases in both surface temperature and snow accumulation during the past 80 years. Note that the left ordinate in the upper plot refers to Dolleman Island and that on the right refers to James Ross Island. Shorter data records from Dolleman Island and other stations suggest an increase in this trend since 1950, with temperatures increasing by about  $0.06^{\circ}\text{C}$  per year and precipitation by approximately 6 mm water equivalent per year. [From Peel et al. 1988; and private communication from D.A. Peel, June 1990.]

smaller, and we certainly are not yet in a position to predict what they might do in response to a warming climate; they might become larger by increased snow accumulation (Figure 2), or they might become smaller by increased melting and ice discharge into the sea.

The importance of research on stratospheric ozone at high latitudes is now widely accepted, and results from that research have undoubtedly had a strong influence on recent major international

agreements aimed at preserving the Earth's ozone layer. This, perhaps, is a case where the special conditions that occur at high latitudes have provided a sufficiently early warning to allow the people of the world to take effective measures to prevent a disaster of their own making.

Because almost all high-latitude lands and oceans are remote, inhospitable, and vast in scale, they are most effectively investigated

by satellite remote sensing. Long-term, global satellite measurements began in the early 1970's with the polar-orbiting weather satellites, the early Landsats, and NASA's Nimbus series of spacecraft. Instruments similar to those aboard these early missions have been launched at irregular intervals ever since, and sufficient data have been acquired to provide almost continuous time series of some of the measurements. A major example with polar applications is the sequence of passive-microwave measurements obtained, first from NASA's Nimbus satellites, and more recently by a Department of Defense weather satellite. This has provided information on the behavior of sea ice that simply could not have been obtained in any other way.

The early instruments were passive sensors; they measured the intensity of natural radiation from the Earth surface and atmosphere at a range of wavelengths. Then, in the late 1970's, three distinct types of radar were launched with the objective of measuring specific characteristics: the radar altimeter, measuring ocean-surface and ice-sheet topography, wave height, and wind speed; the scatterometer, measuring the radar backscatter from wind-induced capillary waves on the ocean, from which sea-surface wind vectors could be deduced; and the Synthetic Aperture Radar (SAR), providing high-resolution, all weather images of ocean, land, and ice surfaces. These proved to be highly successful and, together with the passive sensors that have been progressively improved, they provide the blueprint for many of the Earth-looking sen-

sors that will fly over the next decade. Indeed, after the high days of the 70's, when many new instruments were launched and successfully tested, the 80's have been a barren time, with very few launches and no new sensors. However, this hiatus has allowed time for a rigorous assessment of the capabilities and limitations of the various remote-sensing techniques, and time to begin to develop the data systems that are essential to full exploitation of the vast accumulations of data typically produced by a satellite sensor. Moreover, several of the instruments launched in the late 70's continued to produce excellent data into the late 80's, supplying key time series of observations and helping to retain the interest of researchers using these data.

Over the next decade, there will be a massive expansion in the amount of satellite data that will be available with direct relevance to polar research (Figure 3). In the early 90's, at least one Earth-observing satellite will be launched every year, some of these with strong applications to polar research. Later in the decade, the Polar Platforms of the Earth Observing System (EOS) will carry a range of passive and active sensors into near-polar orbit, with a total data output that, in a few weeks, will exceed all the polar data now in existence. Although this is a daunting prospect, the polar-research community has an excellent opportunity to prepare for the data deluge from EOS. This opportunity is provided by the extensive sets of data already existing, and still being acquired, and by the missions of the early 90's. These data should be used to compile baseline measurements of key geophysical variables, to develop the necessary processing and data-han-

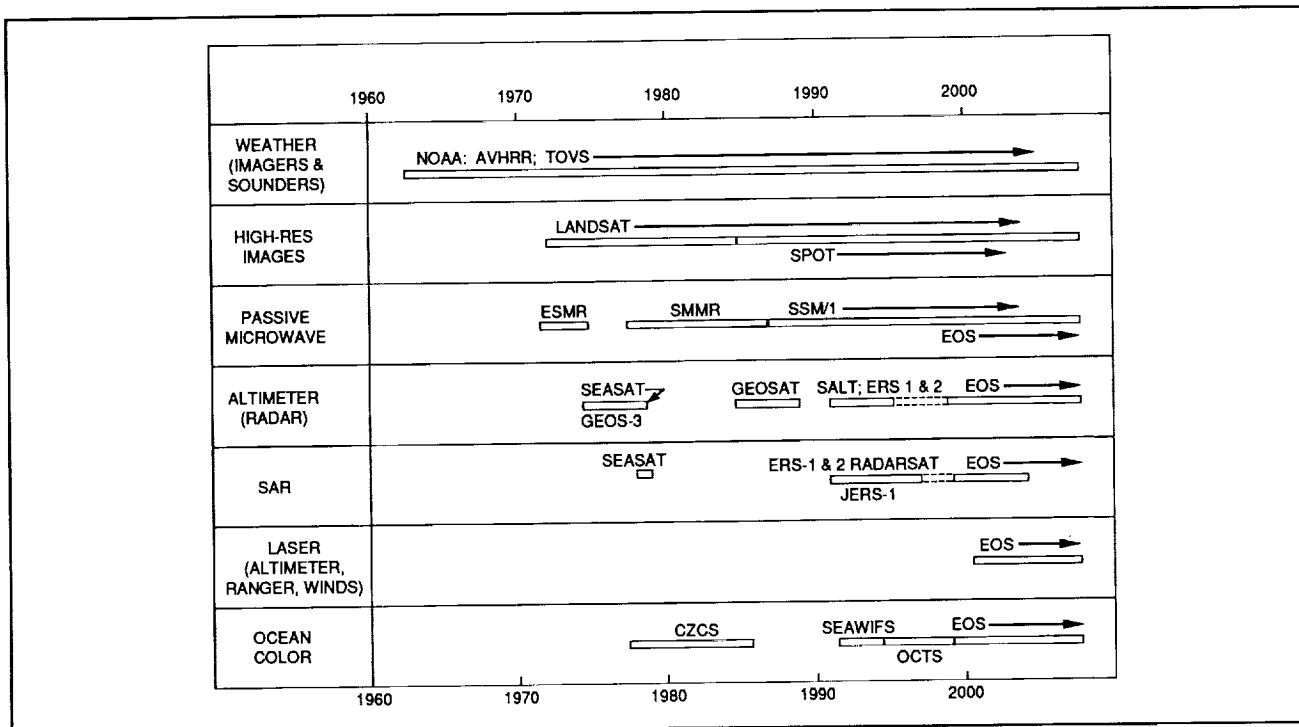


Figure 3. Past, present, and planned satellite missions with major potential for polar research.

ding techniques, to build the understanding of how to use products derived from satellite data to address research problems, and to attract talented new investigators to polar research.

This report presents a review of existing and planned satellite sensors with applications to polar research, a description of the major sets of polar data already acquired by satellites, and a preview of planned missions that will both extend these data sets into the future and provide entirely new types of polar data. In addition, it includes some examples of how these various data should be used to address specific problems. Emphasis is on instruments that measure surface, or near-surface parameters of particular importance to polar research, and we shall discuss only briefly the instruments that sound the atmosphere.

The next Section provides a summary of major polar-research objectives in order to help identify the types of satellite measurement that can be used to address these objectives. While this summary is far from complete, it is an attempt to identify a set of polar research objectives that contribute to larger studies of the global system, with a clear bias towards research that can benefit significantly from satellite measurements. Our emphasis is motivated by a desire to identify a simple theme that unites most of polar research and relates that research to the context of understanding global change. Omission of specific research activities should not be interpreted as a commentary on the value of that research; moreover, in most cases, these omitted activities will also be served by the satellite data identified in this document.

## 2. The Polar Regions and Climate Change

Attempting to identify "important" research is always dangerous. First, what is important depends on the context - the overall goals that motivate the research; and second, our perception of what is important is certain to change as we learn more about the problems. However, without some attempt to classify and to prioritize, a description of polar research becomes an interminable listing of research problems linked solely because they relate to high latitudes. Moreover, the growing national and international interest in "Global Change" provides a natural focus for Earth studies, and a timely rationale by which to set priorities. The reader is referred to the various reports of the Polar Research Board listed in the bibliography for a more thorough discussion of research objectives and priorities at high latitudes, and to the two reports being compiled to guide the NSF Arctic Systems Science (ARCSS) program.

The Global Change program has the goals of understanding the Earth system sufficiently to detect changes within the system, and to predict, with at least some confidence, the probable response of the system to significant perturbations, be they natural or man-made. In this context, the major components of the Earth system with most relevance to the polar regions are: ocean/atmosphere heat exchange and the modification of water masses; radiatively active trace gases in the atmosphere (CO<sub>2</sub>,

methane, ozone, etc.); surface albedo and its effect on the Earth's radiation balance; the response of high-latitude processes to climate change; and paleoclimate (Figure 4). Each of these, with the exception of paleoclimate, can be addressed using satellite data, and in the subsections below we shall briefly review the relevant types of measurement that are either available now or will be in the near future. First, however, we should stress that many other research problems are also served by these same data sets. In particular, solid earth processes, such as coastal erosion, vulcanism, plate tectonics, and surficial erosional and depositional processes, can be studied using data from many of the instruments described in Section 3. Moreover, operational observation techniques and prediction capability in polar regions will benefit from this research.

Each of the Sections below identify satellite instruments that acquire information relevant to the research topic of that Section. For more information on the instruments and applications of the data they acquire, the reader should refer to Section 3.

### 2.1 Ocean/Atmosphere Heat Transfer

High-latitude air/sea interactions have a direct influence on the rate of transfer of heat and water vapor from low to high latitudes. Major factors are the areal extent and characteristics of polar sea ice, and the circulation and density structure of the underlying ocean. Moreover, as an ocean driver, the freezing and melting of sea ice is the high-latitude analogue of evaporation and precipitation; freezing increases the salinity of the

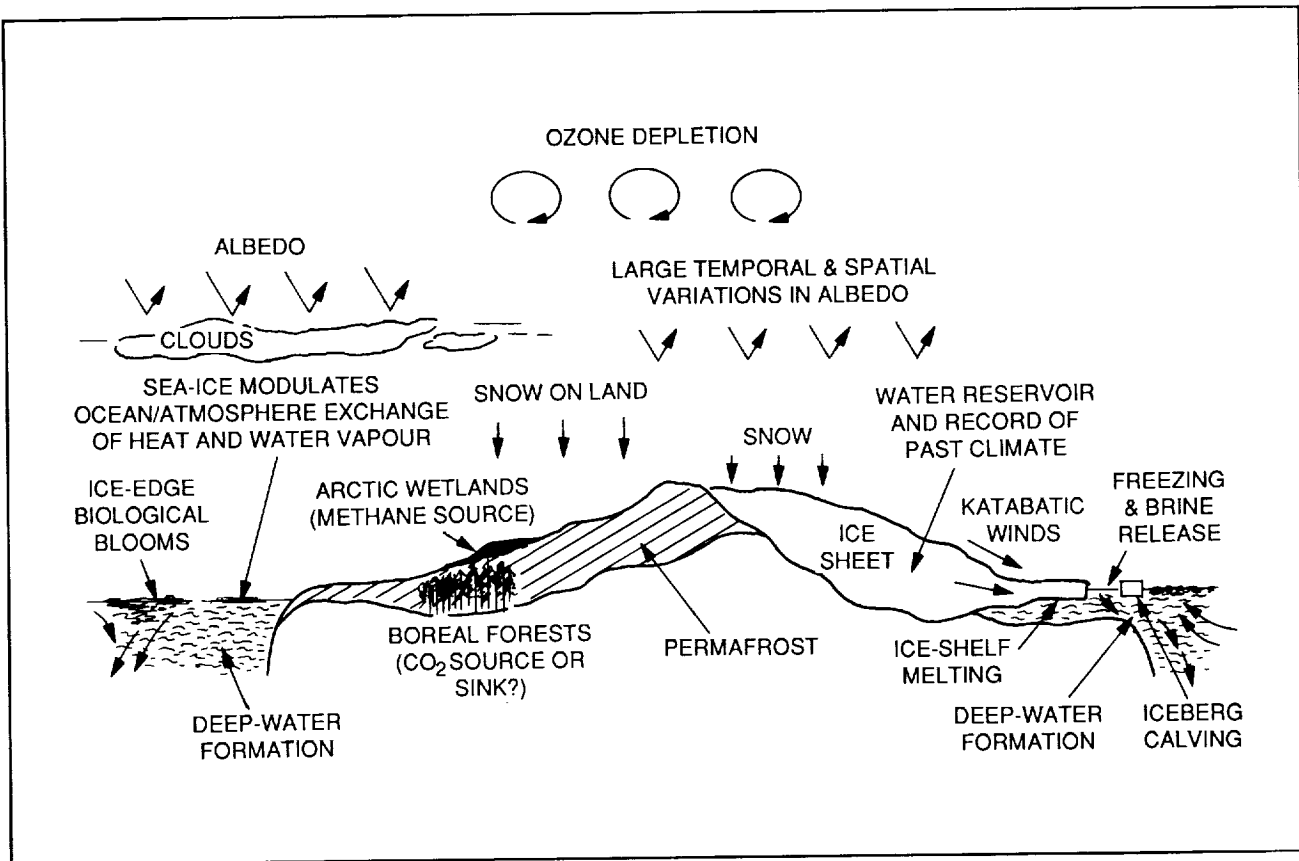


Figure 4. Schematic, showing high-latitude processes important to global change.

underlying ocean, and melting reduces it. Movement of the ice prior to melting redistributes the fresh water and, in particular, can cause significant fresh-water export to lower latitudes; the major sea-ice outflow from the Arctic east of Greenland (Figure 5) represents a fresh-water flux of about  $2800 \text{ km}^3/\text{yr}$ . This is on the same order as the annual discharge of glacial ice from Antarctica but, by contrast, it takes place over a very small region, and is second only in volume to that of the Amazon River (Aagaard and Carmack, 1989).

Heat loss from the ocean to the atmosphere through a sea-ice cover can be up to two orders of magnitude less than from the open sea, and heat within the deep ocean can be further isolated by a

layer of low-salinity water resulting from melting ice. Moreover, sea ice plays a key role in determining the behavior of the thermohaline cells that link the world's oceans and are responsible for redistributing heat and salt around the globe (Figure 6). The deep and bottom waters of the world ocean make contact with the atmosphere through only 5% of the total ocean area, all at high latitudes. Their temperature, oxygen content, and other characteristics are acquired in areas of deep mixing caused by density perturbations associated with brine rejection from freezing sea ice (Gordon, 1986). These key processes occur in the Arctic Ocean, on the vast continental shelves around its margins, in the Greenland, Iceland, and

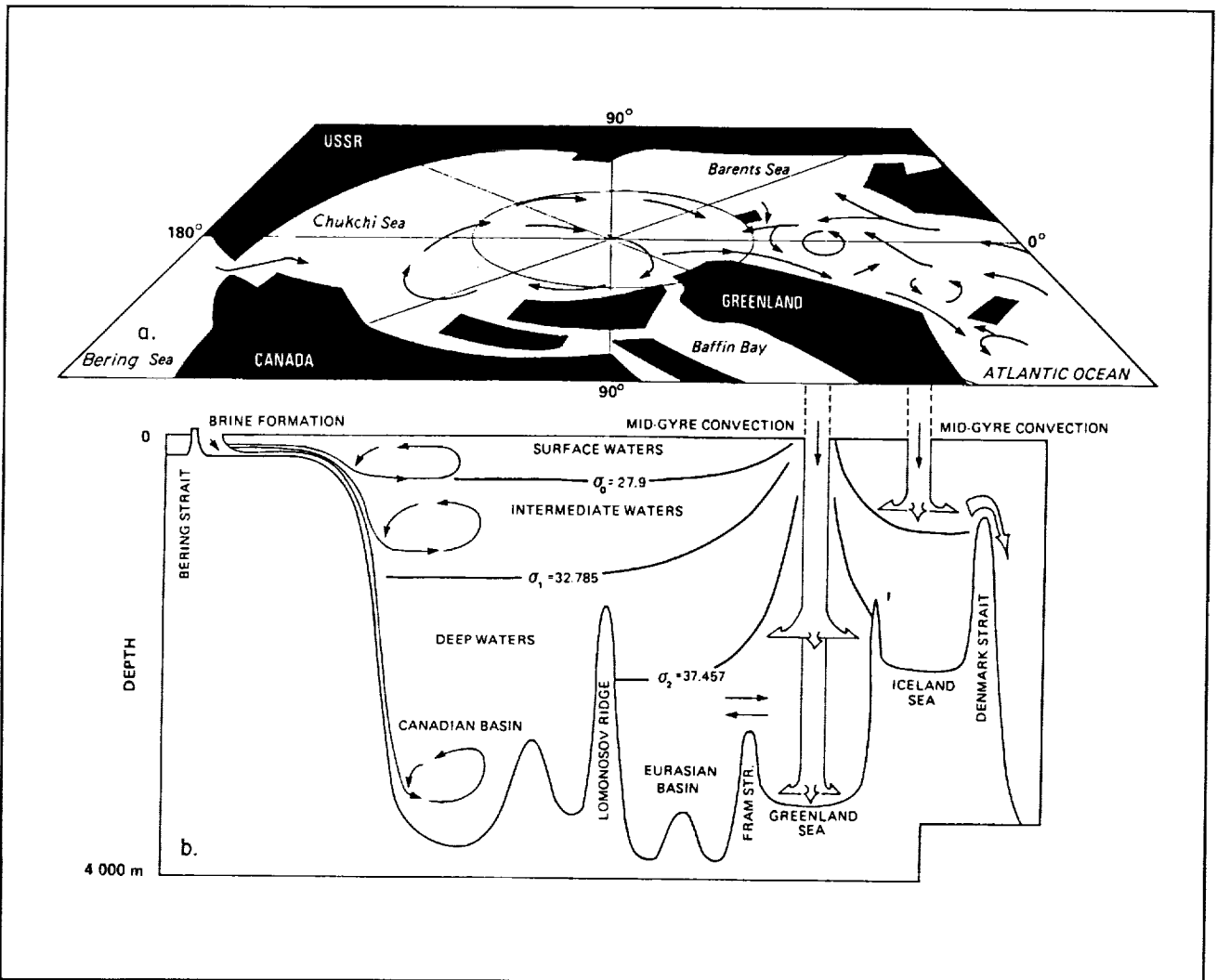


Figure 5. Schematic circulation in the Arctic Ocean and the Greenland and Iceland Seas. The upper panel represents near-surface circulation; the lower panel represents a section from Bering Strait, across the Arctic Ocean, and through the Greenland and Iceland Seas to Denmark Strait, where cold, saline water overflows southward to help form North Atlantic Deep Water, contributing to the global thermohaline circulation depicted in Figure 6. [Aagaard et al., 1985.]

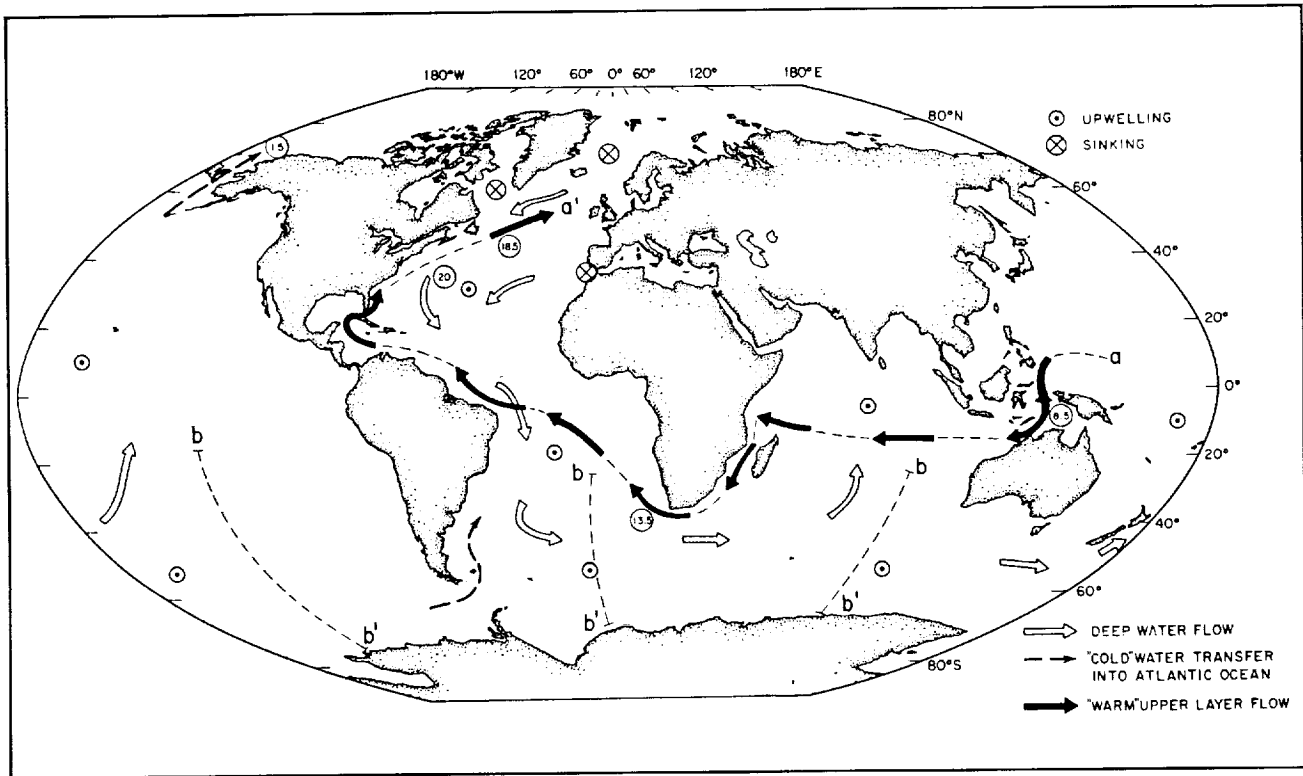


Figure 6. Proposed pattern of the global thermohaline circulation associated with North Atlantic Deep Water (NADW) production. Warm, salty, upper-layer waters required to feed NADW production follow the solid arrows to the northern North Atlantic, where they mix with cold, salty waters formed in the Arctic and sink, primarily in the Labrador and Greenland/Norwegian Seas. As this northern component of the NADW moves southwards (open arrows) within the deep western boundary current, it is joined by the saltier outflow from the Mediterranean Sea. The circled numbers give the volume flux in millions of cubic meters per second. A major area of upwelling of NADW is in the Southern Ocean, where it contributes to the formation of Antarctic deep and intermediate waters (Figure 7). [Gordon, 1986.]

Labrador seas, in the Weddell and Ross seas, and along parts of the coast line in Antarctica (Figures 7 and 8).

Relevant satellite data are obtained from microwave radiometers and Synthetic Aperture Radars (SARs), both providing all-weather, day/night images of the sea-ice cover, and from thermal-infrared radiometers, which provide estimates of surface temperatures on the ocean and ice.

## 2.2 Trace Gases

The 1985 discovery of large, rapid decreases in atmospheric ozone each spring in Ant-

arctica (the "ozone hole") prompted a series of experiments in both the Antarctic and the Arctic, which have shown that polar stratospheric clouds, which form at low temperatures, are the sites of a series of chemical reactions that accelerate the catalytic destruction of ozone by chlorine. The source of the chlorine is almost certainly the chemically inactive, man-made series of chloro-fluorocarbons, which become converted to photochemically-active compounds on the surface of polar stratospheric clouds.

Relevant satellite measurements are obtained by the Solar Backscatter Ultra Violet

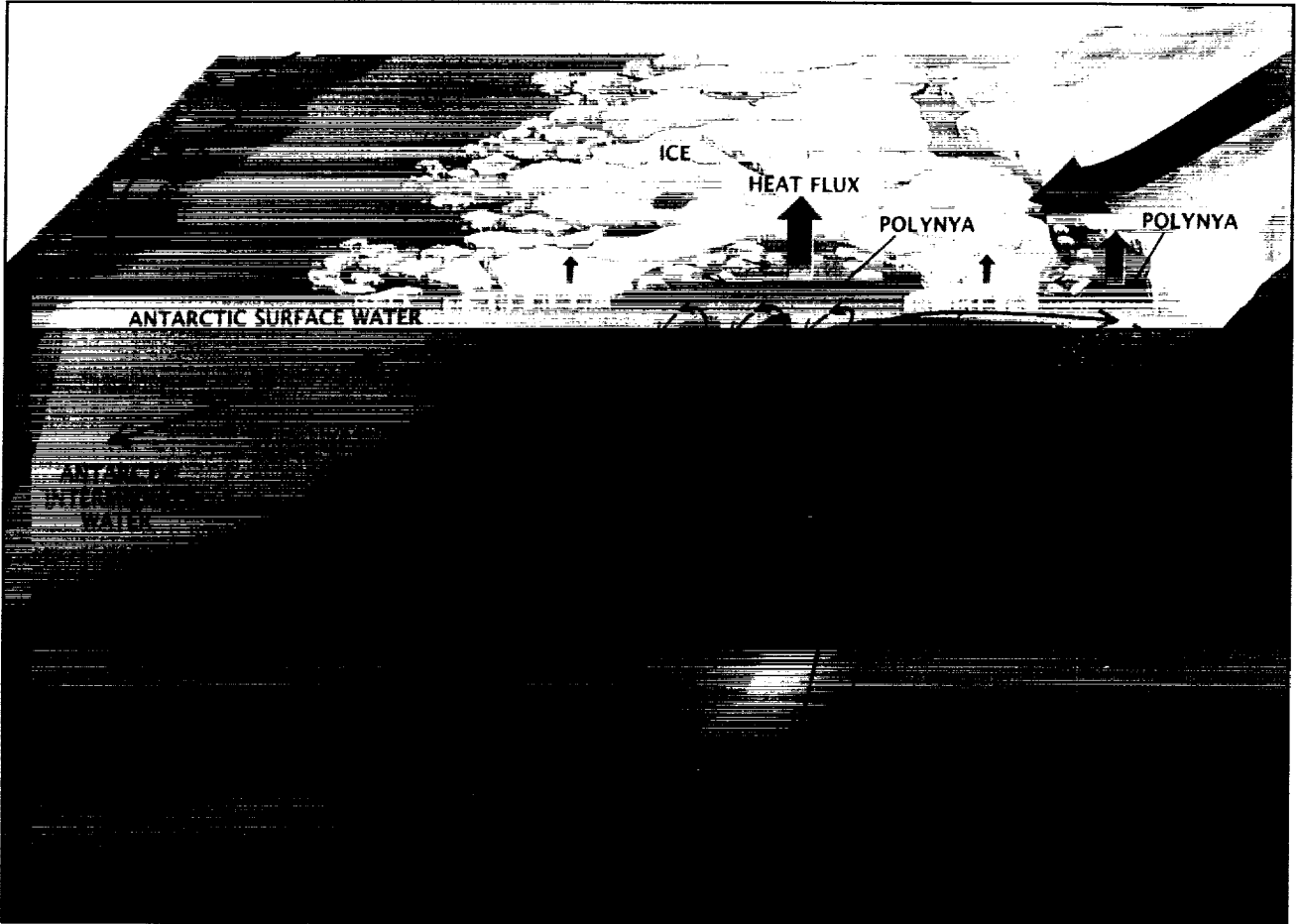


Figure 7. Circulation of the waters around Antarctica. Relatively warm, salty North Atlantic Deep Water rises towards the surface as it approaches Antarctica to become Circumpolar Deep Water (CDW). Although the CDW is warmer than Antarctic Surface Water, it is slightly heavier because of its high salinity, and tends to remain beneath the surface. However, there is only a slight density difference between these two water masses, and quite small perturbations, associated with winds or salt release into the surface waters during ice formation, can enhance mixing and even initiate overturning to bring warm water to the surface. The 200,000 square km Weddell Polynya that persisted through four winters during the 1970's was probably associated with such overturning. Near the Antarctic coast, intense ice formation, in polynyas formed by katabatic winds pushing the sea ice seawards, releases large quantities of salt. The resulting cold, dense body of water sinks to form Antarctic Bottom Water, which moves northwards along the ocean floor. It travels well beyond the Equator, and is the major mass of bottom water in the world. [Gordon and Comiso, 1988.]

ORIGINAL PAGE IS  
OF POOR QUALITY

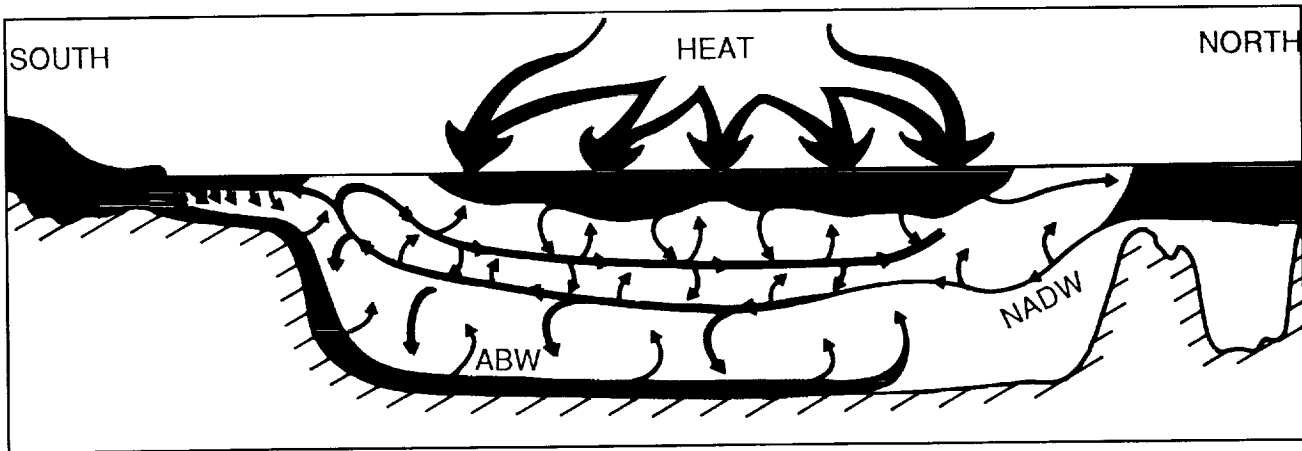


Figure 8. Schematic thermohaline circulation associated with North Atlantic Deep Water (NADW) and Antarctic Bottom Water (ABW). Much of the heat carried by NADW into the Circumpolar Deep Water (CDW) is lost to surface waters around Antarctica, limiting the heat available for melting ice from beneath the large Ross and Filchner/Ronne ice shelves. In the Bellingshausen Sea, however, CDW reaches the coast after minimal cooling, and ice-shelf basal melt rates are perhaps an order of magnitude larger.

(SBUV) and Total Ozone Mapping Spectrometer (TOMS) instruments aboard NASA's Nimbus-7. Data have been collected since 1978, and the TOMS is still operating 11 years later; data quality from SBUV has deteriorated since 1987. SBUV instruments have also been included aboard NOAA polar-orbiting satellites, and a series of TOMS instruments will be launched during the early 1990's by NASA in collaboration with the Russians and Japanese. Both SBUV and TOMS make measurements in the ultra-violet portion of the spectrum, to provide estimates of total ozone and the ozone profile directly beneath the spacecraft (SBUV), and a mapping of total ozone within a swath approximately 3000 km wide (TOMS).

For millennia, peatlands have captured and stored carbon, and they now hold some 15 to 20 percent of land-stored carbon. Under the right conditions, methane-producing bacteria

(methanogens) thrive at peaty sites, and it is estimated that much of the global methane emission is from the Arctic wetlands. Nevertheless, in the past, these peatlands have been net carbon "sinks." However, additional water from increased precipitation or melting permafrost would probably increase the rate of methane emission, and drying-out of the peatlands would attract oxygen-using microbes, to produce enhanced levels of carbon dioxide. Moreover, recent work suggests that increasing sulphate levels associated with acid rain attract sulphate-reducing bacteria to the peatlands, and these bacteria are perhaps 50% more efficient than methanogens at producing greenhouse gases. Consequently, it is quite likely that significant Arctic warming would convert the peatlands from a sink to a source of atmospheric carbon.

ORIGINAL PAGE IS  
OF POOR QUALITY

A recent assessment of the global carbon budget (Tans et al., 1990) suggests that a significant fraction of "industrial" CO<sub>2</sub> is removed from the atmosphere by the terrestrial ecosystem, most probably by temperate and high-latitude forests in the Northern Hemisphere. However, their study also highlights how little is known about the many components of the carbon budget, including the Arctic wetlands and boreal forests.

In response to a warming climate, the mix of Arctic vegetation is likely to change. Indeed, evidence from borehole temperatures in permafrost (Lachenbruch and Marshall, 1986) suggests substantial warming of Arctic regions has occurred over the past century, and there are indications in northwest Alaska of rapid spread of spruce, cottonwood, alder, and willow. This has been accompanied by migration of moose, beaver, and porcupine. Assuming that quantitative links can be found relating temperature and soil moisture to both greenhouse-gas production and vegetation types, then monitoring the vegetation mix from space provides a proxy indication of the flux of greenhouse gases (Figure 9). Relevant instruments are those obtaining medium to high resolution images in the visible, infrared, and microwave, such as the AVHRR, Landsat and SAR. Wintertime SAR data may provide a direct indication of permafrost extent.

Carbon dioxide dissolves in ocean water, with solubility increasing at lower temperatures, and it is absorbed during photo-

synthesis by marine plants in surface waters that form the base of the marine food chain. The near-surface ocean mixed layer is in approximate equilibrium with the atmosphere, and solution of additional carbon is limited by the rate at which photosynthesis extracts dissolved carbon from the surface waters, the rate of precipitation of organic detritus into the deep ocean, and the slow rate of water exchange between the mixed layer and the deep ocean. However, in areas of deep-water formation, predominantly at high latitudes, surface water is funneled into the deep ocean, taking with it dissolved carbon dioxide. Thermohaline circulation induced by this process brings warm surface water to higher latitudes where it is cooled and, because CO<sub>2</sub> solubility increases at lower temperatures, is able to dissolve additional CO<sub>2</sub>. The ocean loses carbon primarily at lower latitudes, where upwelling deep water warms and outgases some of its dissolved load of carbon dioxide. Significant changes in the annual cycle of sea-ice formation and decay are bound to affect deep-water production rates and the thermohaline circulation system, which will have a currently unpredictable impact on the global carbon cycle.

Satellite measurements of ocean color at several frequencies provide estimates of chlorophyll content that can be related to the primary productivity of the surface layers of the ocean.

### 2.3 Surface Albedo

The albedo of snow and ice ranges from 0.3, for melting sea ice with puddles, to 0.9, for fresh, dry snow. There are rapid changes in albedo

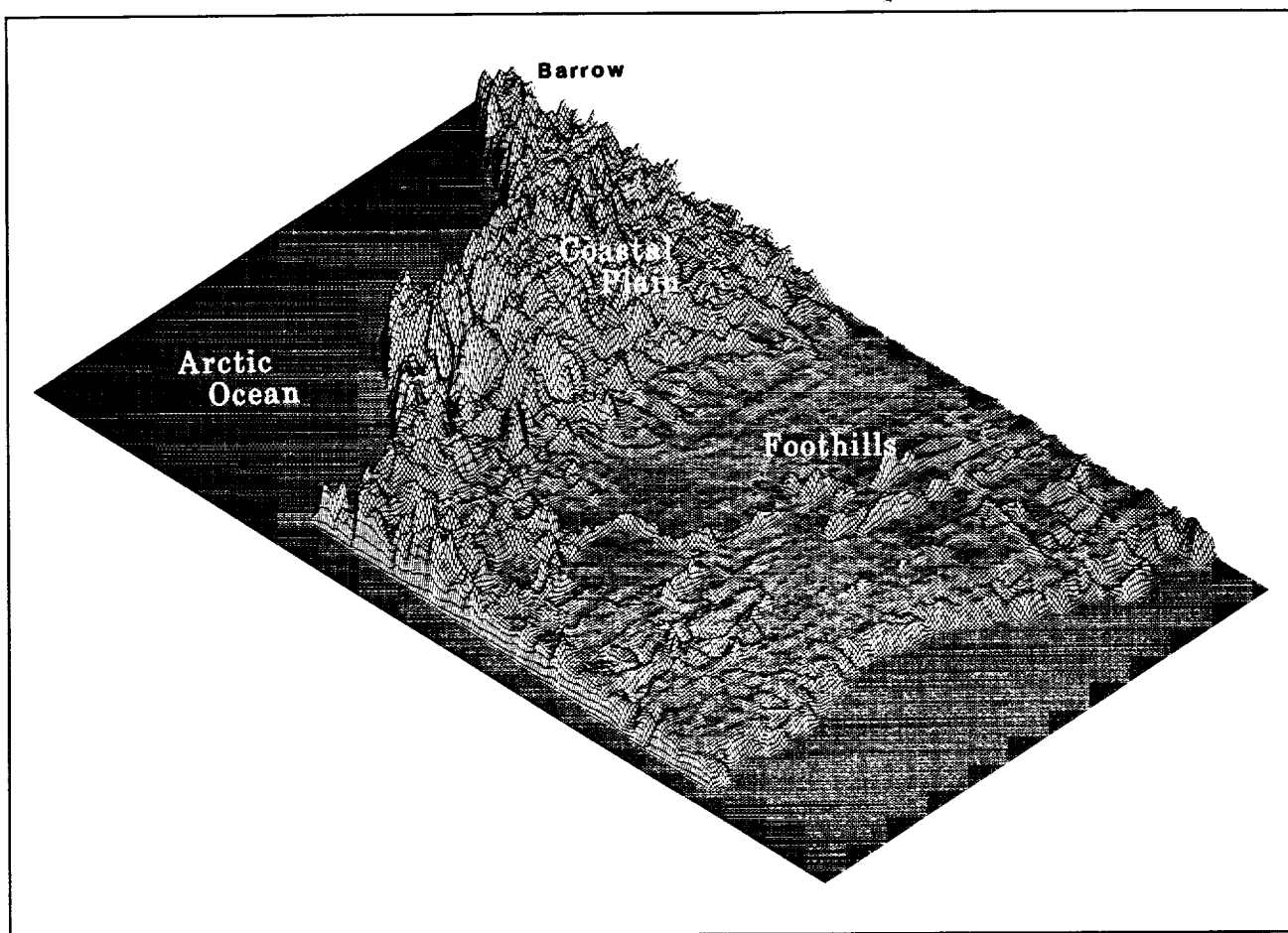


Figure 9. An image depicting the magnitude of methane flux from the western half of the North Slope of Alaska. The poorly drained Coastal Plains display both high emissions and high spatial variability, while the foothills exhibit low emissions and low variability except along river drainages. These estimates are based on measurements of methane emissions from various types of surface with a mapping of surface types by airborne and satellite remote sensing. [Image provided by G. Livinston and L. Morrisey, NASA Ames Research Center.]

during spring and autumn (Figure 10), but their climatic significance is reduced during autumn when the albedo at high latitudes is determined mainly by cloud cover. Moreover, the total solar radiation received at high latitudes is small. The effect of snow and ice albedo as a positive feedback in a warming climate may have been overestimated in some studies, particularly those assigning large albedo values to all snow and ice.

In addition to the natural variability of snow albedo, carbon from industrial pollution may be

causing an appreciable reduction in the albedo of snow. Every spring for the past half century or more, a haze consisting of fine particles has formed over the Arctic, so that the Arctic atmosphere in late winter and spring may contain more man-made aerosols than does, for instance, polluted air off the east coast of the US. This Arctic haze traps heat near the surface and increases both the rate of atmospheric warming and the rate of melting of the surface snow, with as yet unknown effects on local and global climate.

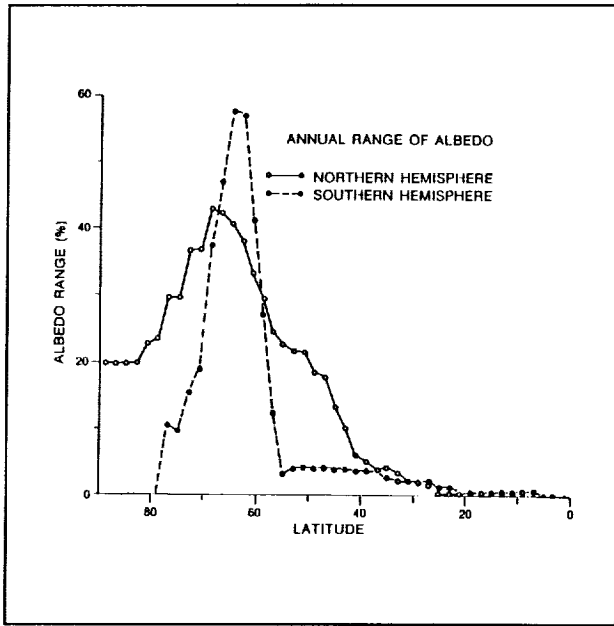


Figure 10. Annual range of zonally-averaged albedo variations in both hemispheres. [Kukla and Robinson, 1980.]

Optical and infrared sensors, such as those aboard weather satellites and Landsat, are useful for snow-albedo studies, but there are major problems involved in obtaining routine estimates of snow and ice albedo over large areas because of natural variability both with time, and with the orientation of the sun with respect to the snow surface.

Attempts have been made to measure the Earth radiation budget, starting with NASA's Nimbus-7 (launched in 1978) which carried three separate instruments operating at a wide range of frequencies to measure solar irradiance and Earth radiation at both coarse and fine spatial resolution. Similar instruments were included on NOAA weather satellites, beginning in 1984, and data from these various instruments provide a time series from which

we are beginning to detect short- and long-term variations in solar irradiance, and to investigate regional patterns of Earth radiation flux. Little use has yet been made of these data for polar research.

## 2.4 Response to Climate Warming

Most attempts to model greenhouse effects indicate that atmospheric warming, particularly in winter, will be enhanced at high northern latitudes. If the consensus of existing model predictions is correct, then we might expect the first clear signs of such warming to be detected in the Arctic (e.g., Hansen et al., 1984; Grotch, 1988).

Recent work by Stouffer et al. (1989) suggests that greenhouse warming in Antarctica may be very slow, primarily because deep mixing increases the thermal inertia of the waters around Antarctica. The importance of this work lies, not so much in its message of reassurance to those eager to discount the threat of rising sea level, but more as a strong indication of the sensitivity of the greenhouse scenario to interactions previously unaccounted for. It stresses the need for rigorous incorporation of realistic simulations of polar processes into global climate models.

The effects of climate warming at high latitudes might be manifest as systematic increases in surface temperatures or, more indirectly, as changes in sea-ice conditions, areal extent of seasonal snow, intensity of summer melting on the Greenland ice sheet, patterns of precipitation, or the total volume of ice on land. Unfortunately, however, there is but a poor existing record of surface temperatures in the Arctic, and most of the

other responses, such as sea-ice extent, possess a large interannual variability from which any long-term trend must be distinguished.

Despite more than four decades of sustained international field investigations costing some hundreds of million of dollars, we still do not know whether the volume of ice on Earth is decreasing or increasing. Results from the field work indicate that some glaciers are increasing in size; others are decreasing. Extrapolations have been made from these observations to infer, for instance, the contribution to sea-level rise made by "small" glaciers and ice caps. Errors in the resulting estimates are very large, and for the big polar ice sheets, we cannot confidently conclude even whether the mass balance is positive or negative. In those few areas where we do have reliable estimates of ice thickening or thinning rates, we cannot explain why the ice is behaving as observed. There is a major need for a comprehensive program to measure ice thickening/thinning rates over all the larger ice sheets, and

to investigate the processes affecting mass balance: snow accumulation and melting; ice-stream and glacier discharge; and ice/ocean interactions.

It is important to continue existing time series, such as estimates of sea-ice and snow-cover characteristics, and to start as early as possible to compile appropriate new time series of relevant data such as permafrost extent, ice-surface temperature, and ice-sheet volume, both to allow detection of climatic trends, and to investigate the processes underlying interannual variations.

Relevant satellite data are acquired by almost all Earth-looking sensors, including visible, thermal infrared, and microwave radiometers, synthetic aperture radars, and radar and laser altimeters.

### 3. The Satellite Instruments

Techniques for satellite remote sensing of the Earth make use of electromagnetic radiation to gain information from some distant region above, on, or beneath the Earth surface. The information is contained in the intensity, the frequency spectrum, the polarization and the time delay of the received energy. The prime objective of this chapter is to review the techniques used for investigating the properties primarily at or near the Earth surface at high latitudes and, to a lesser extent, throughout the polar atmosphere.

Appendix I provides details on how to obtain more information about, and copies of, specific data sets.

#### 3.1 Basic Principles

Electromagnetic radiation ranges in wavelength over more than 20 orders of magnitude (Figure 11) and parts of almost the entire range are used in some type of remote-sensing application. The portion of the spectrum most used in satellite remote sensing of the Earth extends from the visible, with wavelengths of order  $10^{-6}$  meters, through the infrared, to microwaves, with wave-

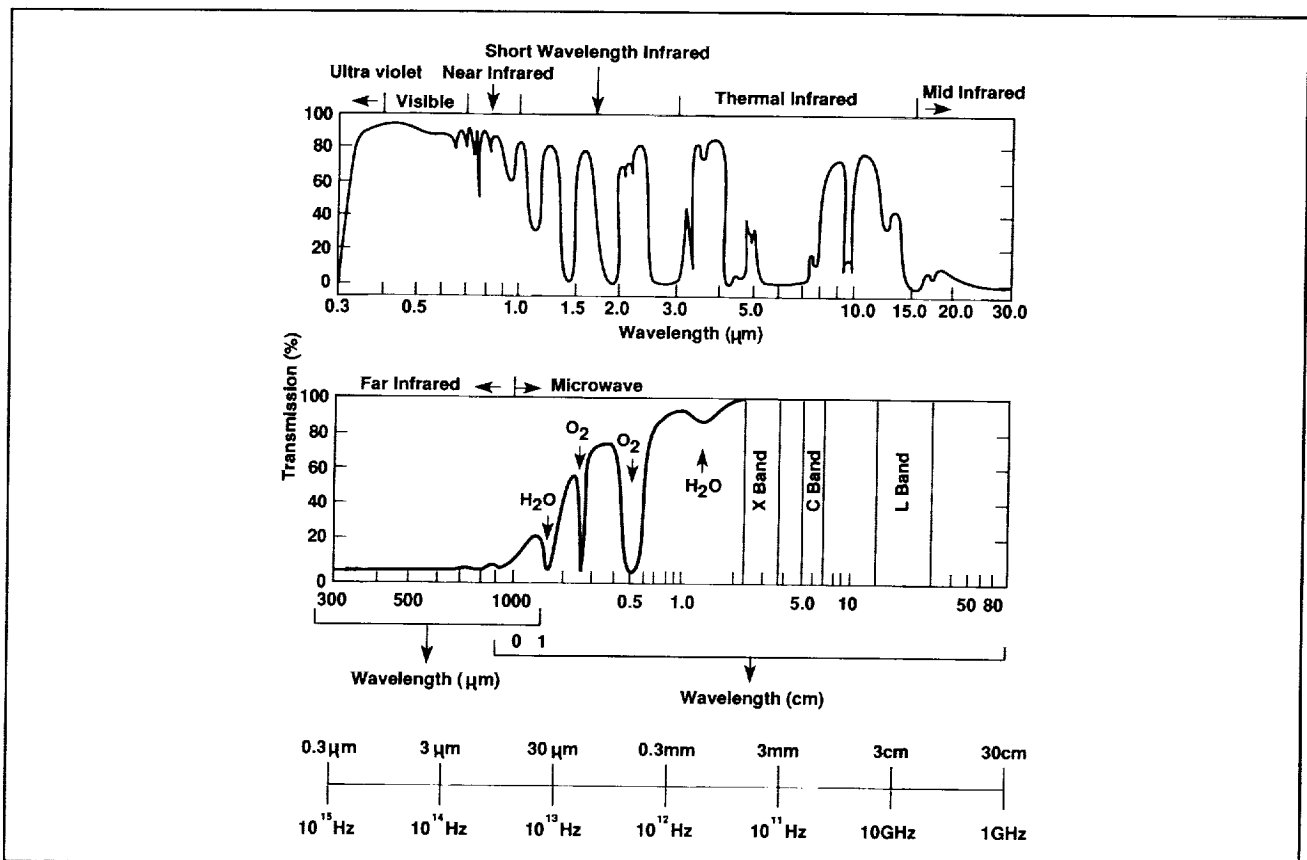


Figure 11. Generalized absorption spectrum of the Earth's atmosphere at zenith. The curve shows the total atmospheric transmission as a function of wavelength. [After Elachi, 1987.]

lengths up to about 1 meter. Radiation at wavelengths shorter than visible is strongly affected by the atmosphere, and that at wavelengths longer than microwave have very poor spatial resolution. Moreover, at wavelengths longer than 30 m (10 MHz), the ionosphere blocks all radiation. In general, the shortest wavelengths provide greatest spatial resolution, whilst the longer wavelengths are less affected by the atmosphere. However, it is possible to obtain high spatial resolution with microwaves (see Section 3.3.1) and, even in the microwave, there are bands that are strongly affected by atmospheric components (Section 3.2.4).

All matter, unless it has a temperature of absolute zero, emits electromagnetic radiation, generally with intensity proportional to its physical temperature. A perfect emitter, known as a “blackbody,” has an emissivity of unity, which means that it emits radiation at the maximum possible rate, a rate that depends only on the temperature of the emitter. Most natural bodies emit radiation at a lower rate, and the ratio of this rate to that of a blackbody at the same temperature is the “emissivity,” which consequently is unity for a blackbody. In general, the emissivity is nearly independent of temperature, and is determined by the nature of the emitter - its chemical composition, crystal structure, grain size, surface roughness, etc. The emissivity is also a function of direction; thus, the viewing direction of a radiometer must be accurately known. The emissivity of a substance is generally different for different radiation frequencies and different polarizations, so that most materials possess unique radiation properties or “signatures” from which they can be identified.

In much the same way, the electrical properties of matter govern the scattering of radiation from the material. Radiation purposefully used to illuminate a material (e.g., from a radar) is scattered to a degree related to the electrical, structural, and chemical properties of the material. Temperature is important only in so far as it modifies these properties.

### 3.1.1 Choice of Frequencies

Figure 11 shows the atmospheric transmission as a function of wavelength. There are many portions of the spectrum where the atmosphere has a high opacity. In the ultraviolet, this is caused mainly by the ozone layer high in the atmosphere; in the visible and near infrared, mainly by water vapor and carbon dioxide; in the far infrared, the atmosphere is almost completely opaque, due mainly to the presence of absorption bands associated with various atmospheric constituents; and in the microwave, the strong absorption bands are mainly caused by oxygen and water vapor. Water droplets in clouds lead to additional absorption and scattering, but this is negligible at the lower microwave frequencies. Observations of the Earth’s surface make use of spectral “windows,” where the atmosphere is almost transparent to radiation. Conversely, the spectral bands with high opacity are used to sound the atmosphere.

Data at visible wavelengths indicate the color of the viewed surface, from which proxy information can be derived on surface characteristics such as rock type, vegetation, snow

cover, and ocean chlorophyll. At the other end of the spectrum, microwave data contain information on surface roughness, sea-ice characteristics, soil moisture, ocean winds etc. In general, radiation at longer wavelengths provides more information from beneath the surface. For example, dry snow on land is readily identified in visible and high-frequency microwave imagery, but low-frequency microwaves pass through the snow, with an attenuation determined by snow depth. The choice of wavelength also imposes constraints on the conditions under which the information can be acquired. Thus, high-resolution imagery is most easily obtained at very short wavelengths, but information from beneath a cloud cover can be obtained only at long wavelengths.

For many substances, the depth from which radiation is emitted or backscattered increases with increasing wavelength. For example, we can learn something about conditions within the upper several meters of an ice sheet or of dry, desert sand using microwaves, whereas visible light and thermal infrared radiation depict conditions at or very close to the surface. However, there are exceptions, notably ocean water, which is almost opaque to infrared and microwave radiation, but through which visible light can pass for several meters.

### 3.1.2 Algorithms

To convert remotely-sensed measurements into information that will be useful to researchers, a number of algorithms are applied. These algorithms calibrate the measure-

ment, to correct it for, say, atmospheric absorption, and extract from it an estimate of the required geophysical parameter. Generally, each of these algorithms requires information from other sources to complement the sensor measurement. For instance: information on the satellite location, or ephemeris, is used to locate the viewed picture element, or "pixel," on the Earth surface; the antenna pattern of a microwave radiometer is used to convert the measured intensity to that corresponding to the pixel; and measurements made at several frequencies and polarizations may be used in the algorithm that derives the geophysical estimates.

The products from each algorithm have some level of uncertainty, which becomes compounded in the derived geophysical quantity, and it is important that users of the data are aware of the limitations imposed by this process. This does not mean that users have to understand the many algorithms used in processing the data; rather, it imposes a requirement on those responsible for data processing to state clearly the accuracies and limitations of derived parameters.

### 3.1.3 Orbits

Two distinct types of satellite are used to obtain remote-sensing data of the Earth from space. A geostationary satellite operates in a high orbit (approximately 36,000 km), where the rotational velocity necessary to balance gravity is identical to the rotational velocity of the Earth. This allows the satellite to remain over approximately the same location, and to image the same hemisphere at almost any desired time interval.

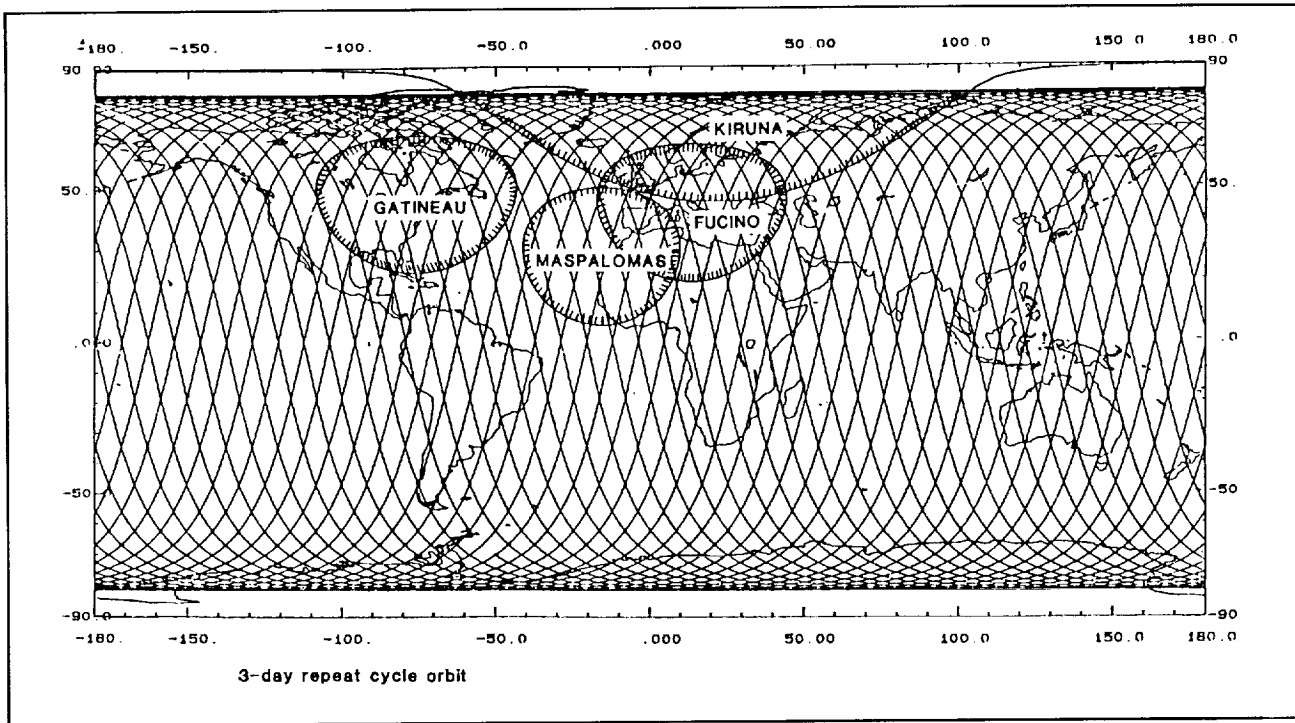


Figure 12. Satellite orbit tracks covered in three days by the European Remote Sensing Satellite ERS-1.

However, the orbit of a geostationary satellite must be approximately in the same plane as the Earth's rotation, i.e., close to the equatorial plane. Consequently, images of the polar regions obtained from geostationary orbit are highly distorted, and they have poor spatial resolution.

A more global view can be obtained from polar-orbiting satellites, with orbits a few hundred km above the Earth, that circle the globe many times each day. Generally, the orbit is not truly polar, but rather offset by about 8 degrees of latitude, and the satellite is at a height of between 700 and 800 km, where it completes approximately 14 revolutions each day, so that each successive orbit track on the Earth surface is separated by about 25 degrees of longitude. Lines of longitude converge towards the poles, so that those parts of the world that are the most difficult to study *in situ* are, fortuitously, those that are best covered by

polar-orbiting satellites (Figure 12). The precise time taken for the satellite to encircle the Earth, the orbit period, is sensitively determined by the height of the satellite, and the orbit period determines the actual separation on the Earth surface between consecutive orbit tracks. This in turn controls the "repeat period" of the satellite - the time taken for the satellite to repeat a particular orbit track. Generally, the repeat period is chosen so that a specific imaging instrument can obtain global coverage within some desired period. Most instruments making measurements in the visible range operate in a "sun-synchronous" orbit, which passes over the equator on each orbit at approximately the same local time. The sun angle in repeated images of a specific area is then determined primarily by the equator-crossing time, the latitude, and the season.

Temporal resolution of a specific sensor is determined by its swath width, its duty cycle and the orbit of its satellite platform. Most frequent coverage of a given location is provided by an imaging sensor with broad swath, continually operating aboard a satellite with a short orbit-repeat period.

### 3.1.4 Remote-Sensing Techniques

For a thorough discussion of this topic, the reader is referred to any of the many specialized texts (e.g.: Stewart, 1985; Elachi, 1987). Satellite sensors measure the intensity of received radiation at some polarization and within a prescribed frequency band. Passive sensors detect the intensity of natural radiation emitted by and reflected from the scanned surface. Active sensors transmit pulses of energy and record characteristics of the signal reflected from the interrogated surface. Most active sensors operate at microwave frequencies, but there is growing interest in the use of lasers to sound the atmosphere, to measure cloud heights and ice-sheet topography, and to measure precise distances to reflectors on the ground. Advantages of active sensors include control over the wavelength, polarization, intensity, pulse shape, and direction of the illuminating radiation, and the ability to measure the transmission time, doppler shift, and shape of the return pulse. This additional information makes possible the measurement from space of parameters such as ocean-surface and ice-sheet topography, wave-heights, wind vectors at the sea surface, wind-vector profiles

above the surface, and crustal motion. In addition, the Synthetic Aperture Radar (SAR) obtains high-resolution radar images of the Earth surface by making use of the range and doppler measurements to extract from the backscattered radar energy information equivalent to that acquired by a very large antenna.

In most cases, data collected by a sensor are stored on tape aboard the spacecraft, and then transmitted at a high data rate, or "dumped," when the spacecraft is within view of a ground receiving station. This introduces a delay of up to a few hours between the time of data acquisition and the time of data receipt on the ground. Recently, Tracking and Data Relay Satellites (TDRS) have been used to relay data that are transmitted from suitably equipped remote-sensing spacecraft. In principle, data can be transmitted to a TDRS in real time, regardless of the satellite location along its orbit.

The spatial and temporal coverage that can be acquired by a specific sensor are currently determined primarily by the resolution and the power consumption of the sensor. Frequent global coverage can be readily obtained with a low-power instrument with coarse spatial resolution, such as passive-microwave sensors. Such instruments can be operated continuously, and they generally have a wide enough swath to ensure overlap between images obtained on consecutive orbits, so that global coverage can be obtained daily. Moreover, instruments with coarse spatial resolution have low data rates, permitting onboard storage of data covering very large areas. Weather satellites also

transmit information continuously to allow real-time acquisition by suitably-equipped users.

High-resolution instruments, such as Landsat and SAR, have comparatively narrow swaths, high data rates and, in the case of the SAR, high power requirements. Although global coverage can be obtained by collecting data over an extended period, these constraints generally limit data acquisition to preselected regions.

### 3.2 Passive Sensors

A radiometer measures the intensity of radiation, within some prescribed frequency band and polarization, from a particular area, or pixel, of the viewed surface, at some known viewing angle. Images are obtained by sequentially measuring the radiance from a series of pixels. Forward motion of the remote-sensing platform ensures scanning along track. Coverage of a broad swath requires either a set of many detectors, each viewing a different portion of the swath (pushbroom), or rotation of a single detector so that it obtains sequential measurements across the swath (scanning). For some purposes it is important to view each pixel at a fixed angle with respect to the vertical, and the detector is rotated so that the envelope of its viewing directions forms a cone that intersects the Earth surface at the desired angle (Figure 13).

Spatial resolution is determined by the pixel size, which is proportional to the wavelength divided by the antenna diameter; highest resolution

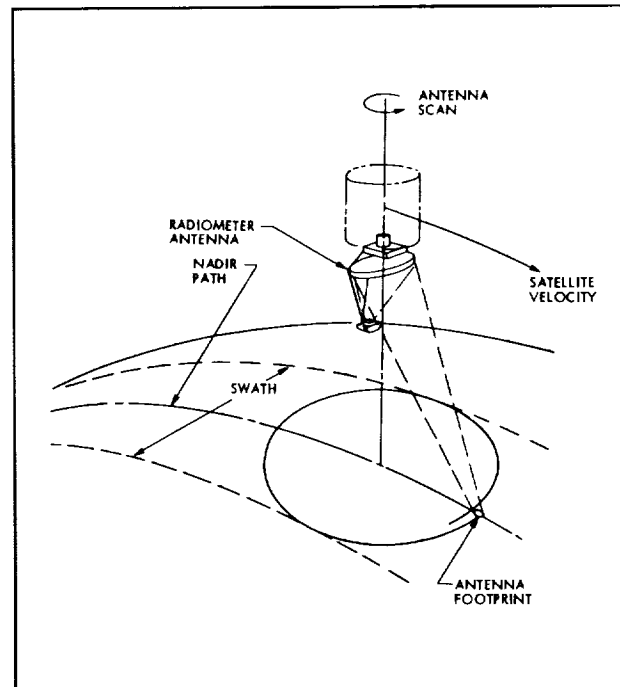


Figure 13. Conical scan configuration. Constant Earth-incidence angle is maintained over the entire swath. [Njoku, 1982.]

is obtained at short wavelengths with a large antenna aperture. With present civilian satellites, spatial resolution ranges from a few meters in the visible to tens of km in the microwave.

In this Section, we shall subdivide passive sensors into four types: microwave; medium-resolution visible and infrared; high-resolution visible and infrared; and sensors that sound the atmosphere.

#### 3.2.1 Microwave Radiometers

Satellite passive-microwave imaging sensors have operated in the 5 -100 GHz range.

Data can be obtained day and night, and are only slightly affected by cloud cover. The swath width is several hundred km, providing almost total global coverage every day and, with existing sensors, pixel size ranges from 12.5 km at a frequency of 85 GHz to about 150 km at 6.6 GHz. All microwave radiation is affected by many different characteristics of the Earth surface and atmosphere, but specific frequencies are affected more by some characteristics than by others (Figure 14). Thus, sea-surface temperatures have a predominant effect at the lower end of the spectrum, and oxygen strongly affects radiation in the 50 - 60 GHz band.

In contrast to a radar, which emits microwave energy and measures the reflected signal, a passive-microwave radiometer simply measures the natural emissions from the viewed surface and from the intervening atmosphere. As with a radar, measurements can be made through a cloud cover and in darkness. Satellite passive-microwave data have been obtained almost continuously since 1972 by a series of NASA spacecraft. The earlier data (from the Electrically Scanning Microwave Radiometer - ESMR) were at a single frequency, 19.35 GHz, but they nevertheless provided a wealth of information on sea-ice cover in both polar regions, which has been published in atlas form (Zwally et al., 1983a; Parkinson et al., 1987). In 1978, Nimbus-7 was launched carrying a Scanning Multichannel Microwave Radiometer (SMMR), which obtained measurements at

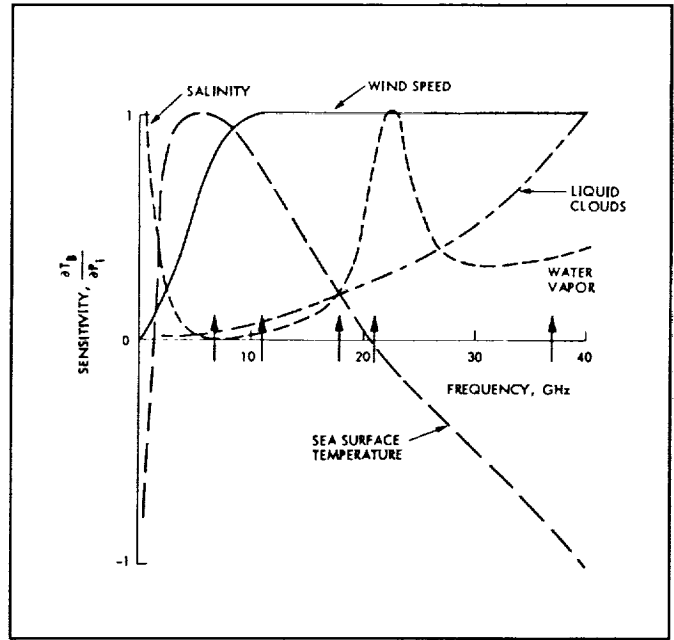


Figure 14. Schematic normalized sensitivity of microwave brightness temperature ( $T_b$ ) to various geophysical parameters ( $P_i$ ) as a function of frequency. Dark arrows indicate SMMR frequencies. [Wilheit et al., 1980.]

both horizontal and vertical polarizations for five frequencies: 6.63; 10.69; 18; 21; and 37 GHz. The two lower frequencies were used to estimate sea-surface temperatures and wind speed; the 21 GHz channels were used to measure atmospheric water content; and sea-ice information was derived from the 18 and 37 GHz channels. In contrast to the ESMR, which scanned the surface across the satellite track, the SMMR scanned the surface conically (Figure 13) so that all data were collected at a  $50^\circ$  angle of incidence.

The SMMR operated successfully until August, 1987. Data were collected continuously along a 780 km swath, with a spatial resolution ranging from approximately 30 km for the 37 GHz channels to 150 km for the 6.63 GHz channels.

Onboard recorders stored global data at latitudes less than  $84^\circ$ . Although, for most of the mission, the SMMR operated only on alternate days, this coverage has provided a unique insight into sea-ice behavior, and a sea-ice atlas summarizing the 9-year data set will be published in 1991 (Gloersen et al., In preparation).

The first of a new generation of passive-microwave radiometers, the Special Sensor Microwave/Imager (SSM/I), was launched in June, 1987 on a spacecraft of the Defense Meteorological Satellite Program (DMSP), thus providing an overlap of about a month with SMMR. Present plans call for continuous coverage by identical instruments at least into the mid 1990's. The SSM/I includes 19.35 and 37 GHz channels (primarily for monitoring sea-ice conditions), a 22.235 GHz channel for measuring atmospheric water, and 85.5 GHz channels for measuring rainfall over land. This also is a conically-scanning instrument, with an incidence angle of  $53^\circ$ . Spatial resolution ranges from 55 km for the 19.35 GHz channels to 12 km at 85.5 GHz. Both horizontally and vertically polarized data are acquired at all frequencies except 22.235 GHz, which is in vertical polarization only. Swath width is 1300 km, and almost total global coverage is obtained every day, except at latitudes higher than  $86^\circ$ .

Ice and liquid water have very distinct microwave emission signatures, primarily because of differences in the way molecules are arranged in each. Moreover, different ice samples can have distinct signatures, partly because of temperature differences and partly because of differences in

texture, the distribution of air bubbles, and impurity content. Snow density, grain size, surface roughness, brine content, and the degree of wetness all influence the radiated energy, and they influence it differently at different wavelengths. Thus, by detecting an appropriate suite of wavelengths, the ice cover can be distinguished from open water and classified according to its surface and near-surface properties.

Over sea ice, passive-microwave data distinguish water from ice and identify the major ice types: new ice, just a few cm thick; first-year ice, up to 2 m thick and generally snow covered; and old ice, that has survived at least one summer, has undergone deformation and cracking, and is of variable thickness with a comparatively hummocky surface. Old ice also has a lower salinity than younger ice, giving it a distinctive microwave signature. Because it is less saline (and therefore harder) than new ice and generally thicker, it represents a significantly greater hazard to shipping. In principle, relative concentrations of the different ice types can be estimated from passive-microwave data at appropriate frequencies. Major problems arise, however, during the summer months when liquid water on the surface significantly affects the microwave emissions.

During the first two years after launch of the SSM/I, the Navy and NASA supported intensive validation of both the instrument and the parameters derived from the acquired data.

Results from these efforts are being prepared for publication. They indicate that the SSM/I is significantly better calibrated than the SMMR, but that there are problems with geolocation of the acquired data which result in misplacement of image pixels by up to tens of kilometers. Part of the error in existing data can be corrected, and improvements have been implemented to the procedure for deriving geolocation which appear to have significantly reduced misplacement errors.

The passive-microwave measurements have been used extensively, both for research purposes and for operational applications, such as the compilation by the Navy/NOAA Joint Ice Center of weekly maps showing sea-ice conditions in both hemispheres. They provided the first total picture of sea-ice conditions, and revealed major features, such as the Weddell Polynya, which had previously been undetected. More recently, there have been detailed quantitative studies of various aspects of atmosphere/ice/ocean interaction, such as the effect of major weather systems on sea-ice formation and decay (Cavalieri and Parkinson, 1981), the balance of multiyear ice in the Arctic Ocean (Rothrock and Thomas, 1989), and the effects of ice formation in polynyas on ocean salinity and the formation of deep water (Gordon and Comiso, 1988; Martin and Cavalieri, 1989).

The existing long time series of passive-microwave data reveals significant interannual variability in sea-ice extent within any one region (Figure 15), but there is no clear

trend in the total ice cover of either the Arctic or Antarctic. However, the global maximum sea-ice extent, as derived from ESMR and SMMR measurements, shows a very clear decrease over the 15 years since observations began (Figure 16). Over the same period, the amount of open water within the pack appears also to have decreased (Gloersen and Campbell, 1988), but part of this apparent decrease could result from calibration drifts in the SMMR instrument (Gloersen et al., in preparation). The reason for the change in global ice extent is not apparent, but it may be associated with systematic changes in the relative timing of seasonal growth and decay of the sea-ice cover in the Arctic and Antarctic.

Examination of passive-microwave images of the Antarctic ice sheet reveals an intriguing similarity between some of the patterns of microwave brightness temperature and patterns of snow accumulation, and there have been attempts to explain this theoretically (Zwally, 1977), and to make use of the observations to deduce snow-accumulation over large areas of the ice sheet (Rotman et al., 1982). Many other parameters affect the microwave emissivity, and considerable research is required before we can confidently state whether such analysis is viable.

For seasonal snow on land, passive-microwave data have been used to distinguish snow extent and the water equivalent of dry snow (Figure 17). The microwave emissivity increases markedly with snow wetness, and it should be possible to use passive-microwave data to indicate the onset of melting and the total extent of summer melting on the ice sheets (Figure 18). Both of

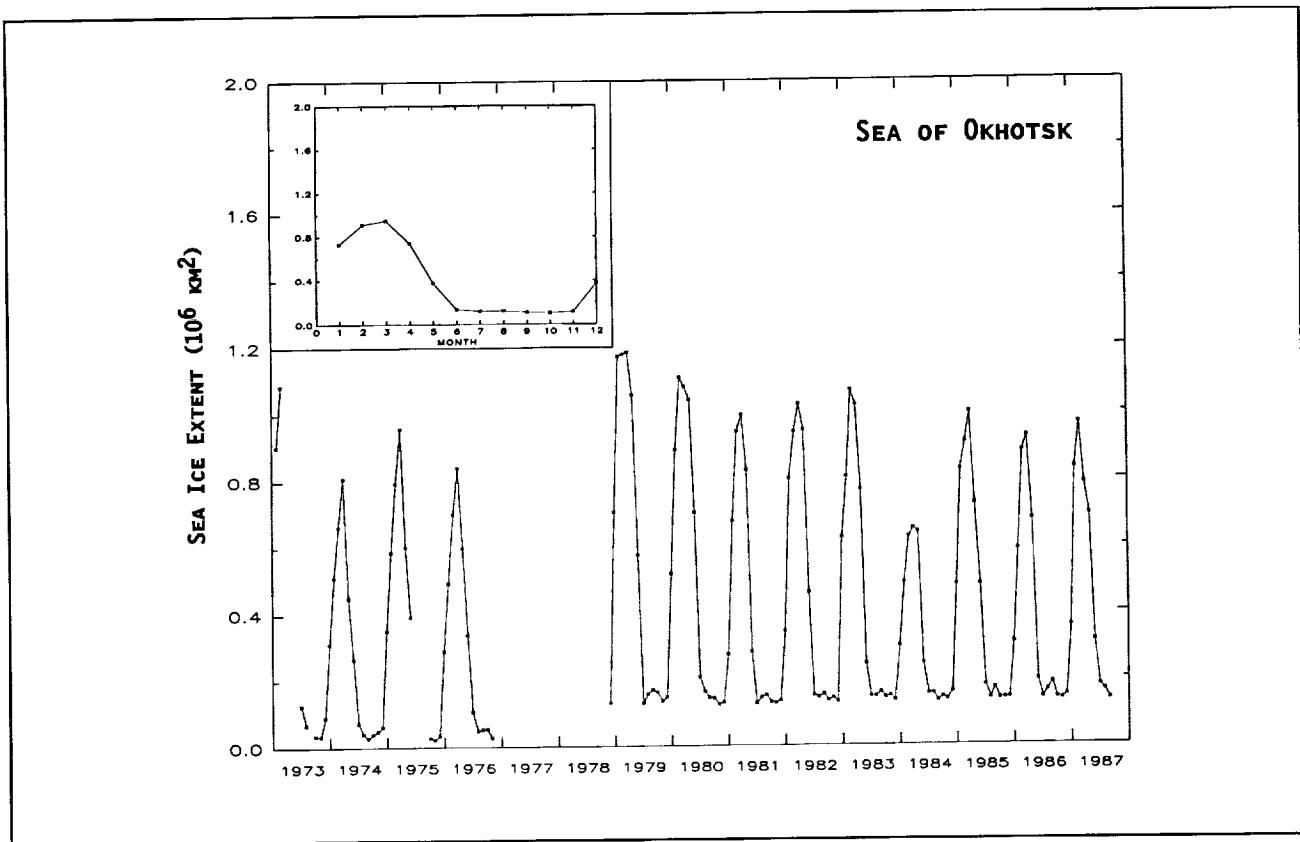


Figure 15. Time series of monthly-averaged sea-ice extents in the Sea of Okhotsk from ESMR and SMMR data (1973 - 1987). The inset shows the average seasonal cycle. In reality, the Sea of Okhotsk becomes totally ice free in summer, and the non-zero values of summer ice extent obtained from the passive-microwave data are caused by land contamination of pixels containing a mixture of land and open water. This problem is greater for SMMR data, with its larger pixels. [Parkinson and Cavalieri, 1989.]

these parameters are likely to be strongly affected by any significant climate change, particularly if it is enhanced at high latitudes. This is an area of research that has hitherto been neglected, and we strongly recommend that data from ESMR, SMMR, and SSM/I be analyzed to extract the melt-zone signal and to establish the foundation for a long time series of such information. This is particularly important over Greenland because climate models predict a major amplification in greenhouse warming at high northern latitudes.

Passive-microwave data over sea ice have been available since 1972, and much effort has

been devoted since then to developing algorithms for converting the data into useful estimates of sea-ice characteristics. Several groups from different countries have demonstrated that sea-ice conditions can be depicted remarkably well using these data. Indeed, it can be argued that, for much of the year, passive-microwave data give more reliable estimates of sea-ice extent and concentration than any other existing technique. Inevitably, traditional sea-ice scientists have been cautious to accept these estimates, particularly when they reveal conditions at variance with conventional observations. Because of the nature of

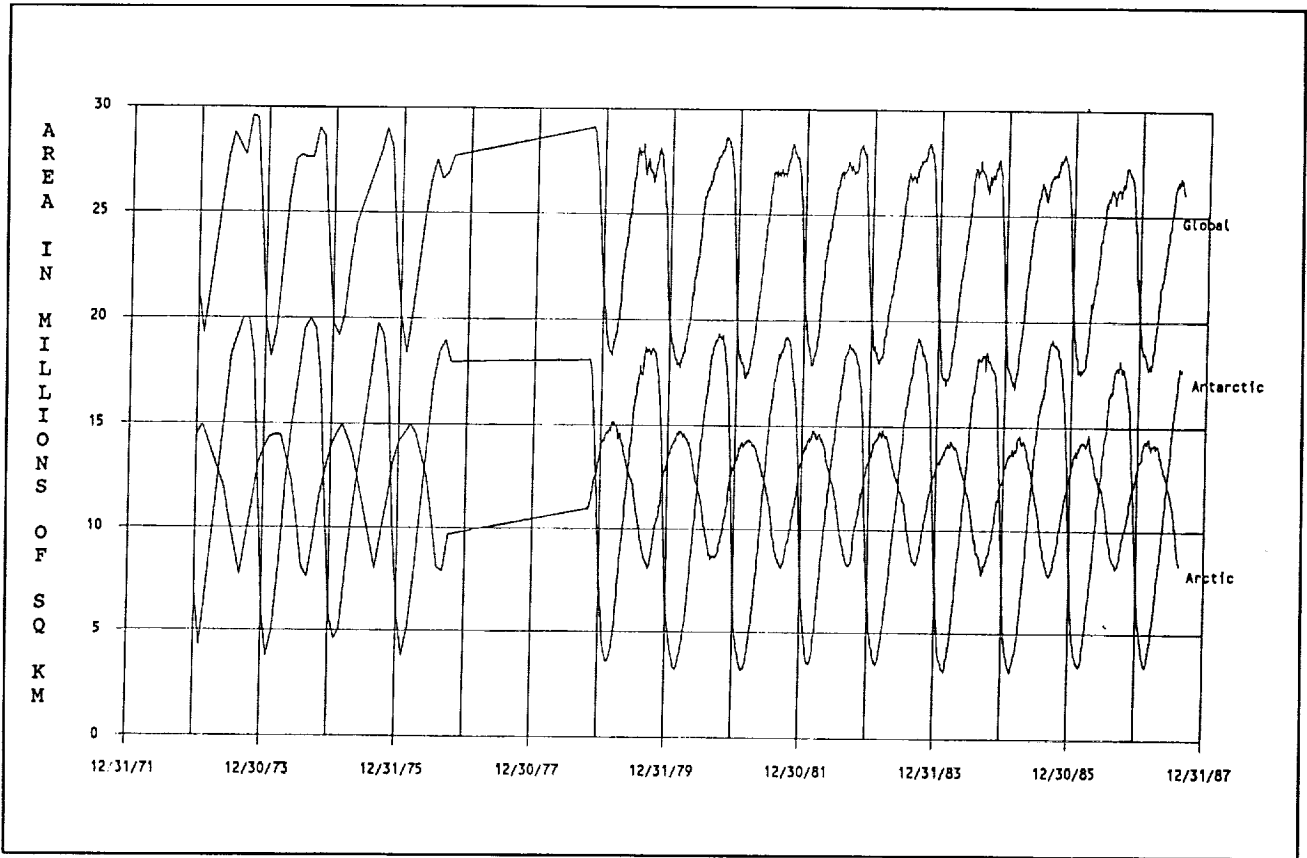


Figure 16. Sea-ice extent in the Arctic and the Antarctic, and their sum: the global ice extent. The area of ice extent shown is the area of ocean enclosed by the sea-ice boundaries as derived from ESMR and SMMR observations. The area of ocean actually covered by ice is always smaller because of the existence of open-water leads and polynyas. There was a hiatus in reliable satellite data during the two-year gap (1976 - 1978) in the time series. Ice extent is readily deduced from passive-microwave observations, and errors on the estimates given in the Figure should be quite small. Although there is little apparent trend in the ice extent of either polar region, the global maximum extent shows a consistent decrease over the entire period. This seems to be associated with a slight decrease in both Antarctic winter and Arctic summer ice extent, combined perhaps with a progressive shift in the relative phasing of the Arctic and Antarctic seasonal ice-extent curves. However, this apparent decreasing trend in global maximum ice extent deserves further investigation. [Gloersen and Campbell, 1988.]

the polar environment, it has been difficult to resolve this situation; *in situ* measurements are too localized, and the only effective validation of satellite passive-microwave data has been provided by other remotely-sensed data. Although this is probably a valid approach, not surprisingly, it has failed to convince the skeptics.

Preparation for SSM/I has, to some extent, forced a welcome convergence between algorithm experts and sea-ice scientists. Mechanisms are in place for intercomparison between the results of different algorithms and for comparison with independent observations. In particular, high-resolution Synthetic Aperture Radar and Landsat imagery, together with upward-looking sonar measurements from submarines beneath the ice

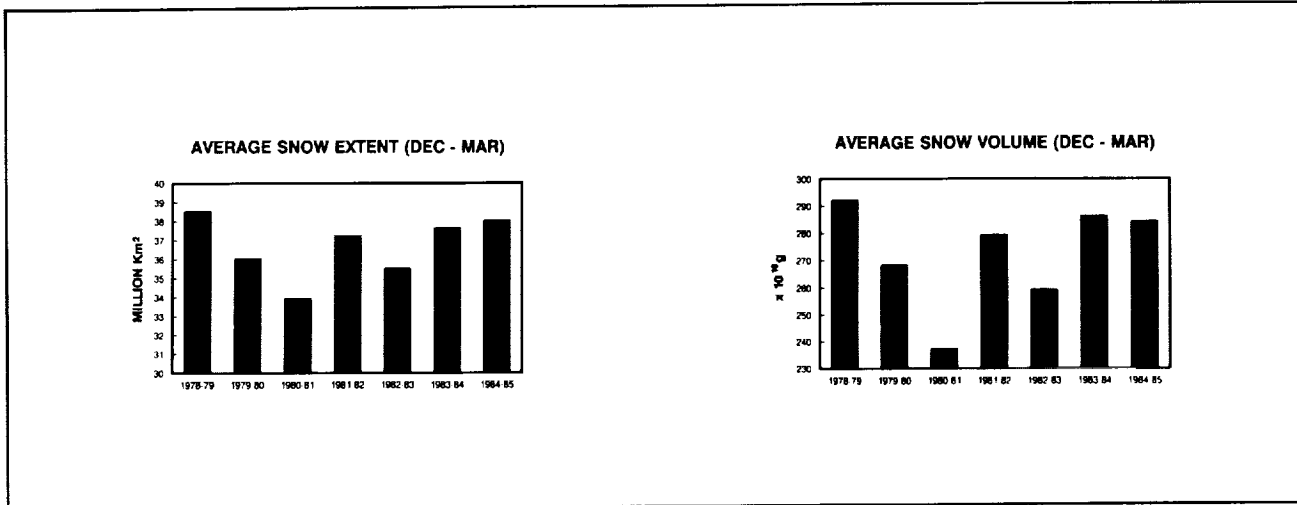


Figure 17. The extent and volume of seasonal snow in the northern hemisphere, as measured using SMMR data. [Hall, 1988.]

ORIGINAL PAGE IS  
OF POOR QUALITY

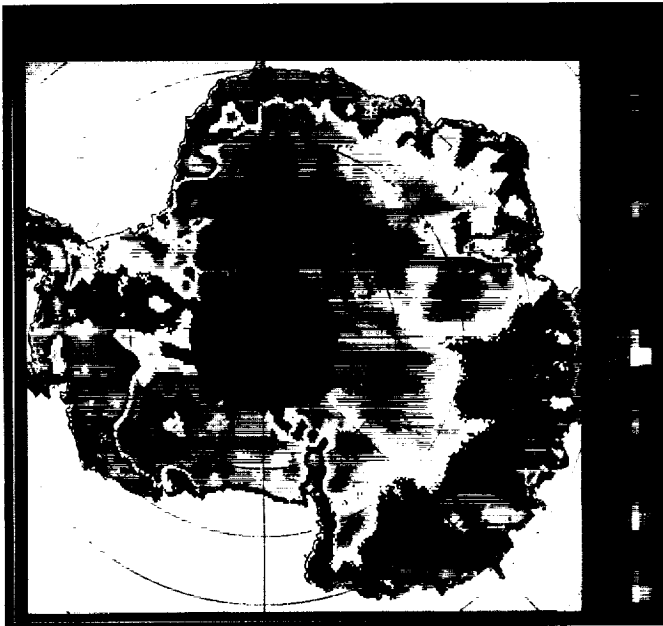


Figure 18. Regions of surface melting derived from passive-microwave measurements. This image shows the polarization ratio (PR) at 18 GHz (defined as the difference between vertically- and horizontally-polarized brightness temperatures divided by their sum) obtained from SMMR data taken over Antarctica in January, 1979. Small amounts of liquid water in the snow significantly reduce the PR, and the blue areas in this image are in locations likely to undergo summer melting. More research is needed before melt zones can confidently be delineated from passive-microwave data, but there is considerable promise in this approach. [Image provided by D. Cavalieri and K. Jezek.]

are being used to validate the airborne and satellite passive-microwave data (Figure 19). Moreover, close involvement of the research community in the validation of SSM/I data should lead to more widespread acceptance of this technique as a research tool. It is time now to use the products of the algorithms to learn more about the sea ice itself; sea-ice parameters derived from passive microwave data should become simply another data set to be used by any lay researcher along with more traditional measurements.

### 3.2.2 Medium-Resolution Visible and Infrared Sensors

Since 1972, instruments of this type have provided continuous coverage of the globe, primarily to monitor weather conditions. An earlier series of weather satellites, beginning in 1962, provided analogue images of clouds and the Earth surface, but data quality was poor. The later instruments are scanning

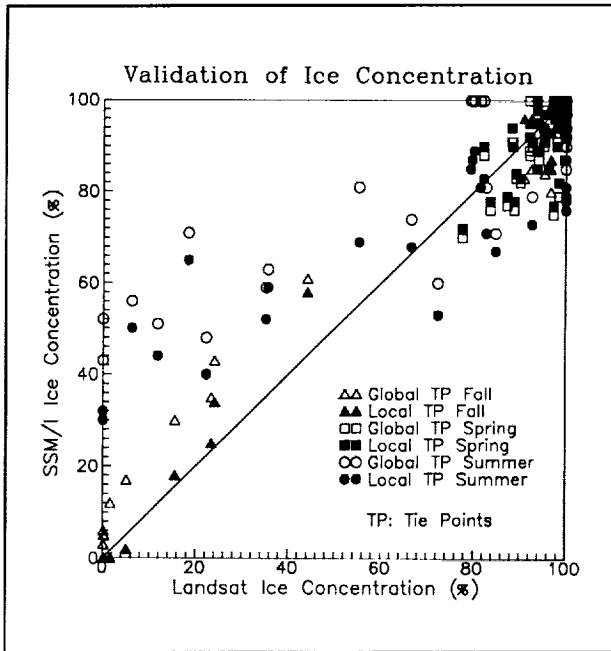


Figure 19. Comparison of ice concentrations derived from Landsat images with those derived from SSM/I data. The estimates from SSM/I data were calculated with an algorithm that utilizes "tie points" for the microwave brightness temperatures of open water, first-year ice, and multiyear ice. Significantly better agreement with the Landsat measurements results if local, rather than global, tie points are used. Nevertheless, there is still considerable room for improvement in the algorithm performance at low ice concentrations. [Steffen, in preparation.]

radiometers operating at several frequencies in the visible, near-infrared and infrared with a spatial resolution of approximately 1 km and a very wide swath. They operate in geostationary orbit and in sun-synchronous orbits.

### 3.2.2.1 Advanced Very High Resolution Radiometer (AVHRR)

These are mounted on the NOAA, polar-orbiting weather satellites, and they acquire information over a 2600 km swath width at five wavelength bands in the visible

(0.55 - 0.9 microns), near infrared (0.725 - 1.10 microns), infrared (3.55 - 3.93 microns), and thermal infrared (10.3 - 11.3 and 11.5 - 12.5 microns). Spatial resolution of real-time data, and of some of the data stored onboard, is 1.1 km at nadir. However, the global data set that is stored aboard the spacecraft for later dumping to ground receiving stations is degraded to a resolution of 4 km. Generally, there are two NOAA polar-orbiting satellites, one overflying at 7:30 am and 7:30 pm local time, and the other overflying at 1:30 am and 1:30 pm. Each provides daily coverage of the entire globe, and far more frequent coverage at high latitudes. Similar data have been acquired continuously since 1972.

AVHRR data are used by NOAA primarily to provide estimates of cloud cover, sea-surface temperatures, seasonal snow cover, and a vegetation-classification index. The Navy/NOAA Joint Ice Center (JIC) also uses these data to compile routine reports of sea-ice conditions in both polar regions. Other derived sea-ice products are extensively produced and used by industry, but these generally are not available to other users. For polar research, AVHRR data have been used to investigate cloud conditions, sea-ice cover, and surface albedo, and to classify Arctic vegetation. As a result of a cooperative effort between NOAA, USGS and the UK National Remote Sensing Centre, a mosaic has been compiled of Antarctica using the higher-resolution AVHRR data (Frontispiece).

Currently, estimates of surface temperature on sea ice and the polar ice sheets are based on

measurements at the few meteorological stations and data buoys, and on 10-meter temperatures acquired in shallow bore holes in the ice sheets, which provide a good indication of the average annual air temperature at the bore-hole site. Analysis of satellite thermal infrared data gives results that are broadly consistent with the surface observations (Figure 20), but they have not been rigorously validated (Orheim and Lucchitta, 1987). This is another area that needs a considerable research effort, to develop techniques for filtering out data from cloud-covered areas, to investigate possible regional and seasonal variations in thermal emissivity, and to compare derived ice-surface temperatures with those obtained at nearby stations and drifting buoys.

Discrimination of clouds from snow is difficult, particularly when the cloud-tops are warmer than the snow. Measurements of radiation at 1.6 microns can help resolve this problem. This channel will be included in future AVHRR instruments and in the Along Track Scanning Radiometer (ATSR) aboard ERS-1, which also will be better calibrated than earlier thermal-infrared radiometers.

### 3.2.2.2 Optical Line Scanner (OLS)

Data similar to those acquired by the AVHRR are obtained by the Optical Line Scanner (OLS) aboard Defense Meteorological Satellite Program (DMSP) spacecraft. There are generally two of these spacecraft, also in sun-synchronous orbits, overflying at 6.00 am and pm, and at 12 am and pm. The OLS operates in two broad bands

(visible and near infrared at 0.4 - 1.1 microns, and thermal infrared at 8 - 13 microns), with a swath width of 3012 km and maximum spatial resolution at nadir of 600 m, which is significantly better than the AVHRR. This provides greater detail in, for instance, mapping open-water leads in sea ice, but the poor spectral resolution (two bands compared with five on AVHRR) is not well suited to land applications such as mapping vegetation types.

### 3.2.2.3 Earth Radiation Budget Experiment (ERBE)

Over times on the order of years, absorbed solar energy is approximately in balance with energy emitted by the Earth and its atmosphere. On shorter time scales and over smaller regions than the entire globe, there are imbalances between absorbed and emitted energy that drive both atmospheric and oceanic circulation systems. This state of overall energy balance and inter-regional energy distribution determines our global climate. Because of close ties between energy balance and many aspects of the climate, measurements of radiation budget are used to help develop and validate numerical models of the atmosphere-ocean system. Moreover, they are needed to detect periodic changes or secular trends in any of the components of the earth radiation budget.

The measurements necessary to estimate the earth radiation budget can be obtained only from satellites, and attempts have been

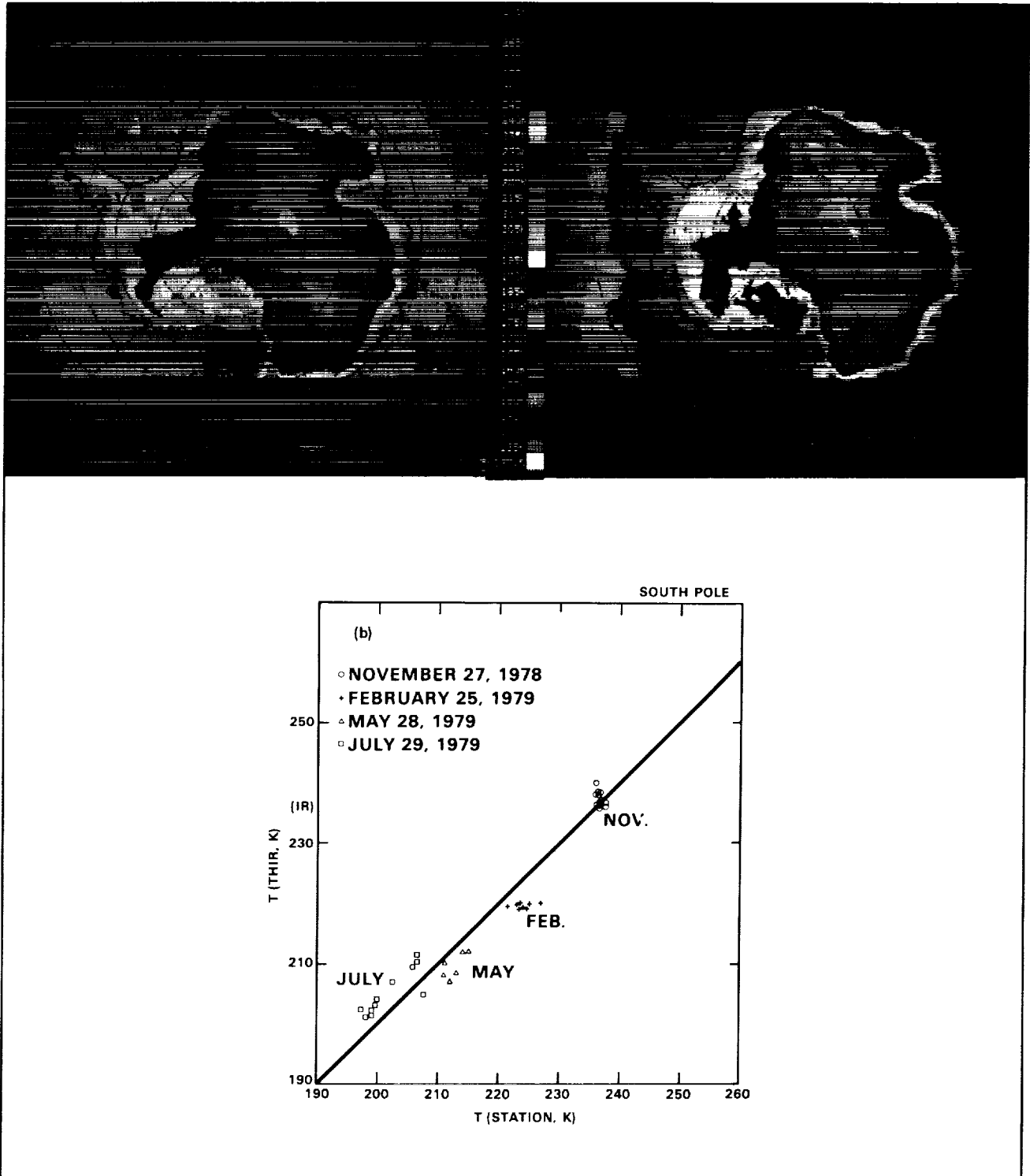


Figure 20. Average surface temperature ( $^{\circ}$ Kelvin) over Antarctica for January (left) and August (right) 1979. These estimates were derived by J. Comiso (personal communication) from satellite thermal infrared data. The lower plot provides a comparison between the satellite-derived estimates and surface measurements at the South Pole. [Comiso, 1983.]

made to achieve this goal since the beginning of the satellite era. Notable amongst these were the Nimbus-7 ERB observations, starting in 1978 with some measurements still being acquired today. Three separate instruments, operating at a wide range of wavelengths, measure solar irradiance and earth radiation, at coarse resolution with a wide field of view (WFOV) radiometer and at high resolution with a narrow field of view (NFOV) radiometer. The NFOV radiometer failed after 20 months, but the other instruments are still operating. It took some years to solve problems associated with calibration of the instruments, but there is now a long-term data set on solar irradiance and earth radiation budget. Reprocessing of data from an earlier instrument aboard Nimbus-6 could extend this data set back to 1975.

The solar irradiance measurements reveal both short-term variations caused, for instance, by sunspots, and a long-term downward trend which has not yet been explained. The WFOV measurements clearly show asymmetry between northern and southern hemisphere tropical radiation budgets after the 1982-1983 El Niño, and the effects of an aerosol cloud in the Arctic resulting from eruption of El Chichon. The NFOV data provide detailed regional information on radiation flux at the top of the atmosphere.

Results from the Nimbus instruments showed that rigorous attention must be paid to error reduction in the instruments, their calibration, and data-processing techniques. Moreover, they showed that a single satellite cannot provide enough data to unravel the effects of synoptic,

seasonal, and diurnal variability. Consequently, the ERBE comprises three satellites, each carrying scanning and non-scanning radiometers. The non-scanning instrument package contains a solar monitor which periodically measures total radiation from the sun for calibration purposes, and four earth-looking radiometers providing WFOV and medium field of view (MFOV) measurements of total radiation and of short-wave radiation. The WFOV radiometers view the entire Earth disc, from one limb to the other, with a radius of about 3000 km, and the MFOV has a footprint of about 1000 km. The scanning instrument package has three radiometers to measure total, short-wave and long-wave radiation at a spatial resolution of 35-60 km, depending on location within the 2500 km swath.

Identical sets of ERBE instruments were launched aboard the Earth Radiation Budget Satellite in October, 1984, and aboard the weather satellites NOAA 9, in December, 1984 and NOAA 10, in September, 1986. Apart from the scanners, all the ERBE instruments are still operating. NASA has no plans for flying similar instruments until the Clouds and Earth's Radiant Energy System (CERES) aboard EOS in the late 1990's. Meanwhile, a French instrument, the SCARAB, will fly aboard a series of Russian METEOR spacecraft, starting in 1991.

### 3.2.2.4 Coastal Zone Color Scanner (CZCS)

Ocean color data were acquired by the CZCS aboard Nimbus 7 from 1978 to 1986, when the instrument failed after exceeding its design lifetime by some six years. These data have a spatial resolution at nadir of 800 m and swath width of 1600 km. The four visible bands (0.433 - 0.453; 0.51 - 0.53; 0.54 - 0.56; and 0.66 - 0.68 microns) and one near-infrared band (0.70 - 0.80 microns) were chosen specifically to observe ocean color and to discriminate land and clouds from the ocean; there was also a thermal-infrared band (10.5 - 12.5 microns) to provide coincident estimates of sea-surface temperature, but this performed poorly, and AVHRR data were used instead. Between 80% and 90% of the radiance received by the CZCS was backscattered from the atmosphere, and this must be removed from the received signal in order to measure ocean color. Consequently, one of the bands on the CZCS was chosen to provide atmospheric corrections. In order to avoid sun glint, the instrument could be tilted fore or aft away from the sun. Occasionally, it was tilted towards the sun to observe oil slicks on the ocean surface.

Primary biological productivity in the ocean results from one-celled plants, phytoplankton, converting nutrients into plant material by using sunlight with the help of chlorophyll. These plants thrive best in the upper few tens of meters of the ocean where there is sufficient sunlight for photosynthesis - the euphotic zone. Chlorophyll in the plants, and

backscatter from the plants themselves change the color of the ocean. Very productive waters appear blue-green or sometimes red in contrast with the deep blue, almost black color of very pure water. Consequently, accurate measurements of ocean color provide estimates of chlorophyll concentration within the surface water, which is closely correlated with the total chlorophyll in the euphotic zone. These estimates of chlorophyll can then be used to study biological productivity over large regions of the ocean. Comparison between the satellite estimates of chlorophyll and those obtained from ships show agreement within about 20%.

Few data were obtained by the CZCS from high latitudes, partly because of cloud cover and partly because of lack of demand. Comparison with *in situ* measurements suggests that data-processing techniques developed for lower latitudes can be applied in polar regions despite the low sun elevation. This lends credence to the estimates of very high chlorophyll values derived from both Arctic and Antarctic data (see covers). Unfortunately, persistent cloud cover in summer, particularly in the marginal ice zone where much of the productivity occurs, seriously limits measurements from space, and it may be necessary to use airborne sensors to complement satellite measurements in polar regions.

Satellite ocean color data have not been available since the failure of the CZCS in 1986. Based on experience with the CZCS data, an improved instrument has been proposed by NASA to be flown on a platform of opportunity. The

instrument, known as the Sea-viewing, Wide-Field-of-view Sensor (SeaWiFS) will have eight bands: 0.402 - 0.422; 433 - 0.453; 0.480 - 0.500; 0.510 - 0.530; 0.555 - 0.575; 0.655 - 0.675; 0.745 - 0.785; and 0.845 - 0.885 microns. The choice of frequencies will permit improved atmospheric corrections, and better instrument performance at high pigment concentrations. The swath width will be 2800 km to provide daily, global coverage at a spatial resolution of 4.5 km. Local area coverage will also be available with a spatial resolution at nadir of 1.13 km. There are tentative plans to launch SeaWiFS aboard a non-NASA platform in 1992/1993.

In the absence of SeaWiFS, the earliest approved mission for an ocean color sensor is the Japanese Advanced Earth Observation Satellite (ADEOS), which will be launched in 1995, carrying a high-resolution visible and infrared imager and an Ocean Color and Temperature Scanner (OCTS). The Moderate Resolution Imaging Spectrometer (MODIS) aboard NASA's Earth Observing System (EOS) will also provide global ocean-color data, but the earliest launch date for this instrument will be in 1998.

Ocean productivity is a fundamental component of the global carbon cycle, and periods of extremely high productivity at sea-ice margins, combined with downwelling associated with deep-water formation, make high-latitude oceans potential carbon sinks. The sustained hiatus in availability of satellite ocean-color data represents a major shortcoming in our attempts to address problems of global change.

### 3.2.3 High-Resolution Imagers

High-resolution data are currently obtained by Landsat-4 and Landsat-5 and by the French Systeme Probatoire d'Observation de la Terre (SPOT) satellite, both of which are operated as subsidized commercial enterprises. Multi-Spectral Scanner (MSS) data have been acquired since 1972, throughout the entire Landsat mission. They comprise four bands in the visible and near-infrared (0.5 - 0.6; 0.6 - 0.7; 0.7 - 0.8; and 0.8 - 1.1 microns), with a spatial resolution of 80 m. Later missions included a fifth, infrared band (10.4 - 12.6 microns) with spatial resolution of 240 m. Thematic Mapper (TM) data, with seven channels, (0.45 - 0.52; 0.52 - 0.6; 0.63 - 0.69; 0.76 - 0.9; 1.55 - 1.75; 2.08 - 2.35; 10.4 - 12.5 microns) have been acquired since 1983. Spatial resolution for the six visible, near-infrared, and infrared channels is 30 m, and that for the thermal infrared channel is 120 m. The swath width for both MSS and TM data is 185 km, and potential coverage extends to approximately 82.5° latitude.

The first of a long series of French SPOT missions was successfully launched in 1986. It obtains data similar to Landsat, but with some important differences. There are two modes: multi-spectral, with two visible bands (0.5 - 0.59 and 0.61 - 0.68 microns) and one near-infrared band (0.79 - 0.89 microns), having a spatial resolution of 20 m; and panchromatic, with one broad band (0.51 - 0.73 microns) at 10 m resolution. Both modes have

a swath width of 60 km. The SPOT orbit covers similar latitude limits to Landsat, but SPOT has an ability to view obliquely, extending coverage to about 85° latitude. This capability also permits stereo viewing from different spacecraft positions, and hence reconstruction of surface topography to an elevation accuracy of approximately 10 meters.

Opportunities to obtain high-resolution radar imagery of Antarctica will be offered in the early nineties by European and Japanese missions, each with the acronym ERS-1, and by the Canadian Radarsat. These spacecraft will carry synthetic aperture radars, which provide 20-30 m resolution radar images in all weather and lighting conditions. The Japanese ERS-1, generally abbreviated to JERS-1, and ADEOS will both carry high resolution visible and infrared instruments.

Important applications of high-resolution imagery to mapping, to glaciological interpretation and to geological reconnaissance have been well demonstrated, and images have also been used for sea-ice and iceberg investigations, vegetation mapping, habitat surveys, and blue-ice mapping for meteorite collection. Repeated surveys permit image comparison to detect changes due, for example, to ice motion, iceberg calving or changes in vegetation. For many of these applications, Landsat data are preferred because of the higher spectral resolution and broader swath width. In what follows, the term "HRV data" refers to any high-resolution visible or infrared imagery.

Accurate maps, particularly ones giving a pictorial indication of the terrain, are important for any research project. Their usefulness in planning and conducting field investigations, as well as in the interpretation of field measurements, cannot be overstated. Mapping from HRV images now involves sophisticated registration and mosaic techniques that minimize position errors and provide maps that are excellently suited to most research requirements. These can be produced at considerably less expense than conventional aerial photography. Both the MSS and the TM images are adequate for mapping, but clearly, the TM and SPOT data provide greater detail (Figure 21).

With the high resolution of HRV data, the image itself becomes a valuable data set for glaciological studies. The reader is referred to the superb collection of Antarctic images published by the USGS in the "Satellite image atlas of the world" (Edited by Williams and Ferrigno, 1989). In regions where other information is available, the image data can be combined with this information (e.g., surface deformation, velocity, ice thickness, surface winds and temperatures, optical leveling, etc.) to extend correlations to areas where there are no *in situ* data. HRV imagery also facilitates interpretation of other satellite data such as altimetry and SAR.

Recent work has clearly demonstrated the importance of the digital images. Enhancement of over-ice imagery has revealed the presence of surface features ranging from subtle undulations associated with ice flow over mountainous terrain to crevasses and melt-water lakes (Swithinbank and Lucchitta, 1986). Quite subtle topographic

relief on ice-sheet surfaces is readily discernable in images that were obtained with a low sun angle, and this information can be used to reconstruct relative surface topography, to delineate glacier catchment basins, and to identify ice stream-lines. US and European investigators are making extensive use of HRV images to map the Siple Coast region and the Filchner/Ronne ice shelf system in Antarctica, and to investigate a variety of glaciological aspects, including ice motion, tributary ice streams and glaciers, and areas of grounded ice within the ice shelf. This work is a major aid in the planning and interpretation of the field measurements.

Apparent stream-lines can be identified in the imagery almost entirely across the major ice shelves. Accurate mapping of these is particularly important because they can be compared with

independent measurements of ice velocity. Differences reveal non-steady-state conditions, and comparisons along a complete flow line provide an insight into past behavior of the ice-sheet/ice-shelf system. The images can also be used to investigate the albedo of the ice-sheet surface. The causes for variability in the albedo are not fully understood, but they are probably associated with factors such as surface melting or snow-grain size and orientation, indicative of local winds.

Comparison of sequential images of the same region provide information on changes that have occurred during the interim between imaging. These include ice motion, ice-shelf advance or retreat, iceberg calving, crevasse patterns, grounded regions within ice shelves, and extent of summer melting. This technique

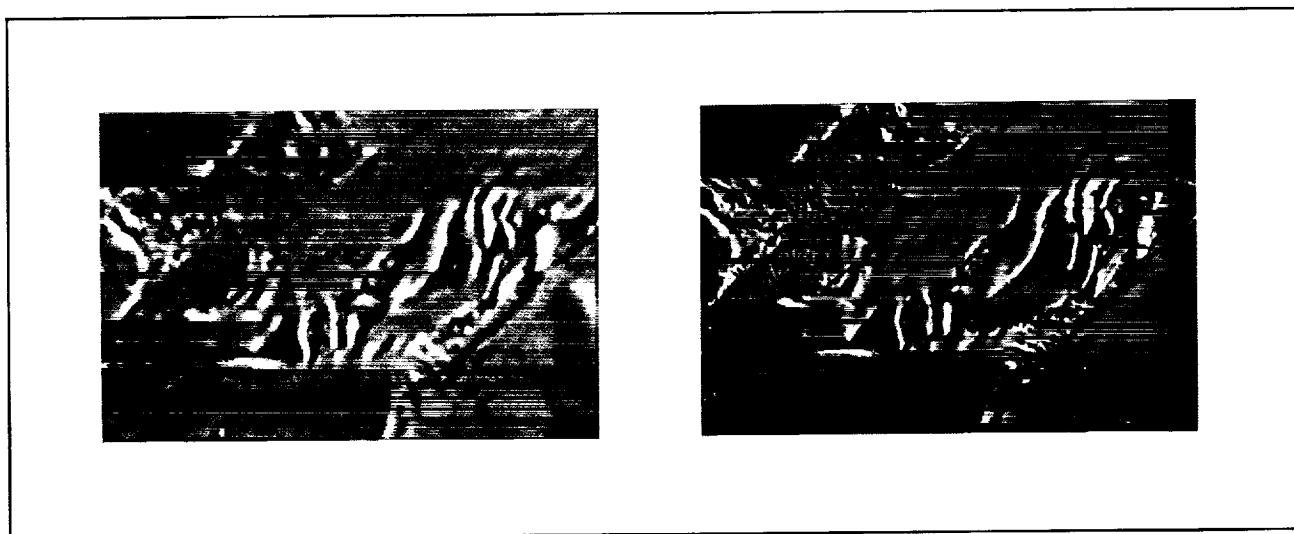


Figure 21. Comparison between Landsat MMS and TM imagery of part of the Jutulstraumen, Antarctica. The images cover a section, approximately 10 km wide, near the rift area at the eastern side of the ice stream. The improved resolution of the TM image (on the right) is readily apparent. [Orheim and Lucchitta, 1987.]

has been widely used to estimate glacier velocity by tracking the location of large crevasses in the images (Lucchitta and Ferguson, 1986). Results from a recent analysis of 14 Antarctic glaciers are shown in Figure 22.

In an attempt to make better use of Landsat coverage, NASA and the USGS are collaborating with other SCAR nations to complement the existing collection of images with new acquisitions (Ferrigno and Molnia, 1989). The resulting collection of images will enable compilation of maps depicting the various morphological features of overflowed parts of the ice sheets (latitudes lower than about 82.5°), and these will represent a particularly valuable resource for planning field investigations and for helping to interpret other data. However, the many images of Antarctica were collected over a period of about 15 years (Williams et al., 1984), and our next major goal should be to establish a long-term program of data acquisition that will provide almost simultaneous coverage of the large terrestrial ice sheets every decade. This would permit the systematic monitoring of changes in the areal extent and surface features of the ice sheets that will be needed by the Global Change Program. Images from SPOT and from the optical sensor aboard JERS-1 will complement those from Landsat, but systematic coverage of large areas is more easily achieved by Landsat, with its broader swath.

Over rock, HRV images provide excellent maps, their broad spatial coverage permits ready identification of large-scale structural

and morphological features, and there is a steady advance in our ability to extract geological information, particularly from TM data. Moreover, much of the geological reconnaissance in polar regions was done in a "broad-brush" manner, with only a very small percentage of rock area actually visited, and HRV data serve to fill in the gaps between visited sites. In addition, they are routinely used to identify blue ice areas on glaciers and ice sheets (Figure 23). These areas are likely to be very sensitive to climate change and, in Antarctica, they contain many meteorites exposed by sustained sublimation of the ice that once encased them. The next generation of USGS maps derived from HRV images will delineate areas of blue ice, which can be readily identified by their spectral signature. Biological applications include habitat surveys and identification and monitoring of vegetation units. HRV images can provide large-area surveys of vegetation types indicative of, for instance, permafrost or wet peatland (Figure 24).

Over the ocean, there has been extensive use of HRV images for numerous sea-ice studies, including detailed analysis of ice cover and motion (McNutt, 1981; Steffen, 1986), and validation of passive-microwave measurements of sea-ice concentration (Steffen, In Preparation).

### 3.2.4 Atmospheric Sounding

Not shown on the plot of atmospheric transmission in Figure 11 are many hundreds of narrow bands with high opacity, each characteristic of some specific molecule, such as methane or nitrous oxide. For each of these bands, the opacity

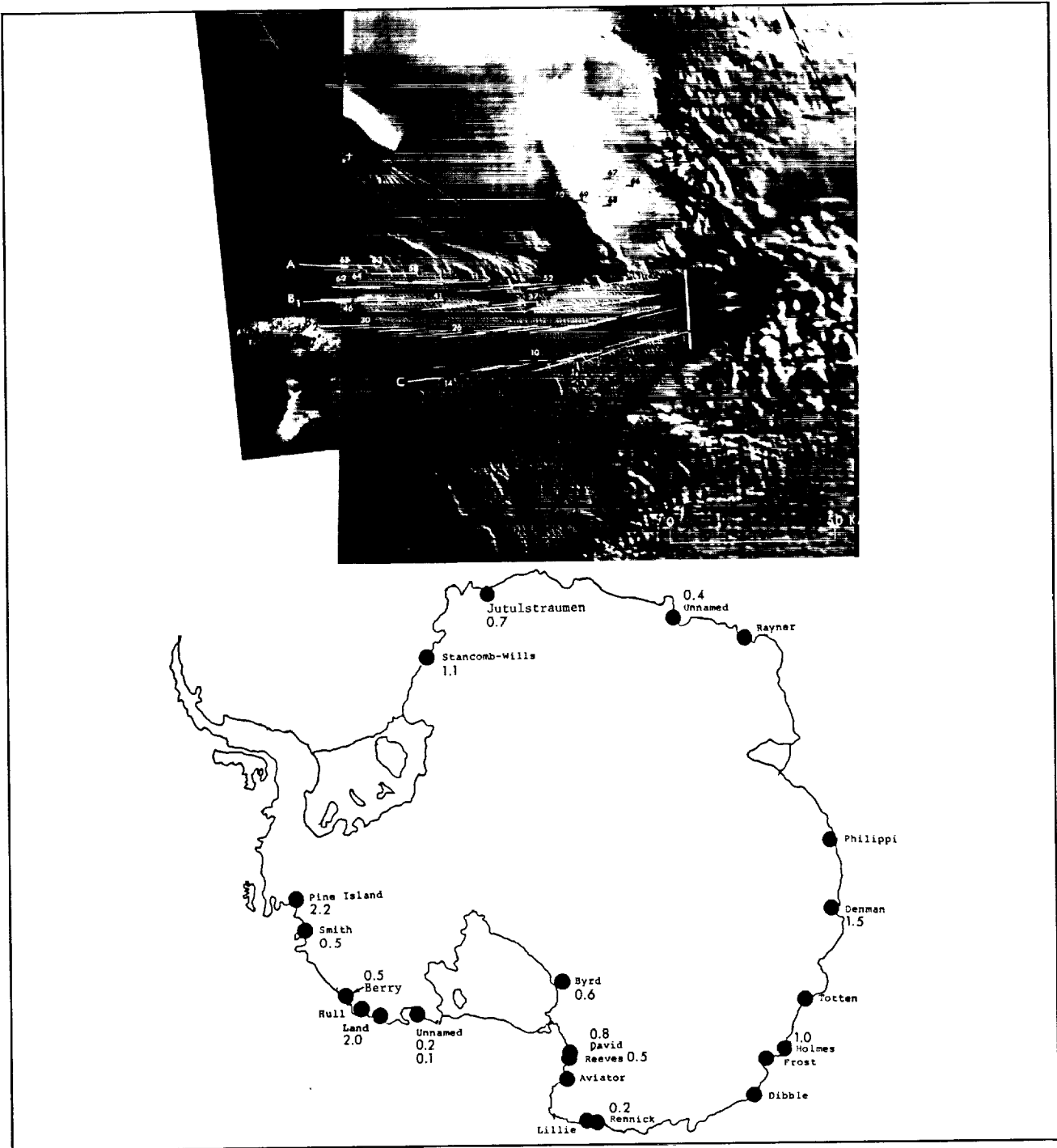


Figure 22. Antarctic outlet-glacier velocities obtained by comparing two sets of Landsat images. The map includes velocity estimates, indicated by the numbers in (km/yr) for some of the glaciers (Macdonald et al. In Press). The image depicts the Stancomb-Wills Glacier Tongue of the Brunt Ice Shelf, Weddell Sea. Movement vectors were obtained by tracing crevasse patterns on Landsat images acquired 12 years apart. Paper print copies of the images were optically matched under a stereoscope. The heavy white baseline is about 10 km west of the grounding line, and glacier movement is to the left. The velocities range from approximately 950 m/year, close to the baseline, to about 1.2 km/year 100 km downstream (Lucchitta et al., submitted). They show excellent agreement with a velocity of 1.3 km/year measured 30 km further downstream in the late 1960's (Thomas, 1973). [Provided by B. Lucchitta.]

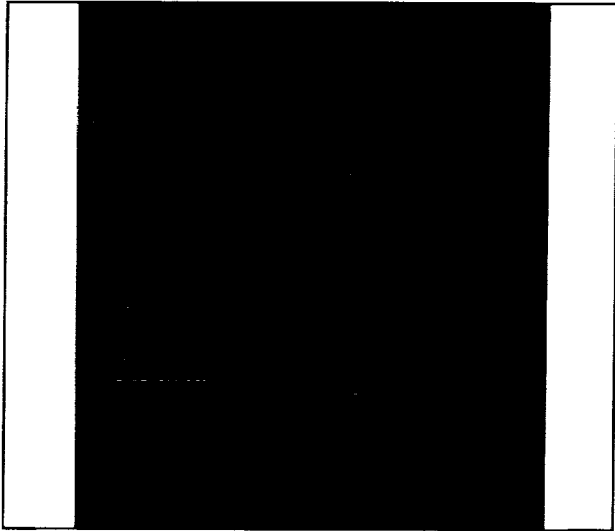


Figure 23. Changes in the area of bare ice on the Pasterze Glacier, Austria derived from Thematic Mapper data. [Hall et al., 1989.]

is affected by the temperature and the amount of the gas that is present, and by measuring the energy intensity at many selected frequencies it is possible to estimate the concentration in the atmosphere of, for instance, liquid water, water vapor, or individual trace gases.

The high-absorption band centered at 55 GHz in Figure 11 is caused by resonance of oxygen molecules, and within this band the precise resonant frequency is associated with a discrete range for the partial pressure of the oxygen, and the absorption at that frequency is determined mainly by the temperature of the oxygen within that pressure range. Thus, by sampling at several frequencies within the 55 GHz oxygen absorption band, temperatures can be estimated as a function of the partial pressure of the oxygen, and hence as a function of altitude. In this way, it is possible to obtain a coarse-resolution temperature/pressure plot for

the entire depth of the atmosphere. Moreover, by sounding the atmosphere nearly horizontally ("limb sounding") substantially improved sensitivity and vertical resolution can be achieved for estimates of the concentration of atmospheric constituents, such as ozone, in the upper atmosphere.

The Tiros Operational Vertical Sounder (TOVS) aboard NOAA weather satellites comprises infrared and microwave sounding units designed to provide temperature and water-vapor profiles of the atmosphere from the surface to 10 mb at a coarse spatial resolution. At high latitudes, the sounder data have not yet received much attention, but they are now under investigation as sources of information needed to evaluate the surface energy budget.

### 3.3 Active Instruments

Active sensors transmit pulses of energy and measure various characteristics of the reflected radiation. The synthetic aperture radar, scatterometer, and radar altimeter operate at microwave frequencies, and can therefore "see" the Earth surface in all weather conditions. The laser ranger, altimeter, and sounder operate in and near the visible range of frequencies, and are limited by cloud cover.

#### 3.3.1 Synthetic Aperture Radar (SAR)

The spatial resolution of a conventional radar is determined by radar frequency and antenna size. This imposes a practical limitation on the

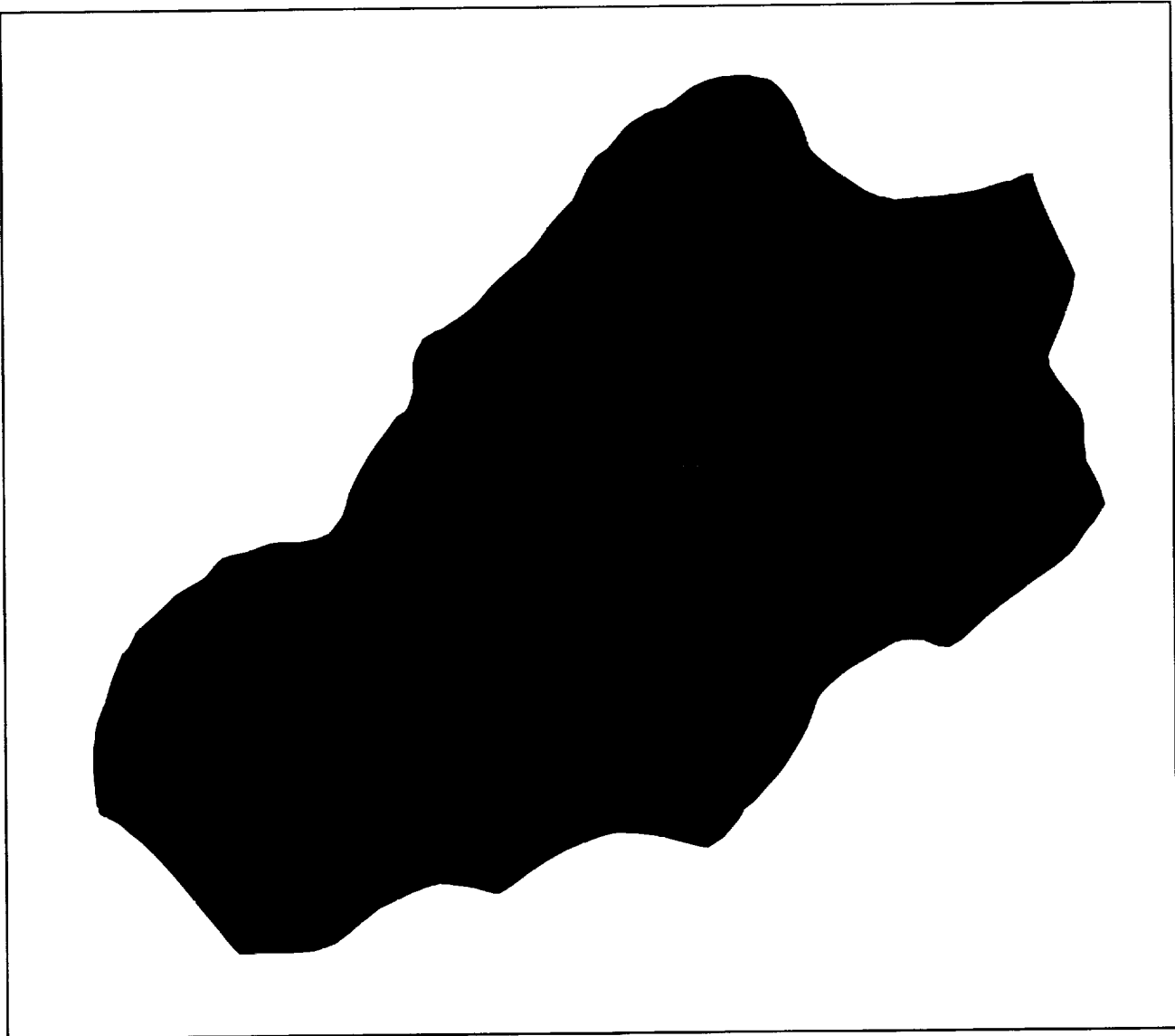


Figure 24. Permafrost zones from Landsat data. A region of boreal forest within the Yukon-Tanana Uplands of central Alaska. A classification using a Thematic Mapper (TM) thermal band and a TM-derived vegetation map indicates the distribution of three permafrost categories with an approximately 80% accuracy. Blue represents frozen ground; tan represents discontinuously frozen ground; and red represents unfrozen ground. [Morrisey et al., 1986.]

achievable resolution. The SAR overcomes this by illuminating a swath off to the side of the spacecraft and discriminating individual resolution cells according to their range and the Doppler shift in frequency of the reflected radiation caused by spacecraft motion. Spatial resolution is on the order of meters to tens of meters. Data are ac-

quired at extremely high rates (on the order of 100 Mbits/second), and they are transmitted immediately to ground receiving stations within view of the spacecraft. It is possible with existing technology to record some of the data onboard the satellite for later transmission, but appropriate recorders are not well proven in

space, and experience with existing recorders used to store slower data streams indicate that they frequently are the first components of a mission to fail.

In addition to providing high-resolution information at frequencies which complement those in the visible and infrared, SAR data have the major advantage of being unaffected by clouds or darkness. Moreover, radar wavelengths penetrate snow and ice to detect shallow subsurface features. Limitations include high power consumption, high data rate and complex data-processing techniques. In addition, swath width is generally narrow (75-100 km), but, by the mid 1990's, Radarsat will acquire coarser-resolution SAR data within a 500-km swath.

Extensive SAR coverage was first obtained by NASA's Seasat in 1978 but premature failure of the spacecraft's power system limited data acquisition to only 3 months. The Seasat SAR operated at L-band (1.275 GHz, or about 24 cm wavelength). A few images were obtained over Greenland, and none over Antarctica. Analysis of these data show that melt zones on the ice sheet can be identified along with melt features such as lakes and streams (Bindschadler et al., 1987). Extensive coverage of Arctic sea ice clearly demonstrated the great potential of SAR for both research and operational applications in ice-covered waters. Over recent years, techniques have been developed for rapidly extracting information on sea ice from SAR images. This includes estimates

of sea-ice concentration and type; ice motion from comparison of sequential images of the same area; and information on ocean waves near the marginal ice zone. Currently, SAR data obtained by aircraft are under investigation. In addition, there is strong interest in SAR applications over land, particularly to complement visible, near infrared, and infrared imagery.

The next opportunities for large-scale acquisition of SAR data at high latitudes will be provided by a C-band (5.3 GHz) SAR aboard the European Remote Sensing Satellite (ERS-1, to be launched early in 1991) and an L-band (1.275 GHz) SAR aboard the Japanese Earth resources Satellite (JERS-1, to be launched in 1992). Highest spatial resolution will be 8 m, but these will be noisy data, and nominal high resolution will be 30 m, with a swath width of 100 km. For ERS-1, data acquisition over polar regions will be limited to approximately 5-20 minutes per day (equivalent to an image strip 100 km wide and 2000-8000 km long), and these data must be acquired in real time by receiving stations at appropriate locations. Excellent Arctic coverage will be obtained by stations in Sweden, Scotland, Norway, Canada, and Alaska (Figure 25), with Sea of Okhotsk coverage available from a Japanese receiving station. Moreover, because a SAR views obliquely to the side of the spacecraft, the northward-looking ERS-1 will be capable of acquiring data between latitudes 85° N and 78° S. In the Antarctic, a Japanese station at Syowa (69° 39' S, 39° 35' E) to serve JERS-1, is being adapted also to receive ERS-1 SAR data, and there will be a German

station at the Chilean O'Higgins Station ( $63^{\circ} 19' S$ ,  $57^{\circ} 54' W$ ) on the northwest coast of the Antarctic Peninsula.

Potential SAR coverage by JERS-1 lies between approximately  $79^{\circ}$  South and  $84^{\circ}$  North. The major advantages offered by JERS-1 are the capability to store SAR data aboard the spacecraft (making it possible to acquire almost global coverage) and the complementary high-resolution visible and infrared data that will also be acquired. Although there will still be limitations imposed by power availability and tape-recorder capacity, JERS-1 could offer major opportunities for Antarctic research. The latitude limits of data acquisition will restrict this research to coastal regions and surrounding sea ice, but this is where prevalent cloud cover limits the use of optical sensors so that SAR will provide maximum benefit.

A third SAR mission, the Canadian Radarsat, has recently been approved for launch in 1995. It will operate at C-band, with a design lifetime of 5 years (compared to 2 years for ERS-1 and JERS-1). This instrument will represent a significant advance over the earlier ones in that both the look angle and the swath width will be adjustable. Swath width will vary between 55 km, with a spatial resolution of 8 m, and 500 km, with a spatial resolution of 100 m. The look angle will be adjustable between  $20^{\circ}$  and  $60^{\circ}$  from vertical, and there will be onboard data storage permitting almost total coverage of the globe. Antarctic coverage will be achieved by altering the spacecraft alignment so that the SAR looks south for a limited period. The Radarsat program will involve

collaboration between Canada, NOAA, and NASA, with NOAA providing data facilities and NASA providing the launch. Table 1 provides a summary of the three SAR missions.

NASA, in collaboration with the University of Alaska at Fairbanks (UAF), has installed a SAR receiving antenna at the Geophysical Institute at the university (Figure 26). A SAR processing system and a data archive and delivery system will handle initially approximately 10 minutes of SAR data per day, imaging almost half a million square km of the Earth's surface (Figure 27). NASA has memoranda of understanding which will permit acquisition of SAR data from ERS-1 and JERS-1 at the Alaska SAR Facility (ASF), and a similar MOU is being negotiated for acquisition of Radarsat data from both polar regions. However, because of limited onboard data storage, synoptic coverage of the Antarctic will require an additional receiving station at, or close to, McMurdo in the Ross Sea to complement the Japanese station at Syowa and the German station at O'Higgins (Figure 25).

A SAR produces high-resolution digital images with intensity proportional to radar backscatter. Correction for distortions induced by surface topography yields geocoded images with locations for each of the image pixels. These images can be used to supplement high-resolution visible and infrared images for many of the mapping purposes described in Section 3.2.3. Other applications include:

**Table 1**  
**SAR Missions**

		ERS-1*	J-ERS-1	RADARSAT
<i>SAR</i>	Frequency	C-band	L-Band	C-band
	Polarization	VV	HH	HH
	Swath	100 km	75 km	50 to 500 km
	Resolution/looks	30 m/4	30 m/4	30 m/4 - 100 m/8
	Incidence	23 degrees	35 degrees	20 - 50+ degrees
	Orientation	Right	Right	Right
	Onboard Storage	none	about 10 <sup>11</sup> bits	about 10 <sup>11</sup> bits
<i>Orbit</i>	Inclination	97.5 degrees	98.5 degrees	98.5 degrees
	Altitude	785 km	568 km	790 km
	Repeat	3 days and 35 days	41 days	13 days
	Type	sun-synchronous	sun-synchronous	sun-synchronous
<i>Mission</i>	Launch	5/1991	2/1992	1995
	Lifetime	2-3 years	2 years	5 years
	Status	Approved	Approved	Approved in Canada, int'l collaboration pending

\* *ERS-1 will be followed by a second, virtually identical, spacecraft (ERS-2), which will extend the European ERS mission well into the mid 1990's.*

- detailed surveillance of the ice-covered ocean including ice-floe sizes, open-water leads and polynyas, icebergs, sea-ice type and, from sequential imagery, sea-ice and iceberg motion;
- all-weather mapping of ice-sheet surface features (melt zones, melt pools, crevasses, undulations, etc.) and surface extent, and the detection of changes in any of these by comparing sequential images;
- proxy information about phenomena that affect fine-scale sea-surface roughness, such as winds, bathymetry, river discharge, and waves;
- topographic mapping on land and clear detection of structural features such as faults;

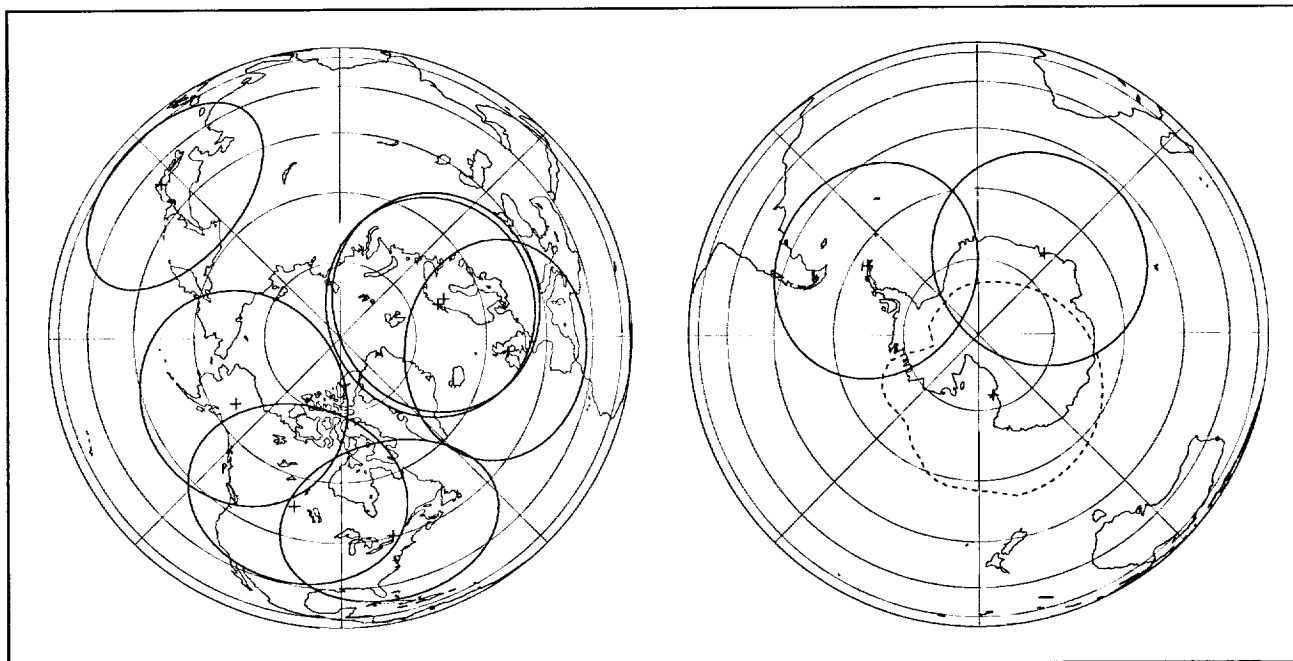


Figure 25. Arctic and Antarctic coverage provided by SAR receiving stations planned for ERS-1. Because of the satellite orbit and the instrument look angle, areas within approximately 400 km of the North Pole and 1300 km of the South Pole will not be covered by the ERS-1 and JERS-1 SARs. These regions will be imaged by Radarsat. Note, however, that there will be no receiving station in the Ross Sea sector of Antarctica during ERS-1 and JERS-1. The broken line depicts the station mask of a receiving station under consideration by the National Science Foundation for installation at McMurdo in time for Radarsat.

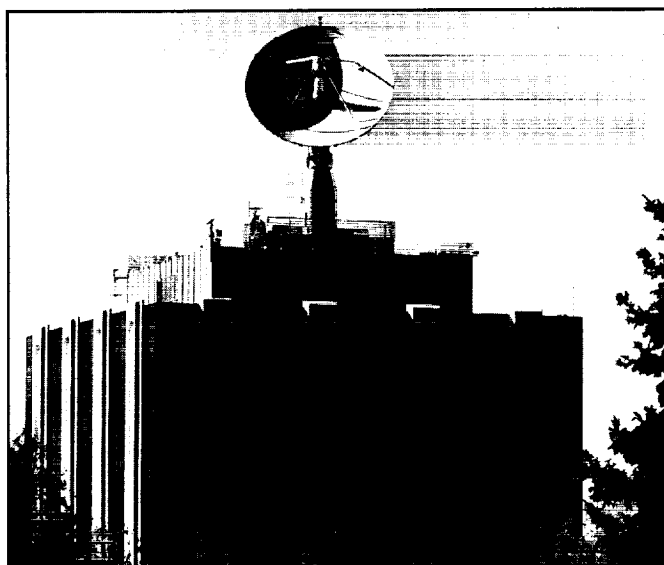


Figure 26. The SAR receiving antenna on the roof of the Geophysical Institute at the University of Alaska at Fairbanks. This antenna will receive data from three satellite SAR missions scheduled for launch during the early 1990's.

- in combination with high-resolution visible and infrared data, SAR can be used to classify surface rock and soil types, surface wetness, and vegetation.

Of these, the sea-ice applications are best understood, and efforts are underway to develop techniques for rapid extraction of sea-ice information from SAR imagery in readiness for both research and operational application of ERS-1 data. These techniques will be incorporated within a Geophysical Processing System (GPS), to be installed at the ASF, that will automatically calculate estimates of sea-ice concentration, ice type, and ice motion from selected SAR images (Figure 28). Similar

## Alaska SAR Facility Functional Block Diagram

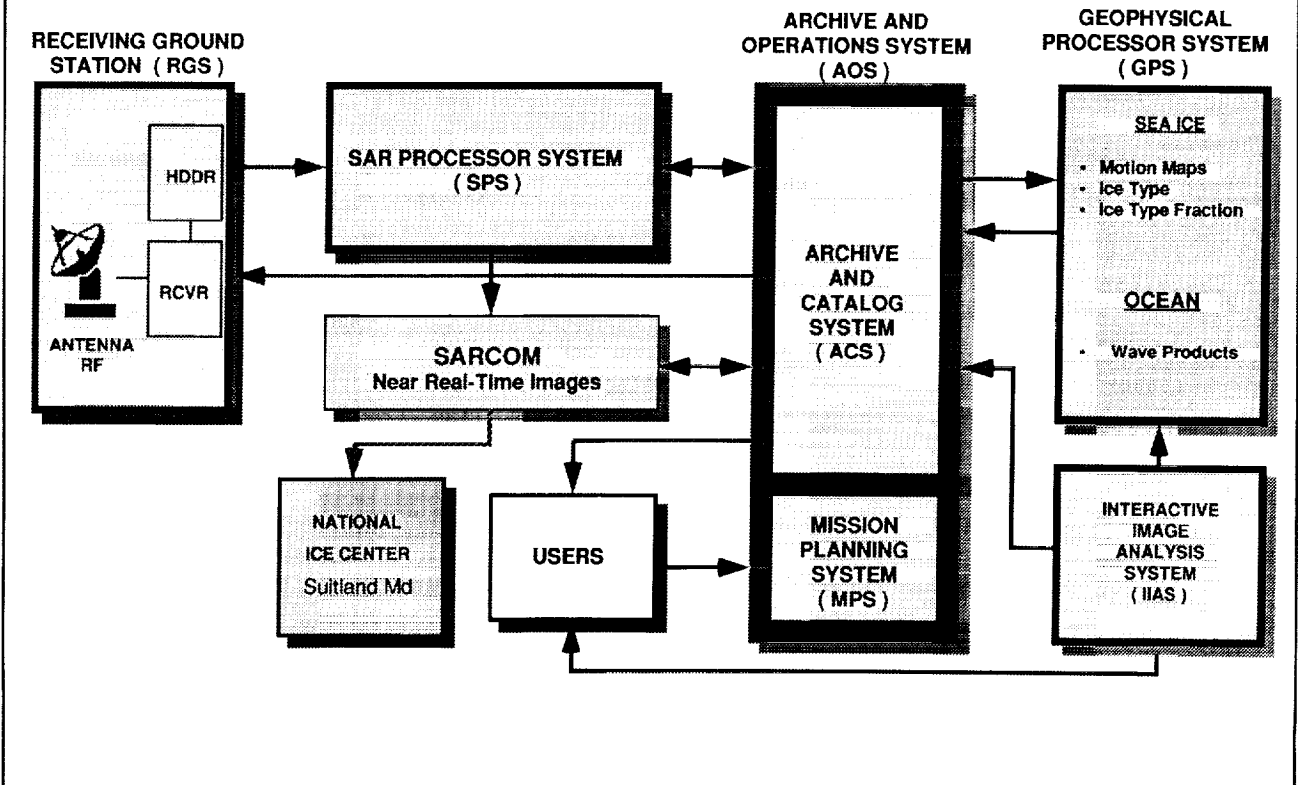


Figure 27. The Alaska SAR Facility, one of NASA's Distributed Active Archive Centers, where data will be received from the satellite, processed to SAR images, archived and distributed. In addition, geophysical parameters will be routinely derived from the SAR imagery on request by users.

techniques will be applied at the Joint Ice Center for operational applications.

Present estimates of the number and sizes of icebergs in the Southern Ocean and of their lifetime vary widely. It is important to improve these estimates because they provide an indirect assessment of the amount of ice discharged into the ocean, and long-term monitoring would reveal sustained increases in

ice discharge. Our first requirement is a baseline set of high-resolution imagery acquired within a short time period. Because of cloud cover and the costs associated with acquiring HRV images for such an effort, the most effective approach will be to use SAR imagery from the European and Japanese ERS-1 missions and the Canadian Radarsat.

Techniques have also been developed for producing digital mosaics of SAR images, and

these will assist in mapping applications. However, much work remains to be done on interpretation of the radar backscatter that is recorded by the SAR. At present, we can look at a SAR image of, say, a glacier and be impressed by the amount of information that the image apparently contains, but we cannot quantify that information.

### 3.3.2 Radar Altimeter

Satellite radar altimeters have flown aboard NASA's GEOS-3 (1975-1978) and Seasat (July - October, 1978), and the US Navy's Geosat (1985 - 1989). These instruments were designed to measure ranges to the ocean surface by transmitting short radar pulses and measuring the time delay until receipt of the reflected pulse. Pulse rate is approximately 1000 per second, and the altimeter attempts to follow the time delay of the half-power point on the leading edge of a composite return-pulse waveform formed by summing 50 consecutive received pulses. Summation takes account of range changes between consecutive pulses by correcting delay times for anticipated range change extrapolated from earlier measurements. In order to obtain high range resolution, return energy is measured only within a data acquisition window of about 190 nanosecond duration - equivalent to a range window extending 15 m above and below the measured surface. The altimeters work well over the oceans, where the return waveform generally has a fairly sharp rise and a slow decay (Figure 29) and measured range changes slowly. The precision of a range measurement, averaged from one second's data over the ocean, is on the order of 10 cm or less.

Although the altimeter illuminates a circle on the ocean surface with a radius of about 12 km (the beam-limited footprint), the area contributing to the return-pulse leading edge (the pulse-limited footprint), from which the range measurements are made, is only about 1 km in radius on a flat surface. Roughening of the surface, for instance by waves, increases the radius of the pulse-limited footprint to as much as 5 km, and it broadens the leading edge of the return-pulse waveform. This effect has two benefits: it ensures that the altimeter-derived range automatically averages the effects of waves; and it provides a means for measuring ocean-wave height from the width of the leading edge.

Over sea ice, the return pulse has a very sharp rise followed by a quite rapid fall, producing a spike, characteristic of a specular reflection (Figure 29). Although the altimeter tracking system was not designed to handle this type of return pulse, it follows the sea-ice surface remarkably well. However, there can be significant errors in the range measurement. Moreover, the Seasat and Geosat data records do not permit reconstruction of the 50-pulse composite waveforms, from which it would be possible to calculate the errors most accurately. Instead, the pulse shape preserved in the record was formed by summing two consecutive 50-pulse composites to provide a ten-per-second data rate. Significant errors in the onboard estimate of range rate over sea ice lead to appreciable broadening of these pulses, and even the formation of twin spikes in some pulses. Nevertheless, range measurements

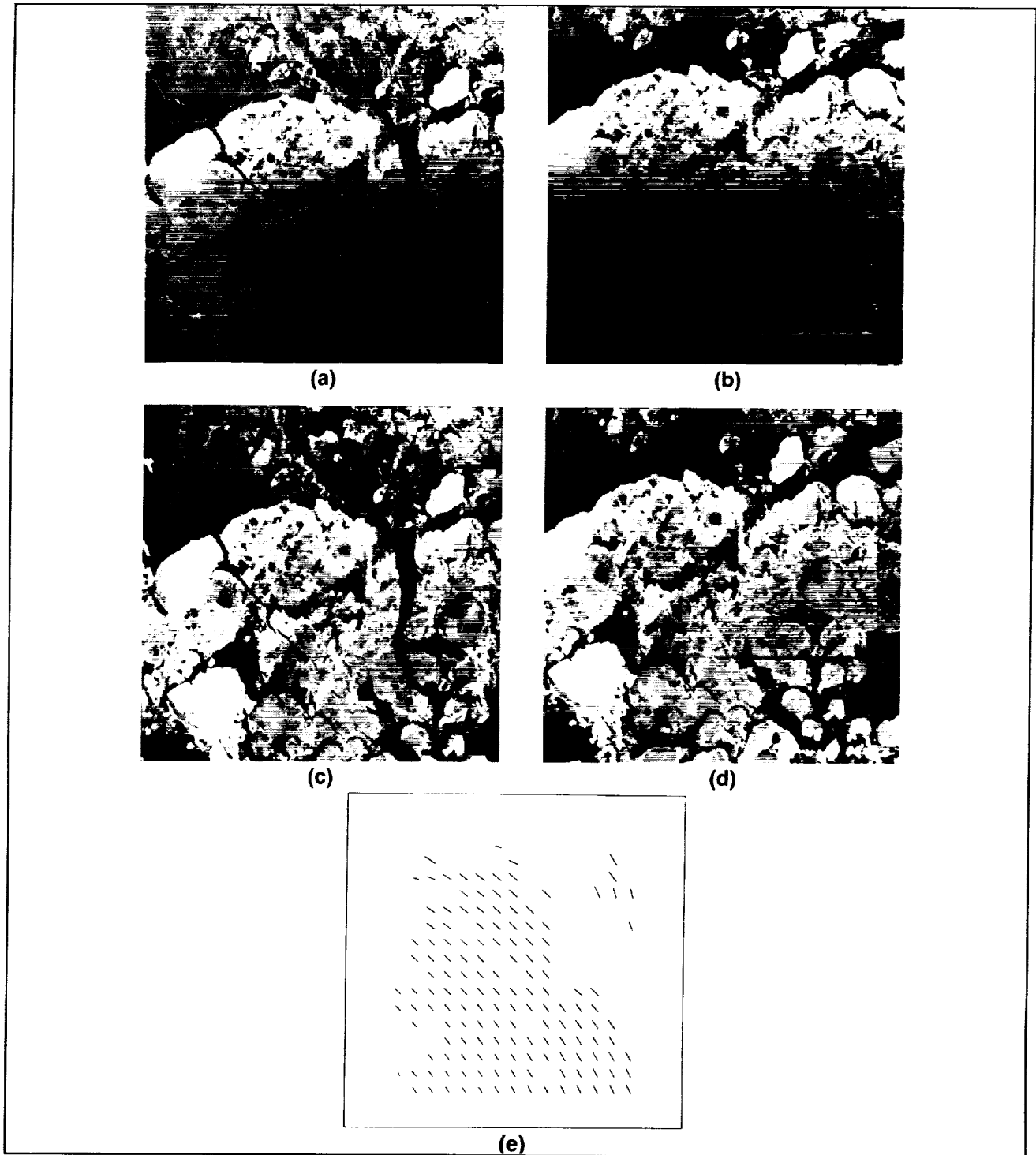


Figure 28. Geophysical products to be derived at the ASF from SAR images. The two Seasat L-band SAR images (a and b) are of the same region with a time separation of three days. In c and d, the images are automatically classified into three ice types based on the relative intensity of their backscatter: rough multiyear - brightest region; smooth multiyear - second brightest; and first year - dark. Automatic tracking of ice flows in the images gives the vectors (e) showing displacement of the ice in three days. The average motion of the sea ice within the images is approximately 2 km/day. [Provided by R. Kwok, JPL.]

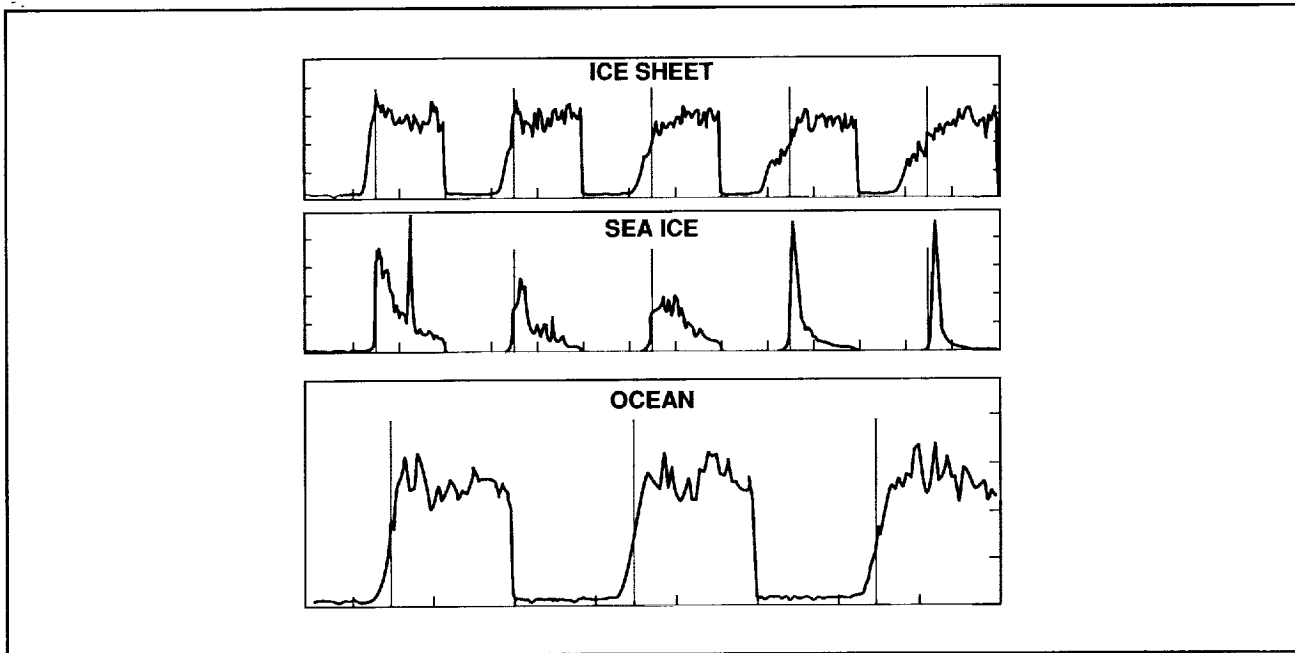


Figure 29. Radar-altimeter return waveforms from an ice-sheet surface, sea ice, and the ocean. The ice-sheet waveforms are quite similar to those from the ocean, but the sea-ice waveforms are very different and generally have a sharp spike signifying a near-specular reflection. The vertical lines mark the location on the waveform automatically "tracked" by the altimeter, and to which ranges are measured. Over the ocean, the automatic tracking is very effective, providing ranges to the average sea surface within the footprint, but over sea ice and the ice sheets, measured ranges are unreliable, and each waveform must be retracked. [After Zwally et al., 1987.]

over sea ice are significantly improved by retracking the data.

Over sloping or undulating terrain, such as the polar ice sheets, the servo-tracking circuit in the altimeter is not sufficiently agile to follow rapidly changing ranges, and the altimeter frequently loses track of the return pulse. In this respect, the more agile tracker of the Geosat altimeter represented a major improvement over Seasat, and it acquired more continuous records over the Greenland and Antarctic ice sheets. However, the altimeter-derived ranges in these records all have significant errors, and each return-pulse waveform must be retracked. This involves correcting each altimeter-derived range over ice for the offset between the altimeter tracking point and the actual half-power

point of the leading edge of the reflected-pulse waveform (Martin et al., 1983). Fortunately, most of these have a similar shape to pulses over the ocean (Figure 29) and, after retracking and other corrections have been applied for atmospheric effects, range precision for the ten-per-second data over smoother portions of the ice sheets is on the order of 30 cm, while over rougher portions it is more commonly on the order of a few meters.

Each corrected range is measured to the closest surface within the beam-limited footprint, with the effects of minor undulations (like sastrugi) averaged out. Consequently, over a sloping surface, the measured range is to

a point that is not directly beneath the spacecraft. Corrections for this slope-induced error can be applied where the slope is constant over large distances, but it is very difficult to correct for the effects of the large undulations that are commonly found on the polar ice sheets. This translates to an elevation error that can be on the order of many meters. Moreover, useful data cannot be acquired over slopes that exceed half the angular beam width of the radar antenna (i.e., slopes steeper than about 1:70). This restriction applies to approximately 10-15% of the Greenland and Antarctic ice sheets, and predominates in the coastal regions where ice velocities are highest, and scientific interest is most pronounced.

Application of radar-altimetry data to ice research involves reprocessing all the over-ice altimeter waveform composites. This has been done for all the Seasat data by NASA investigators (Zwally et al., 1983b), and the resulting corrected measurements of range between satellite and ice surface have been further corrected for orbit errors and reduced to ice-surface elevations with respect to both the Earth ellipsoid and the geoid (approximately sea level). The results have been published in atlas form (Bindschadler et al., 1989), and the corrected ranges and derived ice-surface elevations are available from NSIDC. Data from GEOS-3 are not sufficiently accurate to warrant reprocessing, but all the over-ice data from Geosat is being retracked. The resulting data set will provide the basic information necessary for many glaciological requirements,

such as delineating catchment basins, deducing flowlines, calculating ice-flow driving stresses, and setting boundary conditions for theoretical models, as well as for the production of accurate maps.

Altimetry measurements are obtained only from beneath the spacecraft, and the 10-per-second data rate provides estimates of surface elevation at intervals along the orbit track of approximately 700 m. Cross-track data density is determined by the separation of orbit tracks, and a particularly dense network of data was provided by the first 18 months of the Geosat mission when the satellite was in an orbit with a long repeat period (Figure 30). Unfortunately, coverage from both Geosat and Seasat extends only to 72° latitude, while GEOS-3 reached only to 65°. Nevertheless, the southern half of Greenland and much of the coastal portion of Antarctica are included. The accuracy of individual estimates of surface elevation is on the order of meters, and this is inadequate for detecting changes at a specific location. However, by comparing elevation differences at the many points where a set of satellite orbits cross those from an earlier time, it is possible to reduce significantly the effect of random errors.

A careful study (Lingle et al., 1990) of the extensive data set obtained during the first 18 months of the Geosat mission, indicates that errors are largely random, apart from the slope-induced error, which should remain almost constant at a given location on the ice sheet. Consequently, comparison of a very large number of crossing-point comparisons should provide an indication of the thickening/thinning rate of the ice sheet. Such

an analysis has been applied to the Greenland ice sheet (Figure 31), and indicates that the higher-elevation parts of the ice sheet south of 72° N, thickened by approximately 1.6 meters between 1978 and 1986 (Zwally et al., 1989; Zwally, 1989). Although this result has been questioned because of unknown orbit errors for the two satellites, the effects of these errors were minimized by comparing Seasat and Geosat data over the ocean near to Greenland. If this estimate of ice-sheet thickening is correct, then it has important ramifications, and a high priority should be given to continuing this type of systematic analysis, and to extending it to higher latitudes using data from ERS-1.

Lingle et al.'s (1990) error analysis indicates that radar-altimetry data may also be useful to detect elevation changes in the Greenland ablation area. Here, although errors of individual altimeter measurements can be very large (tens of meters), they appear to be independent, and therefore amenable to reduction by taking averages over sufficiently large areas.

There is a clear need to extend coverage nearer the poles, and this will be achieved by ERS-1, which will carry an altimeter in an orbit reaching 82° latitude. The ERS-1 altimeter is similar to those of Seasat and Geosat, but its tracking is different. In particular, there will be an option to implement an ice-tracking mode which will utilize a wider data-acquisition window in order to maintain track over steeper slopes. Inevitably, range accuracy in this mode will be poor. Over the flatter portions of the ice sheet, the precise

tracking mode will be implemented, and this should permit comparison between ERS-1 results and those from the earlier missions. One major improvement will be preservation in the ERS-1 data record of each 50-pulse composite, yielding a twenty-per-second data rate. This will improve the accuracy of retracked data, and facilitate extraction of additional information, such as sastrugi height and sea-ice characteristics, from the pulse shape.

The joint US/French mission - TOPEX/Poseidon - will carry a system for measuring ocean topography very accurately and for keeping track of relevant errors. It is scheduled for launch in 1992, but its orbit will reach only 66° latitude. Nevertheless, it will provide a highly accurate measurement of ocean-surface topography which will be used as a datum with which to upgrade the accuracy of altimetry measurements from ERS-1, including those at higher latitudes.

It should be stressed that these radar altimeters cannot acquire useful data over surface slopes larger than approximately one degree, and that the ice-sheet surface reconstructed from altimetry data represents a smoothed approximation to the actual surface. The effect of surface slope is to bias this envelope above the real surface, whereas the effect of radar penetration into the ice is to bias the envelope below the real surface. The quantitative effect of radar penetration on the measured range is poorly understood, but model studies (Jezek and Alley, 1988) and

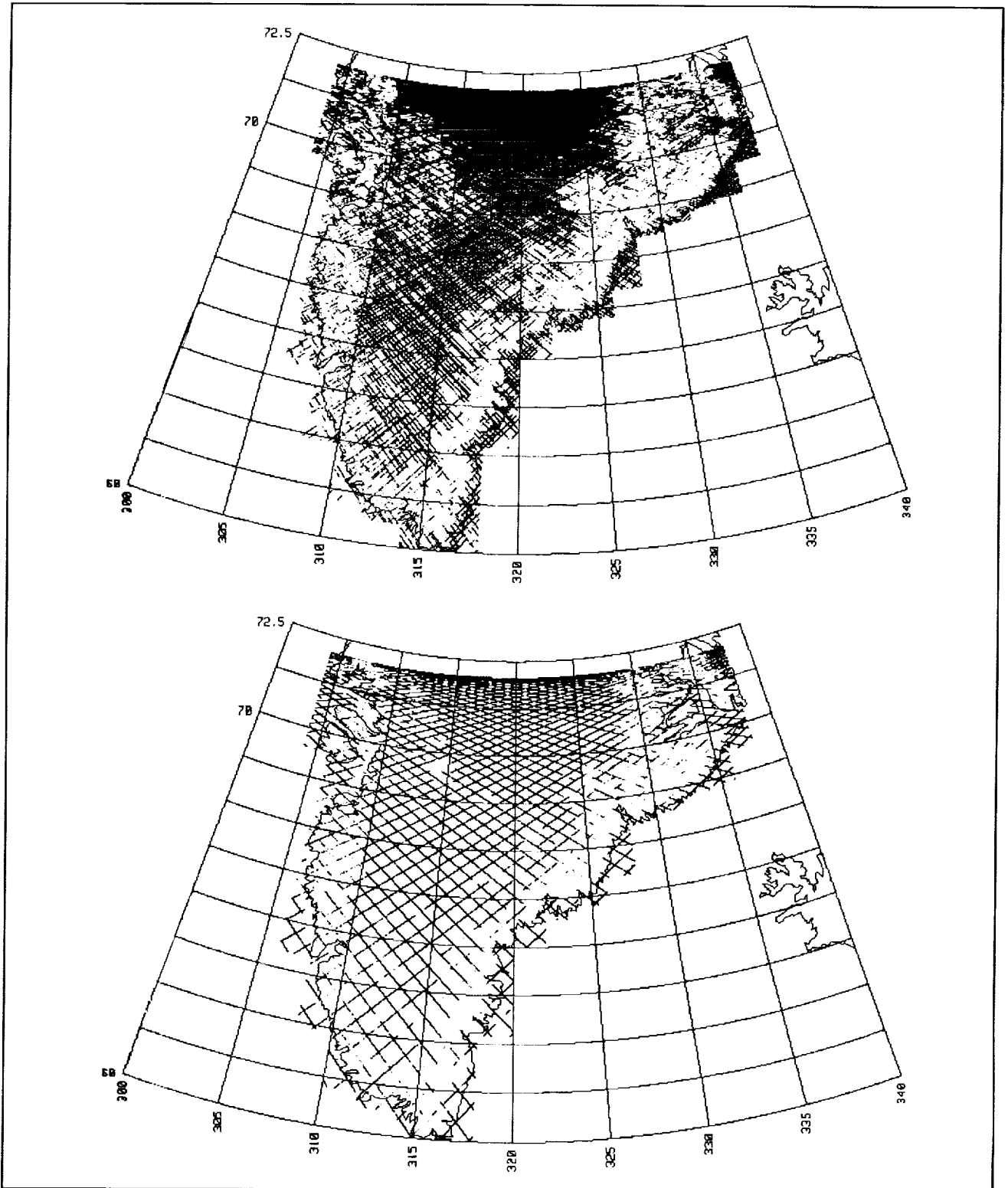


Figure 30. Ground tracks of the Navy's Geosat radar altimeter over the Greenland ice sheet. Each set of tracks refers to a 3-month period (top) when the satellite was in a long repeat orbit and (bottom) when the satellite was in a 17-day repeat orbit. Discontinuities in the tracks represent locations where the altimeter lost track of the reflected signal because of too much smearing of the return pulse by sloping terrain or excessively rapid variations in the range to the ice surface. The extremely dense coverage in the top figure is a result of the long time interval between repeating satellite orbit tracks compared to the 17-day repeat orbit shown in the lower figure. [Zwally et al., 1987.]

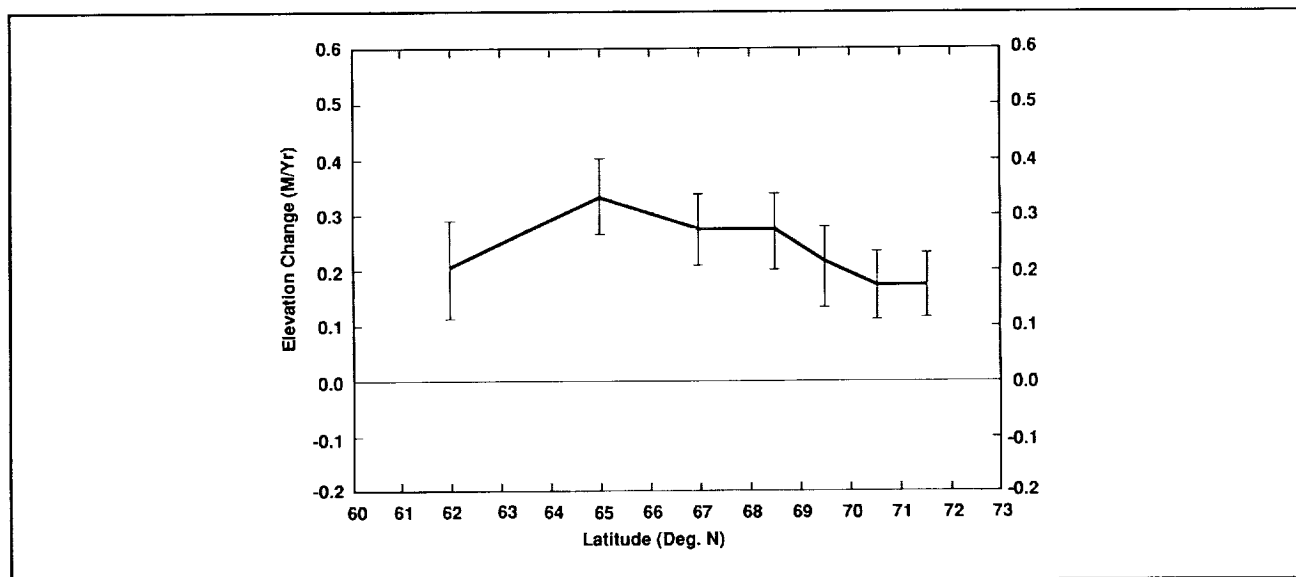


Figure 31. Greenland ice sheet surface-elevation change derived from comparison of Geosat and Seasat radar-altimetry data. The rate of thickening of the ice sheet is plotted against latitude. The error bars are estimates of standard deviation, assuming the errors in each orbit-crossover comparison are independent. [After Zwally, 1989.]

analysis of altimeter pulse shapes over ice (Partington et al., 1989) suggest that it could be significant, and it certainly warrants further investigation. The bias and the degree of smoothing are determined by local surface slopes and by characteristics of the altimeter and its tracking system. It is important to understand this relationship in order to make effective use of the data, particularly if this involves intercomparison of data from different instruments. Nevertheless, satellite radar altimeters provide the best available means of mapping ice sheet topography over vast areas of Greenland and Antarctica.

Other potential applications in high latitudes include:

- measurements of ocean-surface topography, winds, and wave height for which the altimeters were designed (see, for instance, Wunsch, 1981; Chelton and McCabe, 1985);
- measurements of sea-ice surface elevation, from which can be deduced the local geoid and hence indications of seabed topography (Haxby et al., 1983);
- mapping ice-cliff margins of the Antarctic ice sheet, and the margins between sea ice and open water (Thomas et al., 1983; Laxon, 1989);
- investigating ice-surface characteristics such as sastrugi roughness and crevasse intensity (Partington et al., 1989).

### 3.3.3 Scatterometer

This instrument obtains coarse-resolution measurements of radar backscatter from the surface of the ocean. Prime application is the measurement of sea-surface wind vectors.

Over the ocean, radar backscatter is determined by small capillary waves generated by the wind. The orientation of these waves is determined by the wind direction, and the backscatter intensity is affected by the wave orientation with respect to the look angle of the scatterometer. Consequently, the wind scatterometer uses three antennae to measure backscatter intensity from three different look angles, providing sufficient information to estimate both wind speed and wind direction. Over ice, the data may usefully complement passive-microwave and SAR measurements, but interpretation is poorly understood.

Scatterometer measurement of ocean winds was demonstrated by the two-antenna instrument aboard Seasat, and the Active Microwave Instrument (AMI) aboard ERS-1 will be capable of operating alternately as a SAR or as a wind scatterometer. NASA is developing a wind scatterometer (NSCAT) for inclusion aboard the Japanese ADEOS mission, to be launched in 1995.

### 3.3.4 Lidar

Lidar techniques can be used in a variety of applications, including atmospheric sounding, measurement of wind profiles, precisely locating retro-reflectors on the Earth surface, and accurate measurement of surface elevation. The two latter applications have clear relevance to the study of ice sheets. It is very probable that a series of satellite radar altimeters will be capable of detecting elevation changes greater than a few tens of cm in

smooth, nearly horizontal areas of the ice sheets. However, it is certain that they will not detect similar changes in near-coastal, steeply sloping regions where we expect the most rapid changes to be occurring. A laser altimeter operates with a very narrow beam, so that its footprint on the ice-sheet surface is just a few tens of meters in diameter. Consequently, a laser measures ranges to more clearly-defined positions on the earth surface so long as both the satellite position and the laser pointing direction are accurately known. The net result is a greater ability to measure thickening/thinning rates. This means that changes averaged over large areas can be detected over shorter periods, and patterns of change can be discriminated at a far higher spatial resolution than with a radar altimeter.

The first satellite laser-altimeter mission will be the Mars Observatory Laser Altimeter (MOLA), to be launched in 1992. If this is successful, then by the mid 1990s the surface topography of Mars will be better mapped than many parts of the Earth. The earliest opportunity for satellite laser altimetry over the Earth's polar ice caps will be provided by the Geoscience Laser Ranging System (GLRS), planned for inclusion within the Earth Observing System (EOS). The earliest launch date for GLRS will be after the turn of the century. This instrument is designed to operate in two modes: as an altimeter; and as a ranging instrument. The altimeter mode will provide measurements of average surface elevation within footprints some tens of meters in diameter, spaced at intervals of a few hundred meters along track.

The prime application of these data will be to measure rates of ice-sheet thickening/thinning. In addition, the altimeter mode of GLRS will measure sea-ice surface roughness (from the shape of the return pulse) and cloud-top heights. The ranging mode is primarily for studies of crustal motion, but it will be applied over ice to measure ice strain rates over very large distances. Current specifications call for measurement of the relative position of retro-reflectors to an accuracy of millimeters to centimeters. Repeated measurements to targets planted in the surface of an ice sheet will provide accurate estimates of ice strain rate over distances of tens to hundreds of km, and over short time periods. A major issue for the glaciological community is development of suitable targets. They should be low-cost; they must be capable of remaining above the snow surface for many years (preferably more than a decade); and they need to be constructed in a way that minimizes snow and hoar-frost deposits on the retro-reflector. Development and testing of suitable targets should be started as soon as possible.

Pending launch of a satellite laser altimeter, there are plans for airborne laser-altimeter surveys of the Greenland Ice Sheet, with Global Positioning System (GPS) receivers aboard the aircraft, to provide the very accurate navigation required both to identify the ground track and to direct the aircraft as nearly as possible along repeat tracks. This would be a viable way of investigating the Greenland ablation zone or individual drainage basins of particular interest (Figure 32).

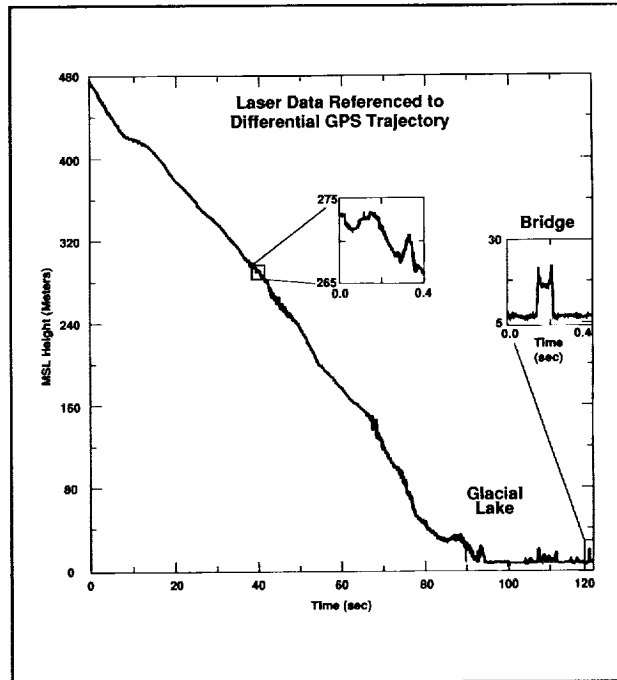


Figure 32. Airborne laser-altimetry measurements over Breidamerkurjokul Glacier in Iceland. The position of the airplane was fixed using Global Positioning System (GPS) receivers. A highly detailed, accurate surface-elevation profile of the entire glacier was obtained in less than two minutes of flight time. [Provided by W. Krabill, NASA Wallops Flight Facility.]

## 4. The Next Decade

A major long-term goal of polar research is realistic incorporation of high-latitude ocean and ice processes within predictive global climate models. This will require fulfillment of these objectives:

- understand the role of the polar oceans and their sea-ice cover in the transfer of heat and moisture between ocean and atmosphere, and the redistribution of heat from low to high latitudes;
- assess the importance of the polar regions in the global carbon cycle;
- identify and quantify the probable responses of the polar oceans, sea ice, terrestrial ice cover, permafrost, and vegetation to climate change.

Satellite observations provide the only means of making the large areal-coverage, synoptic measurements that will be needed, and in the next four sections we shall briefly review the elements of the research program necessary to address these problems. Each section will be necessarily brief, and more details are provided in reports, listed in the Bibliography, from national and international advisory groups, such as the Polar Research Board of the National Academy of Sciences.

### **4.1 The role of the polar oceans and their sea-ice cover in the transfer of heat and moisture between ocean and atmosphere, and the redistribution of heat from low to high latitudes.**

Research should focus on the marginal ice zone, and open water within the pack ice: energy, water, and salt fluxes within ice-covered areas; associated modification of ocean density structure; and processes of deep-water formation.

#### **4.1.1 Required Satellite Sensors**

SAR (for detailed estimates of ice concentration and ice type, identification of leads and polynyas, and for monitoring ice trajectories); passive microwave (to provide estimates of ice concentration and ice type); visible, near infrared, and thermal infrared (to provide surface temperatures and cloud cover); atmospheric sounding (to study interactions between the atmosphere and the ice and ocean); radar altimeter (to provide estimates of ocean eddy kinetic energy and ocean circulation); laser altimeter (to measure sea-ice surface roughness); laser atmospheric wind sounder (an EOS instrument that will measure near-surface winds over ice). Apart from the laser altimeter and wind sounder, these instruments will be operating over most of the next decade. Moreover, data systems are in place or under development to ensure delivery of useful derived products to investigators. The major requirement is for “critical mass” investigator groups capable of applying these data sets in an holistic way to multidiscipline problems.

### 4.1.2 Ancillary Measurements

Synoptic weather observations at manned stations and at a few automatic stations; buoys on the sea ice (measuring surface pressure, temperature, and buoy location, and at a subset of the buoys ocean temperatures, salinities, and currents); upward-looking sonar on sub-surface buoys moored to the ocean bed, and on submarines (to measure the temporal and spatial distribution of sea-ice thickness); a few intensive field campaigns to investigate processes of heat and mass flux from leads and polynyas, and processes of deep-water formation; chemical/isotope tracing of water masses; and bottom-moored temperature/salinity/current sensors in several critical locations for obtaining time series data.

Many of the necessary field investigations will take place over the next decade, sponsored primarily by ONR, NSF, and NOAA. The future of the Arctic Ocean Buoy Program is currently under review to ensure that research and operational needs will be adequately served in the future. The major area for growth is in the development and deployment of automatic weather stations and buoys providing information on ocean parameters and ice thickness.

### 4.2 The role of the polar regions in the global carbon cycle

Research should focus on the processes that influence the rate of solution of carbon dioxide in cold, high-latitude, seasonally ice-covered waters, the transfer of carbon, in solution and as biological detritus, from surface waters to the deep

ocean, and the transfer of carbon between the atmosphere and Arctic wetlands and boreal forests. The ocean component of this work will build on the research described in Section 4.1.

#### 4.2.1 Required Sensors

Ocean-color imager (to provide estimates of biological productivity); SAR and multispectral visible/infrared imager, such as the AVHRR, the Thematic Mapper on Landsat, and the HIRIS aboard EOS (to map vegetation types and permafrost extent). The principal need here is for early launch of an ocean-color imager.

#### 4.2.2 Ancillary Measurements

Sediment traps in the ocean (to measure the flux of biological detritus); field investigation of the annual cycle of biological activity, uptake of carbon-dioxide and other greenhouse gases in high-latitude waters, and the processes that govern the balance between carbon-dioxide absorption/release and methane production in Arctic wetlands. Much of this work is already underway, or is in the planning stage.

### 4.3 The response of the polar regions to climate change

The principal changes likely to occur at high latitudes, that are detectable from space, are in the sea-ice cover, seasonal snow, surface temperatures, ocean productivity, permafrost

extent and its associated vegetation mix, and in the extent and thickness of the terrestrial ice sheets and glaciers. The major components of ice-sheet mass balance that can potentially be measured from space are snow accumulation, surface melting, ice motion, and changes in ice volume. Of these, measurement of changes in ice volume is a direct indication of the mass balance and is the objective with highest priority. However, the other measurements are important in that they provide insight into the processes affecting the mass balance, and this insight will be needed if we are to assemble models that realistically predict the ice-sheet contribution to sea-level change in a warmer world.

Many of the changes anticipated at higher-latitudes would be detectable from long time series of passive-microwave, SAR, radar and laser altimetry, thermal-infrared, ocean-color, and visible/infrared images. Apart from the laser-altimetry data, the necessary measurements will be made almost continuously over the next ten years by a series of approved satellite missions, and the major requirement is for data systems to convert these measurements into appropriate time series.

#### 4.3.1 Required Sensors

Preparations are well underway to make use of passive-microwave and SAR data to monitor sea ice and seasonal snow; research has begun into the use of thermal-infrared data to derive ice-surface temperatures; but there is a need for a systematic effort to use satellite

data to monitor Arctic vegetation and regions of permafrost.

For measurement of the mass balance of the polar ice sheets, required sensors include: radar altimeter (to measure changes in surface elevation over the smoother, near-horizontal portions of the ice sheets); laser altimeter (to measure elevation changes over the rest of the ice sheets); SAR and Landsat (to measure changes in ice-sheet areal extent, and ice velocity on large ice streams and glaciers); SAR, passive microwave, and thermal infrared (to map regions of summer melting); laser ranger (to measure ice-surface strain rates and, with the laser altimeter, snow-accumulation rates). Apart from the laser instruments, all these sensors will be available during most of the next decade, with appropriate data systems either already in existence or under development. The lack of a satellite laser altimeter until the turn of the century will seriously delay full assessment of the ice-sheet contribution to sea-level rise. Consequently, we strongly recommend the use of an airborne laser altimeter, together with GPS navigation, to make an early start on measuring the mass balance of individual ice streams and glaciers (Figure 33).

#### 4.3.2 Ancillary Measurements

The major need is for intensive investigation of specific processes associated with potential changes, such as ocean/ice/atmosphere energy and mass fluxes; carbon-dioxide and methane exchange between the atmosphere and the ocean/land; and snow accumulation and ice discharge/ablation from the terrestrial ice sheets. Some of

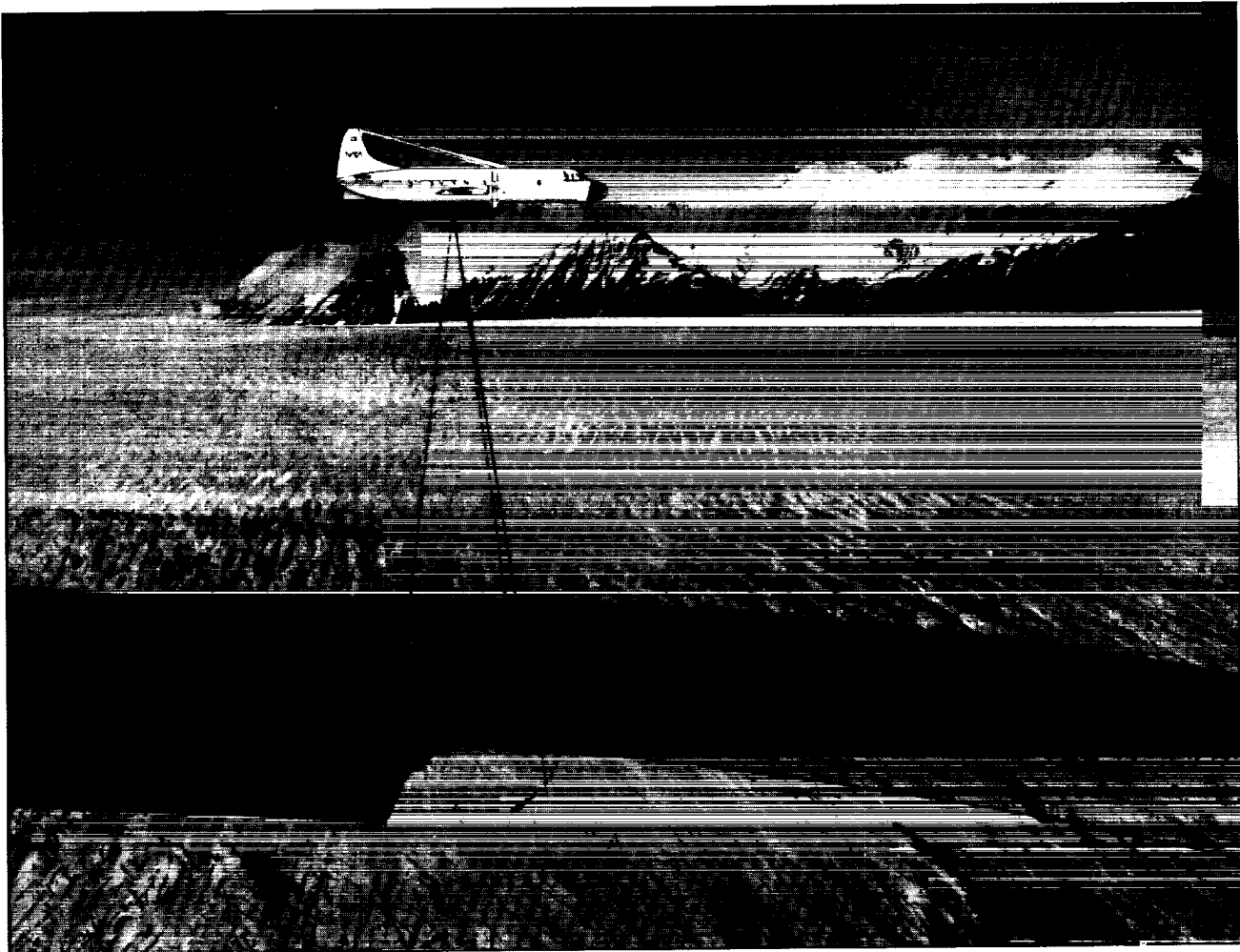


Figure 33. Detection of changes in glacier thickness by laser altimetry. This artist's impression shows how a scanning laser could be used to measure repeat surface profiles of a glacier, with the airplane navigated, using real-time GPS data, to within less than 100 meters of a previous flight path. [Provided by W. Krabill, NASA Wallops Flight Facility.]

these are currently under investigation by projects supported by a number of agencies; others will benefit from the data sets identified above.

#### 4.4 Modeling

The long-term objective of the program summarized above is to put us in a position to predict the likely response of the polar regions to climate change. A set of models will be needed: incorporating what we understand about relevant processes; initiated and validated by what we learn about relevant boundary conditions and current

behavior; and driven by changes in those boundary conditions associated with anticipated climate scenarios. In addition, models will be needed to help interpret the remotely-sensed data in terms of desired geophysical parameters.

There will be an increasing need for modelling at all stages in the interpretation of remotely-sensed data, particularly to provide estimates of parameters that cannot directly be measured. For instance, although sea-ice thickness cannot yet be measured from space,

synoptic passive-microwave, thermal-infrared, and SAR measurements, together with estimates of wind speed from either the laser wind sounder or buoy pressure measurements, permit a Kalman-filter type model in which the satellite data and a physical model “converse” to yield estimates of parameters such as ice thickness, heat and mass fluxes between the ocean and atmosphere, and rates of brine injection into the ocean.

There is also a clear need for more realistic incorporation within global climate models of high-latitude processes, particularly those involving sea ice. This will require a collaborative effort by oceanographers, atmospheric scientists, and sea-ice specialists. Satellite data will be used both to initiate, and to test the performance of resulting models, and to constrain models used for operational forecasting.

## 5. Summary and Recommendations

### 5.1 The Sensors

Most of the sensors needed for polar research either exist now, or are firmly planned for the near future (Figures 3 and 34). Some of them, such as those aboard the NOAA and Defense Department weather satellites, are for operational purposes, and offer the promise of indefinite time series of observations. High-resolution visible sensors, such as Landsat and SPOT, are also likely to continue indefinitely. In addition, almost continuous data will be available from radar altimeters

(Geosat, ERS-1 and 2, and EOS) and from SARs (ERS-1 and 2, JERS-1, Radarsat, and EOS).

With the demise of the CZCS on Nimbus-7, there has been a hiatus in the acquisition of ocean-color data. Early launch of NASA's SeaWiFS, together with the Japanese OCTS, will help fill the gap until the availability of ocean color data from MODIS aboard EOS.

A major omission, over the next ten years, will be a satellite laser altimeter, and there is a clear need for an airborne program of

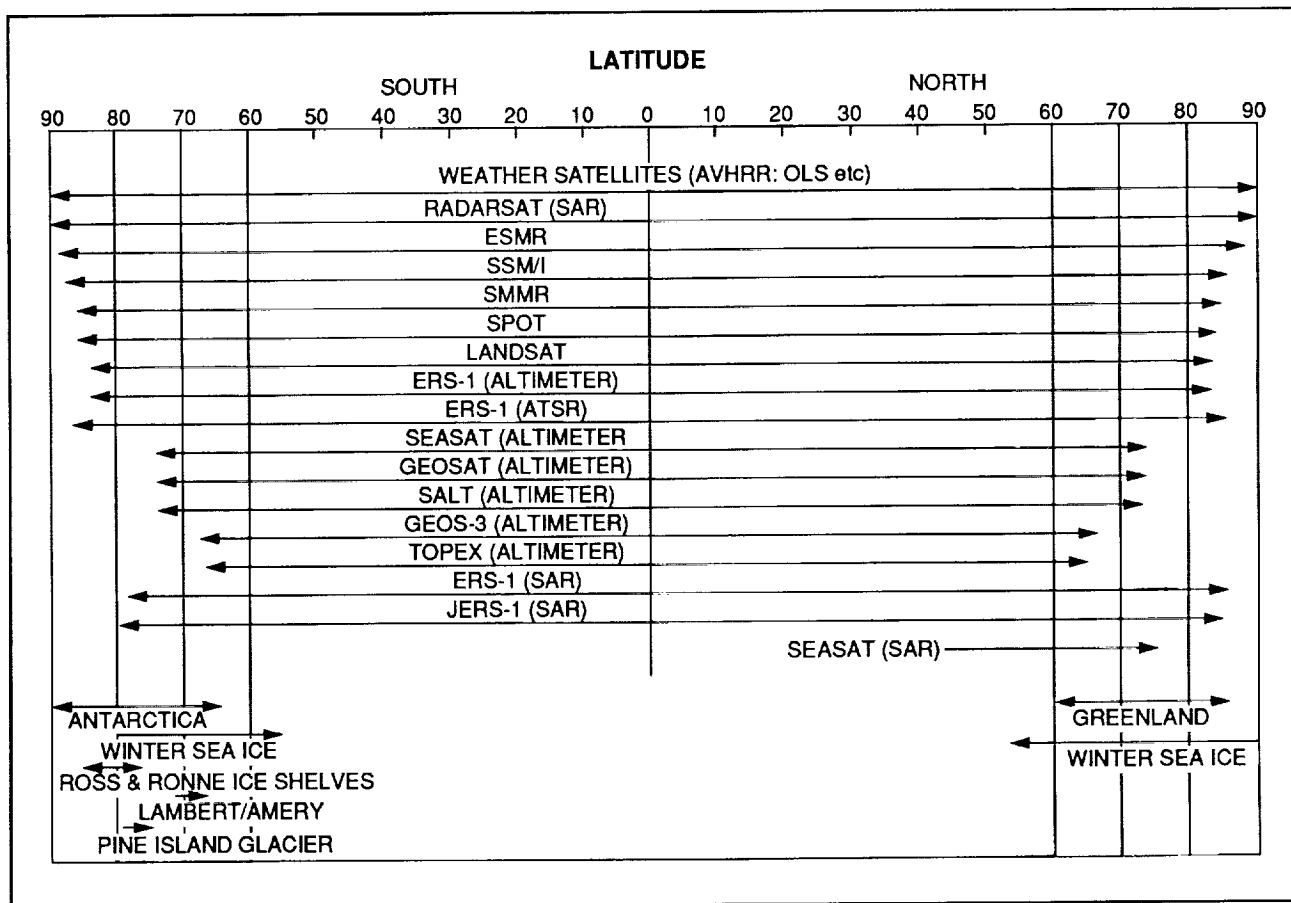


Figure 34. Satellite sensors with high-latitude coverage that will operate during the 1990s.

laser altimetry during this period. For sea-ice observations, we ultimately need a large-swath SAR capable of routinely imaging global sea-ice cover at intervals of just a few days, and Radarsat has the capability to satisfy this requirement.

At present, there is no sensor capable of measuring winds over ice. The Laser Atmospheric Wind Sounder (LAWS) proposed for EOS will provide this information, but it will not be flown until the turn of the century. In the interim, we will be dependent on weather stations and buoys to measure winds and/or surface pressure (from which geostrophic winds can be calculated). Consequently, it is extremely important at least to maintain, and preferably to enhance, the network of data buoys on the Arctic and Antarctic sea ice, and to establish additional remote weather stations at key locations, particularly in Antarctica.

## 5.2 The Data

Satellite data are fast becoming accepted as an essential requirement for most sea-ice and polar-ocean research but, despite the existence of many appropriate data sets, very little ice-sheet research has been attempted using these data. One reason for this is undoubtedly the difficulty of access to these data by traditional glaciologists, partly because the data were not in a user-friendly form, partly because glaciologists have assumed that the remote-sensing specialists would do all the analysis, and partly because of a natural tendency to "stick to the old ways". Conse-

quently, a very small group of specialists, often with little glaciological understanding, have been left with the job of analyzing all these data. Inevitably, progress has been slow, and much time has been devoted to converting the satellite data into user-friendly estimates of geophysical parameters that the lay researcher can understand and use.

Much of this preparatory work is now done and systems are in place, for instance, to convert altimetry data into ice-sheet elevations and to present these in both profile form and as a gridded data set. A stage has been reached when it is imperative for these data to be used as just another source of information by the research community. The availability of satellite data represents a quantum leap in our ability to investigate the polar regions, and a new breed of investigators is needed with the ability and the willingness to make use of them.

## 5.3 Algorithms

Algorithm development is a continuing process, particularly for imaging instruments that provide information at several spectral bands. However, it is important to strike a balance between research with the goal of improving the algorithms, and research that applies the satellite measurements and derived products to some investigation of, for instance, climate or the oceans. Early in the development of any new technique, a heavy investment must be made in the understanding of what information is contained in the measured signal, and in developing algorithms for extracting that information. In the past, this work has generally been done by groups of remote-

sensing specialists who have not always been well-linked to the broader research communities that, potentially, have most to gain from the satellite data. Experience has shown that the best way to forge those links, and to elicit rapid assessment of the value of derived products, is to release data products promptly to as many researchers as possible. Moreover, the hands-on experience, possessed by many of those researchers, of the parameters being derived by the algorithms is a necessary complement to the remote-sensing expertise of the algorithm developers.

Fortunately, the development of optical discs for the storage and easy access of large data sets has made it possible for any scientist to work with almost any type of satellite information, and this development has attracted many more investigators to make use of these data for their research.

#### 5.4 Calibration and Validation

Calibration of satellite sensors provides error estimates for the basic measurements made by the sensors, and hence estimates of instrument-induced errors in the derived parameters. Of particular importance to the Global Change program is the relative calibration of similar instruments from which long time series of data are compiled. Experience has shown that satellite data are ultimately applied to a host of applications for which they were not originally designed, and instrument calibration is frequently the factor which limits the extent of these applications. Thus, attempts have been made to extract climate trends from, for instance, sea-surface temperatures derived from weather-satellite data, but if there is a

climate signal it is probably less than the errors due to calibration. Nevertheless, the calibration of these satellites was perfectly adequate for their original purpose. Consequently, precise calibration has become a first priority for future sensors, with provision for continuous monitoring during the life of the instrument.

Validation of derived estimates of geophysical parameters can be extremely difficult. Satellite instruments record phenomena over time and space scales that are very different from those detected by other instruments. Measurements refer to a very short time interval and, for most sensors, quite a large area. For instance, estimates of sea-ice concentration derived from passive-microwave data refer to conditions instantaneously averaged over hundreds of square kilometers. In many cases, only airborne sensors can acquire comparable information, and they in turn must be validated against very localized surface measurements. Similarly, satellite estimates of ocean winds are instantaneous averages for large areas of the ocean, whereas surface measurements are taken at one location and averaged over significant time intervals. Consequently, it is important to establish a suite of appropriate aircraft sensors for use in validation campaigns, particularly in the polar regions. Because of their greater spatial resolution, these instruments can generally be easily validated against surface observations. Appendix II provides a brief listing of some of the airborne sensors currently available.

## 5.5 Data Systems

For many years satellite data were virtually inaccessible to scientists not directly involved in the satellite program. Data storage was cumbersome; data formats were ill-described; information about the data was, at best, poorly documented; competing algorithms were hotly contested amongst the satellite cognoscenti; and data systems, where they existed, were little better than leaky warehouses. The decade of the eighties has seen a growing awareness of these problems, and several attempts to address them have been made in the form of Pilot Data Systems. These systems have explored different hardware and software options for processing and distributing data. Early attempts focussed on systems that would provide any investigator with instant electronic access to multiple data sets via a large, central computer that would be available also for data manipulation, overlaying, image analysis, etc. More recently, the ability to store large amounts of data in an easily accessible form on optical disc and the availability of low-cost powerful desk-top computers have shifted the focus to broad distribution of well-defined data sets, with the software necessary to read and manipulate the data. Not only is this approach less costly, it appears to be receiving wide approval from users.

The need for continued improvement of data systems is well recognized by all the relevant funding agencies, particularly in view

of the massive increase in satellite data anticipated over the next decade.

Successful archival and distribution of data from many different instruments will probably require a number of different data systems, each specializing in specific instruments, with requirements driven by the prime applications of that instrument. However, there will be an increasing demand from individual investigators and groups of collaborators, for data from several instruments overlaid onto their region of interest. Consequently, there must be close communication between the various data systems, during both their development and implementation phases, to ensure compatibility of data format, data-gridding procedures, and map projections.

## 5.6 Recommendations

- 1. Develop the capability to use passive-microwave, SAR, infrared, and atmospheric-sounding data from satellites to calculate values for the fluxes of energy, water, and salt at the polar ocean/ice/atmosphere interfaces.**

This will require the development of data systems to bring together and appropriately process all the various satellite data, and the development and testing of models, driven by the satellite and *in situ* data sets, to derive estimates of the various fluxes. Our objective should be to complete this development during the lifetime of ERS-1, with the goal of implementing an "operational" system during the lifetime of Radarsat (after 1994). It will also be important to maintain, and preferably to

enhance, the network of data buoys on and beneath the Arctic and Antarctic sea ice, and to establish additional remote weather stations at key locations, particularly in the Antarctic.

**2. Establish a SAR receiving station at, or close to, McMurdo Station, Antarctica prior to 1995, when Radarsat is scheduled for launch.**

Regular SAR coverage will be needed to satisfy the previous recommendation, and Radarsat will provide our first opportunity to collect approximately weekly coverage of all ice-covered waters in both hemispheres, but only if these waters are included within the acquisition masks of SAR receiving stations. Figure 25 clearly indicates the need for a station at McMurdo.

**3. Develop an effective aircraft remote-sensing program that complements satellite and surface measurements, and bridges gaps between present and planned satellite missions.**

Specific requirements include:

- (i) *A high priority for an integrated aircraft program is the routine collection of radio-echo-sounding measurements of ice thickness. This measuring capability has been well demonstrated, but many of the earlier surveys were flown with inaccurate navigation systems, and the availability of aircraft navigation by the Global Positioning System of satellites (GPS) offers major opportunities for highly accurate surveys. Such surveys will yield maximum benefit if several sensors are routinely flown together.*

- (ii) *Airborne laser-altimeter surveys of key ice-sheet regions, using both a scanning laser and a nadir-looking laser in conjunction with GPS navigation. Such a program could be applied to localized regions of particular interest, pending availability at the turn of the century of satellite laser data from GLRS aboard EOS which will provide the global areal coverage required to quantify the ice-sheet contribution to sea-level rise. Other instruments that could usefully fly on the same aircraft include a radar altimeter, a radio-echo sounder to measure ice thickness, a gravity meter, a magnetometer, a large-format camera, a video camera, and a thermal-infrared and a microwave radiometer.*

- (iii) *Multifrequency, multipolarization SAR data should be collected over polar ice and land surfaces to prepare for the upcoming series of satellite SAR missions.*

**4. Provide adequate, readily accessible, and user-friendly data systems.**

Data archival and distribution are not glamorous tasks, and yet they require active involvement from the research community to ensure that research applications are well served and that products have adequate quality control. Such service deserves greater acknowledgement and reward than it has received in the past. For example, we should consider ways in which individuals and groups responsible for data systems can be adequately referenced and acknowledged in research

publications, and academic institutions should take full account of data services in tenure and salary decisions.

Requirements of a data system include:

- (i) *Catalogues that provide users with a rapid, brief, and current summary of what data are available from this and other data centers, and how they can be obtained.*
- (ii) *Formats, gridding systems, map projections, etc that allow for easy overlay of multiple sets of different types of data acquired from different data centers.*
- (iii) *Well-documented algorithms, user guides, etc that help the user gain access to the data and to understand their heritage and limitations.*
- (iv) *The research community must be willing and able to make use of satellite remote sensing data to address major research issues.*

This last may be our most urgent requirement. In the past, there has been insufficient communication between the remote-sensing community and the researchers who are the potential users of the data. Many remote-sensing specialists have regarded remote sensing as an end in itself, and have focussed on aspects of remote sensing that have had little relevance to the needs of the research investigators. At the same time, these investigators have tended to regard remote sensing as outside the domain of their research. More recently, the two communities have

started to communicate more energetically, and this process could be encouraged by:

- *more liberal funding policies towards proposals to make novel use of existing satellite data and data products for addressing identified research problems;*
- *an exchange program to encourage investigators and their students to spend some time working with a remote-sensing group. Such programs exist within NASA, but they should be extended to make it easy for, say, a NSF-funded investigator to spend time at a NASA center.*

**5. Global models of climate, of ocean circulation, and of the carbon and hydrologic cycles should take account of relevant processes occurring at high latitudes.**

This, perhaps, is the principal message in the recent work of Stouffer et al., (1989), in which they show that processes of heat transfer in the Southern Ocean may significantly slow the rate of greenhouse warming over Antarctica. Their work represents an important beginning, but we still have much to learn about these and other important high-latitude processes, and it is highly likely that more surprises await us as these processes are incorporated into the models. This could be facilitated by the establishment of modelling projects that have as their initial focus the polar regions rather than the mid latitudes. Essential elements would include the modelling activity itself, appropriate process studies to provide intuition for model development, and remotely sensed data to initialize and to validate the model.

---

**REFERENCES**

- Aagaard, K., J.H. Swift, and E.C. Carmack. 1985. Thermohaline circulation in the Arctic mediterranean seas. *Journal of Geophysical Research*, Vol. 90, No. C3, pp. 4833-4846.
- Aagaard, K. and E.C. Carmack. 1989. The role of sea ice and other fresh water in the Arctic circulation. *Journal of Geophysical Research*, Vol. 94, No. C10, pp. 14485-14498.
- Bindschadler, R.A., K.C. Jezek, and J. Crawford. 1987. Glaciological investigations using the synthetic aperture radar imaging system. *Annals of Glaciology*, Vol. 9, pp. 11-19.
- Bindschadler, R.A., H.J. Zwally, J. A. Major, and A.C. Brenner. 1989. Surface topography of the Greenland Ice Sheet from satellite radar altimetry. NASA Special Publication No. 503, Washington, DC 20546, 105 pages and 17 maps.
- Cavalieri, D.J. and C.L. Parkinson. 1981. Large-scale variations in observed Antarctic sea ice extent and associated atmospheric circulation. *Monthly Weather Review*, Vol. 109, pp. 2323-2336.
- Chelton, D.B. and P. McCabe. 1985. A review of satellite altimeter measurement of sea-surface wind speed with a proposed new algorithm. *Journal of Geophysical Research*, Vol. 90, No. C3, pp. 4707-4720.
- Comiso, J.C. 1983. Sea ice effective microwave emissivities from satellite passive microwave and infrared observations. *Journal of Geophysical Research*, Vol. 88, No. C12, pp. 7686-7704.
- Elachi, C. 1987. Introduction to the physics and techniques of remote sensing. Wiley-Interscience Publications, John Wiley & Sons, 413 pages.
- Ferrigno, J.G. and B.F. Molnia. 1989. Availability of Landsat, Soyuzkarta, and SPOT data of Antarctica for ice and climate research. *Antarctic Journal of the US*, Vol. 24, No. 4, pp. 15-18.
- Gloersen, P. and W.J. Campbell. 1988. Variations in the Arctic, Antarctic, and global sea-ice covers during 1978-1987 as observed with the Nimbus-7 SMMR. *Journal of Geophysical Research*, Vol. 93, No. C9, pp. 10666-10674.
- Gloersen, P., W.J. Campbell, D.J. Cavalieri, J.C. Comiso, C.L. Parkinson and H.J. Zwally. In Preparation. Arctic and Antarctic sea ice, 1978-1987, satellite passive microwave observations and analysis. NASA Special Publication.
- Gordon, A.L. 1986. Interocean exchange of thermocline water. *Journal of Geophysical Research*, Vol. 91, No. C4, pp. 5037-5046.

- Gordon, A.L. and J.C. Comiso. 1988. Polynyas in the Southern Ocean. *Scientific American*, Vol. 258, No. 6, pp. 90-97.
- Grotch, S.L. 1988. Regional intercomparisons of general circulation model predictions and historical climate data. DOE/NBB-0084, U.S. Department of Energy, Washington, DC 20545, 291 pages.
- Hall, D.K. 1988. Assessment of polar climate change using satellite technology. *Reviews of Geophysics*, Vol. 26, No. 1, pp. 26-39.
- Hall, D.K., A.T.C. Chang, J.L. Foster, C.S. Benson, and W.M. Kovalick. 1989. Comparison of *in situ* Landsat derived reflectance of Alaskan glaciers. *Remote Sensing of the Environment*, Vol. 28, pp. 23-31.
- Hall, D.K. and J. Martinek. 1985. Remote sensing of ice and snow. Chapman and Hall, New York, 189 pages.
- Hansen, J., A. Lacis, D. Rind, P. Russell, I. Fung, R. Ruedy, and J. Lerner. 1984. Climate sensitivity: Analysis of feedback mechanisms. In: *Climate Processes and Climate Sensitivity* (J. Hansen and T. Takahashi, Eds.), American Geophysical Union, Washington, D.C. pp. 130-163.
- Haxby, W.F., G.D. Kerner, J.L. LaBreque, and J.K. Weissel. 1983. Digital images of combined oceanic and continental data sets and their use in tectonic studies. *Eos*, Vol. 64, No. 52, pp. 995-1004.
- Jezek, K.C. and R.B. Alley. 1988. Effect of stratigraphy on radar altimetry data collected over ice sheets. *Annals of Glaciology*, Vol. 11, pp. 60-63.
- Kukla, G. and P. Robinson. 1980. Annual cycle of surface albedo. *Monthly Water Review*, Vol. 108, pp. 56-68
- Lachenbruch, A.H. and B.V. Marshall. 1986. Changing climate: geothermal evidence from permafrost in the Alaska Arctic. *Science*, Vol. 234, pp. 689-696.
- Laxon, S.W.C. 1989. Satellite radar altimetry over sea ice. Unpublished Ph.D. dissertation, University of London, 246 pages.
- Lingle, C.S., A.C. Brenner, and H.J. Zwally. In Press. Satellite altimetry, semivariograms, and seasonal elevation changes in the ablation zone west of Greenland. *Annals of Glaciology*, Vol. 14
- Lucchitta, B.K. and H.M. Ferguson. 1986. Antarctica: measuring glacier velocity from satellite images. *Science*, Vol. 234, pp. 1105-1108.

- Lucchitta, B.K., J.G. Ferrigno, and R.W. Williams. Submitted. Monitoring the dynamics of the Antarctic coastline with Landsat images. International Symposium on Glacier-Oceans-Atmosphere Interactions, Sept. 24-29, 1990, Leningrad, USSR.
- Macdonald, T.R., J.G. Ferrigno, R.S. Williams, and B.K. Lucchitta. In Press. Antarctic Journal of the U.S.
- Martin, S.L. and D.J. Cavalieri. 1989. Contributions of the Siberian Shelf polynyas to the Arctic Ocean intermediate and deep water. *Journal of Geophysical Research*, Vol. 94, No. C9, pp. 12725-12738.
- Martin, T.V., H.J. Zwally, A.C. Brenner, and R.A. Bindshadler. 1983. Analysis and retracking of continental ice sheet radar altimeter waveforms. *Journal of Geophysical Research*, Vol. 88, No. C3, pp. 1608-1616
- McNutt, L. 1981. Ice conditions in the eastern Bering Sea from NOAA and Landsat imagery: winter conditions 1974, 1976, 1977, and 1979. NOAA Technical Memorandum, ERL PMEL-24, 179 pages.
- Morrisey, L.A., L.L. Stong, and D.H. Card. 1986. Mapping permafrost in the boreal forest with thematic mapper satellite data. *Photogrammetric Engineering and Remote Sensing*, Vol. 52, No. 9, pp. 1513-1520.
- Njoku, E.G. 1982. Passive-microwave remote sensing of the Earth from space - a review. *Proceedings of the IEEE*, Vol. 70, No. 7, pp. 728-750.
- Orheim, O. and B.K. Lucchitta. 1987. Snow and ice studies by thematic mapper and multispectral scanner Landsat images. *Annals of Glaciology*, Vol. 9, pp. 1-10.
- Parkinson, C.L. and D.J. Cavalieri. 1989. Arctic sea ice 1972-1987: seasonal, regional, and interannual variability. *Journal of Geophysical Research*, Vol. 94, No. C10, pp. 14499-14523.
- Parkinson, C.L., J.C. Comiso, H.J. Zwally, D.J. Cavalieri, P. Gloersen, and W.J. Campbell. 1987. Arctic sea ice, 1973-1976: satellite passive-microwave observations. NASA Special Publication No. 489, 296 pages.
- Partington, K.C., J.K. Ridley, C.G. Rapley, and H.J. Zally 1989. Observations of the surface properties of the ice sheets by satellite radar altimetry. *Journal of Glaciology*, Vol. 35, No. 120, pp. 267-275.
- Peel, D.A., R. Mulvaney, and B.M. Davison. 1988. Stable-isotope/air temperature relationships in ice cores from Dolleman Island and the Palmer Land Plateau, Antarctica Peninsula. *Annals of Glaciology*, Vol. 10, p. 130-136.

- Peel, D.A. In Press. Ice-core evidence from the Antarctic Peninsula region. In: R.S. Bradley and P.D. Jones (eds.): *Climate since 1500 A.D.* Unwin Hyman.
- Rothrock, D.A. and D.R. Thomas. In Press. The Arctic Ocean mutliyear ice balance, 1979-1982. *Annals of Glaciology*, Vol. 14.
- Rotman, S. R., A.D. Fisher, and D.H., Staelin. 1982. Inversion for physical characteristics of snow using passive radiometric observations. *Journal of Glaciology*, Vol. 28, pp. 179-185.
- Steffen, K. 1986. Atlas of the sea ice types, deformation processes, and openings in the ice. *Zürcher Geographische Schriften*, heft 20. Geographisches Institut. Eidgenössische Technische Hochschule Zürich. 55 pages.
- Steffen, K. In preparation. In: NASA DMSP SSM/I sea-ice validation program - final report. Edited by D.J. Cavalieri, NASA Technical Memorandum.
- Stewart, R.H. 1985. *Methods of satellite oceanography*. University of California Press. 360 pages.
- Stouffer, R.J., S. Manabe, and K. Bryan. 1989. Interhemispheric asymmetry in climate response to a gradual increase of atmospheric CO<sub>2</sub>. *Nature*, Vol. 342, pp. 660-662
- Swithinbank, C. and B.K. Lucchitta. 1986. Multispectral digital image mapping of Antarctic ice features. *Annals of Glaciology*, Vol. 8, pp. 159-163.
- Tans, P.P., I.Y. Fung, and T. Takahashi. 1990. Observational constraints on the global atmospheric CO<sub>2</sub> budget. *Science*, Vol. 247, pp. 1431-1438.
- Thomas, R.H. 1973. The dynamics of the Brunt Ice Shelf. *British Antarctic Survey Scientific Report No. 79*.
- Thomas, R.H., T.V. Martin, and H.J. Zwally. 1983. Mapping ice-sheet margins from radar-altimetry data. *Annals of Glaciology*, Vol. 4, pp. 283-288.
- Wilheit, T.T., A.T.C. Chang, and A.S. Milman. 1980. Atmospheric corrections to passive-microwave observations of the ocean. *Boundary-layer meteorology*, Vol. 18, pp. 65-77.
- Williams, R.S. Jr, J.G. Ferrigno, T.M. Kent, and J.W. Schoonmaker, Jr. 1982. Landsat images and mosaics of Antarctica for mapping and glaciological studies. *Annals of Glaciology*, Vol. 3, pp. 321-326.
- Williams, R.S. Jr, J.G. Ferrigno, and T.M. Kent. 1984. Index map and table of optimum Landsat 1,2 and 3 images of Antarctica. U.S.G.S. Open-File Report 84-573 (1:5M scale map; table).

- 
- Williams, R.S. Jr and J.G. Ferrigno, (Editors). In Press. Satellite image atlas of the world. U.S.G.S. Professional Paper 1386-B, containing a chapter on Antarctica by C. Swithinbank, with sections on 'The Dry Valleys of Victoria Land' by T.J. Chinn and 'Landsat images of Antarctica' by R.S. Williams Jr and J.G. Ferrigno.
- Wunsch, C. 1981. The promise of satellite altimetry. *Oceanus*, Vol. 24. No. 3, pp. 17-26.
- Zwally, H.J. 1977. Microwave emissivity and accumulation rate of polar firn. *Journal of Glaciology*, Vol. 18, pp. 195-215.
- Zwally, H.J., J.C. Comiso, C.L. Parkinson, W.J. Campbell, F.D. Carsey, and P. Gloersen. 1983a. Antarctic sea ice, 1973-1976: Satellite passive microwave observations. NASA SP-459, Washington, D.C. 206 pages.
- Zwally, H.J., R.A. Bindschadler, A.C. Brenner, T.V. Martin, and R.H. Thomas. 1983b. Surface elevation contours of Greenland and Antarctica ice sheets. *Journal of Geophysical Research*. Vol. 88, No. C3, pp. 1589-1596.
- Zwally, H.J., J.A. Major, A.C. Brenner, and R.A. Bindschadler. 1987. Ice measurements by Geosat radar altimeter. *Johns Hopkins APL Technical Digest*, Vol. 8, No. 2, pp. 251-254.
- Zwally, H.J., A.C. Brenner, J.A. Major, R.A. Bindschadler, and J.G. Marsh. 1989. Growth of Greenland Ice Sheet: measurement. *Science*, Vol. 246, p. 1587-1589.
- Zwally, H.J. 1989. Growth of Greenland Ice Sheet: interpretation. *Science*, Vol. 246, pp. 1589-1591.



## Appendix I

### Information on Data Archives, What They Hold, and How to Access Them.

#### Passive-Microwave Data

All SSM/I data are available for both research and operational applications. NASA has established a data system at the National Snow and Ice Data Center (NSIDC), which is responsible for routine processing, archival, and distribution of the data to the research community. Significant problems have been encountered with the geolocation of the SSM/I data, with errors that appear to be caused by a combination of ephemeris errors and a "wobble" in the spacecraft axis, and there is an urgent need for a full assessment of just what is causing these errors. These problems delayed release of gridded SSM/I data sets until January 1990, when NSIDC began to issue gridded microwave brightness temperatures on compact optical discs (CDROM's). Similar products from the ESMR and SMMR instruments are also available from the NSIDC, and CDROM's containing gridded estimates of ice concentration and type derived from the SMMR and SSM/I data will be released in 1991. For additional information, contact:

R. Weaver  
NSIDC  
Campus Box 449  
University of Colorado  
Boulder, Colorado 80309-0449

There have been extensive validation exercises conducted by Navy and NASA investigators; results from these are presented in "DMSP SSM/I calibration/validation" Volume I, coordinated by J. Hollinger, Naval Research Laboratory, 1989; and "NASA DMSP SSM/I sea-ice validation program - final report", edited by D. Cavalieri, NASA Technical Memorandum, In preparation.

#### AVHRR Data

AVHRR data are available in three forms:

High Resolution Picture Transmission (HRPT) data, with spatial resolution at nadir of 1.1 km, are transmitted continuously from the spacecraft, and can be received by suitably equipped ground stations;

Local Area Coverage (LAC) data are essentially the same as HRPT data, but are recorded on request aboard the spacecraft over approximately 10% of the orbit; and

Global Area Coverage (GAC) data, at 4 km spatial resolution, are derived from the full resolution data and recorded aboard the spacecraft for later transmission to ground stations, to provide total coverage of the Earth.

Polar AVHRR data are available in hard copy form from the Joint Ice Center or in digital form from NOAA archives. However, deterioration of tapes holding many of the older digital data may prevent retrieval of some historical data.

AVHRR data from the Arctic are routinely received at the NOAA receiving station at Gilmore Creek, near Fairbanks, Alaska. This station receives HRPT, LAC and GAC data, and retransmits them to the NOAA central archive where the LAC and GAC data are routinely archived on magnetic tape, along with some small percentage of the HRPT data. The GeoData Center at the Geophysical Institute of the University of Alaska at Fairbanks receives fax hardcopy prints of HRPT data acquired at Gilmore Creek from the National Weather Service, and archives approximately 2 - 3 passes per day (out of 12 - 14 total). In addition, since the summer of 1989, the GeoData Center has been routinely archiving a small subset of the HRPT coverage as digital data sets on tape. At present, The GeoData Center holds approximately 14,000 hard-copy AVHRR scenes on film or fax, and some 300 scenes on digital data. For more information, contact:

T. George  
GeoData Center  
Geophysical Institute  
University of Alaska  
Fairbanks, Alaska 99775-0800.

Full-resolution HRPT data acquired at receiving stations at Palmer and McMurdo, Antarctica are archived at the Antarctic Remote Sensing Facility (ARSF) at Scripps Institution of Oceanography. Data from only a selection of satellite passes are received. A data-processing and image-analysis system is available at McMurdo, primarily for operational applications, with an identical system at Scripps. These systems are designed to process and display a variety of geophysical data from the sensors aboard the NOAA and DMSP spacecraft. For more information, contact:

R. Whritner  
Antarctic Remote Sensing Facility  
Ocean Research Division, A-014  
Scripps Institute of Oceanography  
La Jolla, California 92093

### **OLS Data**

The global OLS data set, acquired since 1973, is archived in hard-copy form at the National Snow and Ice Data Center. Digital OLS data, which have not hitherto been preserved, may also be archived in the future by NSIDC. Real-time OLS and SSM/I data from overflying DMSP spacecraft are also acquired at the Palmer and McMurdo receiving stations in Antarctica. For additional information, contact:

R. Weaver  
NSIDC  
Campus Box 449  
University of Colorado  
Boulder, Colorado 80309-0449

or

R. Whritner  
Antarctic Remote Sensing Facility  
Ocean Research Division, A-014  
Scripps Institute of Oceanography  
La Jolla, California 92093

### **Ocean Color Data**

The central archive and distribution facility responsible for providing access to the entire CZCS data set is the National Space Science and Data Center (NSSDC) at NASA/GSFC. A detailed description of the data sets available to users and a list of regional browse, distribution, and analysis centers for higher level CZCS products is given in Feldman et al, (EOS, Vol. 70, No. 23, June 6, 1989). Digital products range from Level 1 (calibrated radiances for all six CZCS channels, at full spatial resolution, with Earth location information) to Level 3 (six derived products, including phytoplankton pigment concentrations, gridded at approximately 20-km resolution, at a variety of time intervals). There are no routine film or hard-copy products.

To facilitate user selection of images and data requests, an analog optical-disc browse and data-order capability has been developed, which allows the user to scan rapidly through the 4-km resolution browse images, select specific scenes, and generate an order for digital products with the option of submitting the order by electronic mail. For additional information, contact:

G. Feldman  
Code 636.0  
NASA/Goddard Space Flight Center  
Greenbelt, Maryland 20771

### **High-Resolution Visible Images**

There is extensive Landsat coverage of high northern latitudes, particularly Alaska, where data are received and hard copies are archived locally by the GeoData Center at the University of Alaska in Fairbanks (see above for mailing address).

The vast majority (more than 10000) of Antarctic images were acquired in 1972-1974 in connection with a Landsat research project. Hard copies (positive prints and/or negative film) of each of these images (in all 4 MSS channels) are stored at the US SCAR (Scientific Committee for Antarctic Research) Library, in Reston, Virginia. A detailed examination indicated that more than half of these have less than 10% clouds, providing coverage of 70% of overflown parts of Antarctica - or about 55% of the entire continent. Many areas were successfully imaged on several occasions. Unfortunately, most of the digital data have been lost because of deterioration of the magnetic tapes, and only about 250 images are now available in digital form on computer compatible tapes (CCT's); most of these are in the SCAR library.

Few additional Antarctic images were acquired between 1974 and 1983, but since 1983 about 3700 scenes have been acquired by Landsats 4 and 5. Most of these are from West Antarctica, the Filchner/Ronne ice shelf and Coates Land, and nearly all are TM scenes. The SCAR Library holds negatives of the MSS scenes, but there are very few positives, and even fewer CCT's. First estimates of cloud cover indicate that less than 30% of the Landsat 4 and 5 images contain much useful information.

There are now several SPOT images of the polar regions, and the extensive Antarctic coverage by the Russian Soyuzkarta missions is available for purchase. Currently, there is underway a concerted international effort to acquire additional Antarctic images, partly to fill gaps in the existing coverage, and partly for the detection of change. In the US, this effort is sponsored by the USGS and NASA, and they are stored at the SCAR Library. Taken along with data from the earlier missions, this collection represents almost total cloud-free coverage of overflown parts of Antarctica, with repeat coverage of more than half the region. For more information, contact:

J. Ferrigno  
 US Geological Survey  
 927 National Center  
 Reston, Virginia 22092

In 1985, the Landsat program was commercialised under the Earth Observing Satellite Company (Eosat). There are no restrictions on application of the Antarctic Landsat 1, 2 and 3 data held by the SCAR Library. Most of the scenes held by the SCAR Library from later missions are in hard-copy form, but this ensures that Eosat has digital data for these images available for purchase. Costs for Landsat, SPOT, and Soyuzkarta images are summarized in the Table (from Ferrigno and Molnia, 1989).

**Comparison of sensor resolution, area of coverage, and cost of Landsat, Soyuzkarta, and SPOT data.**

<i>Spacecraft</i>	<i>Sensor</i>	<i>Resolution (in meters)</i>	<i>Approximate area of scene (in square kilometers)</i>	<i>Least expensive photo product</i>	<i>Cost per square kilometer</i>	<i>CCTs</i>	<i>Cost per square kilometer</i>
Landsat	TM	30	32,400	\$ 700 (new)	\$0.0216	\$3,600	\$0.111
	TM	30	32,400	\$ 300 (archival)	\$0.0093		
	MSS	80	32,400	\$ 300 (new) \$ 90 (archival)	\$0.0093 \$0.0028	\$ 660	\$0.0204
Soyuzkarta	KFA-1000 Panchromatic	6	3,600	\$ 777 (1988)	\$0.2158		
	KATE-200 Multispectral	20	32,400	\$ 610 (1988)	\$0.0188		
SPOT	Panchromatic	10	3,600	\$1,500	\$0.4167	\$2,200	\$0.611
	Multispectral	20	3,600	\$1,300	\$0.3611	\$1,700	\$0.4722

## SAR Data

SAR data from ERS-1, JERS-1, and Radarsat acquired within a radius of approximately 3000 km of Fairbanks, Alaska will be received at the Alaska SAR Facility (ASF), processed to full-resolution (30 m) imagery, and archived within the Archive and Operations System (AOS) of the ASF. A subset of the images obtained will be passed in near-real time to the Navy/NOAA Joint Ice Center, to assist with the production of ice forecasts. A lower-resolution (240 m) product will also be produced, and these images will be issued routinely on CD-ROMs to approved investigators. The precise definition of an "approved" investigator depends on the details of the Memorandum Of Understanding defining NASA access to data from the relevant mission. For ERS-1, access will be

provided to investigators approved by ESA following an Announcement of Opportunity that was issued in 1985, and to investigators approved by NASA.

Full-resolution images, custom-processed products, and derived parameters from the Geophysical Processing System will also be available from the AOS, and it will be possible for investigators to make advance requests for SAR coverage of specific locations at desired times. These requests will be prioritized and collated by the ASF Project Scientist, and relayed to the relevant Mission Planning Office. Products that will be available from the ASF are summarized in the Table.

### ASF Data Products for ERS-1

<u>Product Type</u>	<u>Distribution Media</u>	<u>Data Characteristics</u>
<b>Standard Products:</b>		
Computer Compatible Signal Data	CCT, DOD	12 second segment
Complex Image Data	CCT, DOD	8 m pixel spacing 30 x 50 km area 10 m resolution
Full-Resolution Images	CCT, DOD, Film	12.5 m pixel spacing 30 m resolution 80 x 100 km
Low-Resolution Images	CCT, DOD, Film	100 m pixel spacing 240 m resolution 80 x 100 km area
<b>Geo-Coded Products:</b>		
Geo-Coded Full Res.	CCT, DOD, Film	12.5 m pixel spacing 30 m resolution 80 x 100 km area
Geo-Coded Low Res.	CCT, DOD, Film	100 m pixel spacing 240 m resolution 80 x 100 km area
<b>Geophysical Products:</b>		
Ice Motion Vectors	CCT, DOD	Ice Displacement Vectors 5 km grid 100 km x 100 km (nominal)
Ice Type Classification	CCT, DOD	Ice Type Image 100 m pixels 100 km x 100 km (nominal)
Ice Type Fraction	CCT, DOD	Fraction of Ice Classes 5 km grid 100 km x 100 km (nominal)
Wave Product	CCT, DOD	Wave Direction & Wavelength 6 km x 6 km subsections From Full-Res image
Other Geophysical Products	CCT, DOD	TBD

CCT: Computer Compatible Tape  
DOD: 5.25" Digital Optical Disks

Film: 8" x 10" Format  
TBD: To Be Determined

Additional information can be obtained from:

G. Weller  
Alaska SAR Facility  
Geophysical Institute  
University of Alaska  
Fairbanks, Alaska 99775-0800.

Access to ERS-1 SAR data from outside the ASF mask will be restricted to ESA-approved investigators and to those who wish to purchase the data.

Both JERS-1 and Radarsat will store SAR data aboard the spacecraft. Some of these images will be dumped to the ASF, and it is anticipated that NASA-approved investigators will have access to a subset of these data, which could be acquired from almost any location.

### **Radar-Altometry Data**

Seasat and Geosat radar altometry data over Greenland and Antarctica have been analysed to provide estimates of ice-surface elevations. The Seasat results for Greenland have been published as an atlas (Bindschadler et al., 1989) with a listing of the gridded elevation measurements derived from the radar-altometry data. These measurements, together with similar estimates from Antarctica and gridded elevations from Geosat, can be obtained from NSIDC. For further information, contact:

R. Weaver  
NSIDC  
Campus Box 449  
University of Colorado  
Boulder, Colorado 80309-0449

The raw altometry data, including waveforms, and derived estimates of ice-surface elevations along the orbit tracks, can be obtained from:

H.J. Zwally  
Code 971.1  
NASA/Goddard Space Flight Center  
Greenbelt, Maryland 20771

## Appendix II

### Airborne Remote-Sensing Instruments that Complement the Satellite Sensors.

- **Synthetic Aperture Radar (SAR)**

Airborne multi-frequency, polarimetric SARs are operated by NASA-Jet Propulsion Laboratory (JPL) and the Naval Air Development Center (NADC), and the Canadian Center for Remote Sensing (CCRS) has a multi-frequency, polarised SAR. Data from a polarimetric SAR can be used to reproduce the SAR image for any combination of transmitted and received polarisations, whereas the CCRS instrument can acquire images with only a limited set of transmit/receive combinations. Polarimetric data contain maximum information about surface characteristics, and they represent a powerful validation tool. Moreover, they provide strong guidelines for the design of future satellite sensors.

#### JPL SAR Characteristics

	<b>C-Band</b>	<b>L-Band</b>	<b>P-Band</b>
Wavelength (cm)	5.66	24.02	68.38
Antenna Size (inches)	55 x 6.5	63 x 18	72 x 36
Bandwidth (MHz)	20 or 40	20 or 40	20 or 40
Look Angle (deg)	0 - 70	0 - 70	0 - 70
Swath Width (Km)	16	16	16
Polarization (all bands)	Horizontal and Vertical		
Aircraft Altitude	30,000 (ft)		

An important issue that must be resolved before airborne SAR data can be used by a broad spectrum of investigators is the cost of data acquisition and processing. This is particularly applicable to

polar investigations, many of which require a large areal coverage. Data processing should be sufficiently flexible to satisfy the needs of investigators, some of whom require the highest resolution over small areas whilst others would prefer a lower resolution over large areas.

For additional information, contact:

J. Crawford  
Mail Code 300-323  
Jet Propulsion Laboratory  
4800 Oak Grove Drive  
Pasadena, CA 91109

- **Microwave Radiometers**

The higher spatial resolution possible with an aircraft radiometer permits quite detailed discrimination of different types of surface, particularly when the instrument is used in unison with a SAR. Moreover, the low data rate makes data processing comparatively straightforward. At present, the Naval Oceanographic and Atmospheric Research Laboratory (NOARL) KA band Radiometer Mapping Sensor (KRMS) can be used for this purpose. This is a scanning radiometer, operating at 33.6 GHz, with a swath width approximately 2.5 times the aircraft ground clearance, and spatial resolution at nadir of 0.15 times the ground clearance. This instrument should be upgraded to provide digital data, and possibly an additional frequency.

For additional information, contact:

D. Eppler  
Polar Oceanography Branch  
NOARL  
72 Lyme Road  
Hanover, NH 03755-1290

Data from the SSM/I are acquired at an incidence angle of  $53^{\circ}$ , and comparable aircraft measurements are obtained with the Aircraft Multichannel Microwave Radiometer (AMMR) viewing the surface at a similar incidence angle in the same range of microwave frequencies as those on the SSM/I.

For additional information, contact:

D. Cavalieri  
Code 971  
NASA/GSFC  
Greenbelt, MD 20771

- **Radar Altimeter**

Radar altimeters are routinely used to measure aircraft ground clearance. More elaborate instruments, with extremely high precision, have been developed for a variety of applications. In particular, a pulse-compression radar, similar to those aboard Seasat and Geosat, is being modified at the University of Massachusetts for use over ice in conjunction with other sensors, such as the laser altimeter and radio-echo sounder.

For more information contact:

C. Swift  
Department of Electrical and Computer Engineering  
University of Massachusetts  
Amherst, MA 01003

- **Topographic Profiling Airborne Laser Altimeter**

A compact, airborne laser altimeter has been developed by NASA for topographic profiling studies of land surfaces. With this device, laser-altimeter measurements are typically acquired along the nadir track of the aircraft and consist of laser pulse time-of-flight data at pulse rates up to 50 Hz.

For aircraft installation, the compact laser altimeter transmitter and receiver are mounted together over an aircraft nadir port. Both transmitter and receiver are contained within a cylindrical volume of 0.4 m diameter and 0.5 m in length that weighs 50 kg. The aluminum frame also serves as a reference mechanical mount for a 12-bit roll & pitch gyro package and vertical accelerometer. Data from these auxiliary devices are used to characterize laser-altimeter pointing attitude and vertical motion of the aircraft. The data system is contained within a standard electrical equipment rack 0.5 m wide, 0.6 m deep, and 1 m high that weighs 120 kg.

Laser-altimeter-data acquisition is possible, under clear atmospheric conditions, from approximately 150 m to 12.5 km altitude. The laser divergence slightly overfills the receiver field-of-view of 2.5 mrad. Thus, the laser footprint on the surface is 2.5 m diameter per kilometer of altitude. At an aircraft speed of 100 m/sec, the 50 Hz ranging rate of the laser altimeter will produce continuous data at altitudes of 800 m or above. Single-pulse timing precision is 1 nsec and can be upgraded to 156 psec, or 2 cm in range.

For more information, contact:

J. Bufton  
Code 970  
NASA/GSFC  
Greenbelt, MD 20771

- **Airborne Oceanographic Lidar**

The NASA Airborne Oceanographic Lidar (AOL) can be operated in either of two modes. In the temporal mode, the sensor resolves the timing of the reflected laser pulse in 0.7 nsec channels over a period of 250 nsec. In the fluorosensing mode, laser stimulated fluorescence from water, ice, or ground targets is spectrally resolved between 380 nm and 740 nm in 32 contiguous channels of 11.25 nm width. In either mode, the AOL also functions as a high precision laser altimeter measuring the range between the sensor and the overflown surface. This range-measurement capability permits the AOL to conduct airborne surveys of topographic surfaces including water and ice. Temporal mode applications that have been successfully demonstrated include glacier topography, tree height determination, and surveying topography through forest-covered areas. Ongoing engineering modifications to the sensor design will allow the depth resolution of oceanic scattering layers. In the fluorosensing mode, the AOL has demonstrated that surface-layer chlorophyll can be measured with an airborne laser fluorosensing system. The AOL has supported a number of major oceanographic experiments in this mode of operation. Fluorosensing applications also include the measurement of phycoerythrin (an auxiliary photopigment of marine phytoplankton), oil film thickness, fluorescence conversion efficiency, and dissolved organic matter fluorescence.

Various laser transmitters are used with the AOL. High power (10 millijoules per pulse), low pulse repetition rate (10 pulses per second) lasers are used for fluorosensing applications. A low power (approximate 1 millijoules per pulse), high pulse repetition rate (up to 500 pulses per second) laser is used for topographic surveys. The AOL is equipped with a mirror assembly which can be set to provide 0, 5, 10, or 15 degree off-nadir angle profiles. the mirror is mounted-off axis and can be spun at 5 Hz to produce a conical scan at any of the above off-nadir angles.

The gross weight of the instrument is 1,100 pounds. However, the weight of the sensor varies somewhat depending on the laser transmitter and associated cooling requirements. When operated in a scanning mode at a 15 degree off-nadir angle the AOL produces a scan swath equal to approximately 50% of the aircraft altitude. The present configuration of the AOL is unique to the NASA P-3A aircraft. However, modifications that would allow the deployment of the sensor on longer-range aircraft are under consideration.

The operating altitude of the AOL is effectively 400 m or less with the present laser transmitters. The range of the present NASA P-3A aircraft is ~1,400 miles for low-altitude survey applications and 1,800 miles for high-altitude transit to the investigation site. NASA has recently acquired a P-3B aircraft, which would provide coverage over ~2,700 miles for low-altitude survey applications and 3,600 miles for high-altitude transit.

For more information, contact:

F. Hoge  
NASA/Wallops Flight Facility  
Wallops Island, VA 23337

- **Ocean Color Sensor**

The Ocean Data Acquisition System (ODAS) is an aircraft-borne/ocean-color system consisting of three radiometers with 15 nm bandwidths centered on wavelengths of 460, 490, and 520 nm, and a data acquisition and transmission package. It is generally flown at an altitude of 150-300 meters, giving spatial resolution of 5-50 m at a ground speed of 100 knots (~50 m/s), and operates as a line-of-flight (not scanning) instrument. Data from the radiometers are recorded on a mass-storage device linked to a PC aboard the aircraft, and can also be transmitted via radio Modem to a land- or ship-based PC data-acquisition system. Two algorithms have been used to convert the ODAS data to estimates of chlorophyll concentration. Navigational data (Loran-C) and data from a temperature sensor (PRT-5) and a broad-band sky sensor (400-700 nm) are stored together with radiances from the radiometers. The sampling interval is 0.1 sec, except for the Loran-C which updates at approximately 8 sec intervals. A typical file includes a record of 2 to 15 min duration corresponding to an individual flight line.

For more information, contact:

W. Esaias  
Code 971  
NASA/GSFC  
Greenbelt, MD 20771

- **Radio-Echo Sounding**

Most earth science investigations over the ice sheets of Antarctica and Greenland require knowledge

of ice thickness obtained from airborne surveys using an ice-penetrating radar. Information gleaned from these surveys includes both ice and bedrock elevation, as well as the structure of the ice sheet (e.g., internal layers and distribution of crevasses) and the electromagnetic properties at the ice/rock interface. At present, the US capability includes radars ranging in frequency from 50 to 150 MHz with peak power ratings ranging from 1,000 to 10,000 watts. The most powerful of these radars, a 10,000 watt, 60 MHz unit has been underutilized for most of the last decade because of the expense of operating the four-engine transport aircraft which served as its platform. New efforts to field this radar in a more efficient twin-engine aircraft are being undertaken cooperatively by Ohio State University and the US Geological Survey. Previously, the radar has proven itself capable of penetrating to depths of up to 4,500 m in the "cold" ice of East Antarctica; absorption in the warmer ice of West Antarctica limits its penetration depth to about 3,500 m. Efforts to use the side-looking characteristics of this radar to image the subglacial bedrock are also just beginning.

Because airborne ice-penetrating radar has been and will continue to be the foundation for many earth science activities on the ice sheets, it should be included as part of any comprehensive airborne investigations over these ice sheets. The cooperative effort by Ohio State University and the USGS to re-establish a US capability to sound the thickest portions of the polar ice sheets represents a step toward including ice-penetrating radar as part of any comprehensive airborne experimental platform.

For more information, contact:

D. Blankenship  
Byrd Polar Research Center  
Ohio State University  
125 South Oval Mall  
Columbus, OH 43210

- **Airborne Gravity Measurements**

The Naval Research Laboratory (NRL) has developed a prototype airborne gravity measurement system. The core of the system is a LaCoste and Romberg air-sea gravity meter mounted on a three-axis stable platform. Corrections to the gravimeter data for altitude and variations in altitude are determined from a combination of highly precise radar and pressure altimeters. The original prototype system was designed for use over oceanic areas. Pressure measurements are also made to extend use of the airborne system to terrestrial regions where occasional radar altitudes over points of known topographic height can be obtained. The radar heights are used to relate the pressure altitudes to absolute altitudes and to determine the slopes of the isobaric surfaces. Vertical accelera-

tions due to horizontal velocity over a curved, rotating earth (Eötvös correction) and precise two-dimensional positions are determined from a Texas Instrument P-code Global Positioning System Receiver.

The updated system was tested over eastern North Carolina and the Outer Banks, an area that is difficult to survey by conventional means. Over one-third of the region consists of low-lying swampy terrain and another one-third is the shallow water of the Pamlico and Albemarle Sounds. Neither the land method nor the shipboard gravity surveying method is well suited for these types of areas. Flying at an altitude of 600 m at 375 km/hr, an area over 10,000 km<sup>2</sup> with a nominal track spacing of 9 km by 9 km was covered in less than 18 hours of flying time. A comparison by the Defense Mapping Agency showed a 2.8 mGal rms and a 0.2 mGal mean difference between ground truth data and the airborne data at grid points when both data sets were interpolated to a common 9-km grid.

For more information, contact:

J. M. Brozena  
Naval Research Laboratory  
Code 5110  
Department of the Navy  
Washington, DC 20375

- **Global Positioning System (GPS)**

The Department of Defense (DoD) has developed and is implementing a world-wide, satellite-based navigation and positioning system called the Global Positioning System. While the prime purpose is to provide navigation information for the majority of the military's requirements via tracking a coded signal, known as P-code, commercial and other non-military applications needing precise navigation and positioning information can also benefit from the Clear/Acquisition (C/A) portion of the signal structure. The performance of military P-code receivers is 10-15 meters for world-wide, autonomous navigation. The C/A code receivers provide 25-30 meter information, except when the DoD purposely degrades the capability to the 100 meter level. As an augmentation to the original intent of the GPS, a class of receivers has been developed in which the phase of the L-band carrier is tracked to provide very precise pseudo-range measurements for a number of applications. In particular, government agencies such as the National Geodetic Survey and the Defense Mapping Agency are now routinely using carrier-phase tracking GPS receivers for many surveying applications. More recently, this carrier-phase tracking technology has been extended to positioning moving vehicles relative to a fixed receiver, and is known as differential carrier phase tracking, or interferometric kinematic positioning.

For the past several years NASA , NOAA, and the Navy have been developing techniques for airborne GPS navigation in connection with airborne gravimetry and airborne laser altimetry. Flight tests involving laser altimeters and GPS receivers operated in a differential-carrier phase mode have shown that the relative accuracy of the GPS corrected laser ranging data is at the 10-12 cm level. Analytical studies indicate that there is a potential for extending this capability to the 5 cm level and perhaps better. These earlier tests were conducted with single frequency GPS receivers operated over a baseline of less than 100 km. Since many survey applications require baselines in excess of 100 km, a series of field tests are underway using dual frequency GPS receivers to determine degradation in relative positioning accuracy as a function of distance and to establish practical baseline length limitations. Since the dual frequency data provides correction information for ionospheric propagation errors, it is anticipated that a considerable improvement in the baseline operational length will result from these flight tests. With this emerging capability and the appropriate laser and radar sensors, a host of airborne remote sensing projects become feasible, including:

- Monitoring of ice-volume changes in polar regions
- Ocean and sea-ice surface roughness and topographic mapping
- Comparison of laser and radar altimetry
- Land topography
- Airborne gravimetry.

For more information, contact:  
W. Krabill  
NASA/Wallops Flight Facility  
Wallops Island, VA 23337

## Suggested Readings

***Arctic Systems Science (ARCSS) Planning Documents: Ocean-Atmosphere-Ice Interactions.*** 1990. Joint Oceanographic Institutions Inc. *and Land-Atmosphere-Ice Interactions.* In preparation. To be published by Arctic Research Consortium of the U.S. (ARCUS).

These documents summarize the recommendations made by two workshops which focussed on key Arctic research initiatives related to Global Change.

***Satellite remote sensing of polar regions: applications, limitations and data availability.*** R. Massom, In press, Belhaven Press, London.

Provides extensive details on the full range of satellite sensors that overfly the polar regions.

***SeaRISE: A multidisciplinary research initiative to predict rapid changes in global sea level caused by collapse of marine ice sheets [Proceedings of a NSF/NASA workshop].*** 1990. NASA Conference Publication # 3075. 55 pp.

Describes a research initiative that addresses the coupled atmosphere-ocean-cryosphere-lithosphere system with the goal of predicting the contribution of marine ice sheets to sea-level change over the next decades to centuries.

***Prospects and Concerns for Satellite Remote Sensing.*** *Ad hoc* Panel on Remote Sensing of Snow and Ice, 1989. Polar Research Board. 44 pp.

This report assesses the remote sensing needs of the snow and ice community, examines the specifications of future satellite systems, identifies those instruments and orbits that will meet some of the needs, and examines issues relating to data processing and existing data bases for snow and ice research.

***Science Plan for the Alaska SAR Facility Program.*** 1989. JPL Publication 89-14. 87 pp.

Science objectives, opportunities, and requirements are discussed for the application of SAR data at high latitudes to oceans, ice, and land research. A full description is provided of upcoming SAR missions and of the Alaska SAR Facility (ASF) and data products that will be available from the ASF.

***The Role of Antarctica in Global Change.*** Scientific Committee on Antarctic Research, 1989. Cambridge, ICSU Press, on behalf of SCAR, illustrated. 28 pp.

This document sets out the ways in which Antarctic science and the Scientific Committee on Antarctic Research can contribute to the International Geosphere-Biosphere Program now being planned under the auspices of the International Council of Scientific Unions. Four major, interconnected, interdisciplinary research thrusts define the proposed Antarctic component of the IGBP: detection of global change in Antarctica; study of critical processes linking Antarctica to the global system; extraction of paleoenvironmental information; and assessment of ecological effects.

***Arctic Interactions: Recommendations for an Arctic component in the IGBP.*** UCAR Office for Interdisciplinary Earth Studies, 1988. Report 01ES-4. 45 pp.

Identifies Arctic processes that have important global interactions, and aspects of the coupled Earth system that can best be investigated in the Arctic.

***Physical Oceanography and Tracer Chemistry of the Southern Ocean.*** *Ad hoc* Committee on Antarctic Physical and Chemical Oceanography, 1988. Polar Research Board. 82 pp.

A "Strategy" series report that focuses on the circulation and mixing of the Southern Ocean. The report recommends research on: the antarctic circumpolar current, sea-ice zone, subpolar gyres, and continental margins.

***Priorities in Arctic Marine Science.*** *Ad hoc* Committee on Arctic Marine Science, 1988. Polar Research Board. 73 pp.

This "Strategy" series report identifies two important and poorly understood arctic marine research areas requiring further emphasis: ecosystem dynamics of the arctic shelf and adjacent seas, and circulation of the Arctic Ocean. The report also identifies a program plan for addressing priorities and the logistics and technology necessary to implement the proposed research.

***Satellite image atlas of glaciers of the world.*** Edited by R.S. Williams, Jr. and J.G. Ferrigno, 1988. U.S. Geological Survey, Washington, D.C.

A series of volumes containing many examples of Landsat images of glaciers from all parts of the Earth. The volume entitled "Antarctica" was published in 1988.

***International Research in the Antarctic.*** Fifield, 1987. Oxford University Press, for SCAR and the ICSU Press, Walton Street, Oxford. 146 pp.

This book describes the historical background to the present-day extensive scientific interest in Antarctica, the achievements of Antarctic science, of the Working Groups and Groups of Specialists of the Scientific Committee on Antarctic Research, and their involvements with other international bodies of scientists and scientific institutions.

***United States Arctic Research Plan.*** Interagency Arctic Research Policy Committee, 1987. Washington, D.C. 334 pp.

A comprehensive five-year program plan for the overall Federal effort in Arctic research

***Antarctic Solid-Earth Sciences Research: A Guide for the Next Decade and Beyond.*** *Ad hoc* Committee on Antarctic Geosciences, 1986. Polar Research Board. 40 pp.

This report advocates a directed change in the U.S. approach to antarctic geosciences research, including following a research plan, providing direction, providing a much greater utilization of available new technology, concentrating research activities on a few selected geographic regions, and establishing broad reconnaissance studies.

***U.S. Research in Antarctica in 2000 A.D. and Beyond: A Preliminary Assessment.*** 1986. Polar Research Board. 35 pp.

This report presents unweighted lists of major research goals that the antarctic scientific researchers of today think will be of importance to antarctic science in the next century.

***A Programme for International Polar Oceans Research (PIPOR).*** 1985. ESA SP-1074. 42 pp.

Report of a science working group formulating a coordinated plan for international polar ocean research using satellite and *in situ* measurements.

***Glaciers, Ice Sheets, and Sea Level: Effects of a CO<sub>2</sub>-Induced Climatic Change [Report of a Workshop Held in Seattle, Washington, 13-15 September 1984].*** Committee on Glaciology, 1985. Polar Research Board. 348 pp.

This volume contains the proceedings of a workshop held in Seattle, Washington on 13-15 September 1984, and provides an executive summary of consensus issues.

***National Issues and Research Priorities in the Arctic.*** 1985. Polar Research Board. 124 pp.

This report contains the Polar Research Board's recommendations to the National Science Foundation for a five-year Arctic research plan.

***Oceanography from space: A research strategy for the decade 1985-1995, Parts 1 and 2.*** 1984. Joint Oceanographic Institutions Inc., Washington, D.C. 20 pp. and 32 pp.

A two-part report from the Joint Oceanographic Institutions' Satellite Planning Committee describing a proposed research program utilizing both satellite and *in situ* measurements.

***Passive Microwave Remote Sensing for Sea Ice Research [Report of the NASA Science Working Group].*** 1984. Applied Physics Laboratory, University of Washington. 55 pp.

Assesses sea-ice research applications of passive microwave data from future satellite missions.

***Satellite Remote Sensing for Ice Sheet Research.*** 1984. NASA Technical Memorandum, No. 86233. 40 pp.

Reviews research applications to ice sheet research of high-resolution visible and SAR imagery, infrared, passive-microwave, and scatterometer measurements, and surface topography information from laser and radar altimeters.

***The Polar Regions and Climatic Change. Ad hoc Committee on the Role of the Polar Regions in Climatic Change,*** 1984. Polar Research Board. 59 pp.

In recognizing the important role of polar regions in climate change, this report concludes that two principal focuses for future research should be: the development of models of the global climate system with special attention to improved simulation of climatic processes in the polar regions; and better understanding of the global-scale response of the oceans to atmospheric changes in polar and subpolar latitudes.

***The Polar Regions and Climatic Change, Appendix. Ad hoc Committee on the Role of Polar Regions in Climatic Change,*** 1984. Polar Research Board. 113 pp.

This volume consists of three signed appendices that provide much of the background material and documentation considered by the *ad hoc* Committee on the Role of the Polar Regions in Climatic Change in framing their conclusions and recommendations.

---

## Acknowledgements

This report was sponsored by the National Science Foundation, the National Aeronautics and Space Administration, the Office of Naval Research and the National Oceanic and Atmospheric Administration. Its compilation took considerably longer than I originally had hoped, and its completion owes much to the guidance and encouragement that I have received from Jane Dionne of the NSF. I thank her for her patience and persistence.

S. Abbot, D. Blankenship, J. Brozena, D. Cavalieri, J. Comiso, J. Crawford, D. Eppler, W. Esaias, G. Feldman, F. Hoge, W. Krabill, R. Kwok, B. Lucchitta, and D. Peel generously provided me with previously unpublished illustrations and technical material that I have included here. My thanks also are due to the many colleagues who reviewed the report at various stages during its completion: K. Aagaard, J. Baker, R. Bindschadler, F. Carsey, A. Gordon, S. Jacobs, K. Jezek, C. Parkinson, D. Rothrock, R. Tipper, W. Weeks, and S. Wilson. I owe particular thanks to Lynne Claflin, Andrea Johnson, and Grace Torres of Joint Oceanographic Institutions Incorporated for preparing the material for publication.

## Glossary

ABW	Antarctic Bottom Water
ADEOS	Japanese Advanced Earth Observing Satellite
AMI	Active Microwave Instrument
AOL	NASA Airborne Oceanographic Lidar
AOS	Archive and Operations System
ARCSS	Arctic Systems Science
ARSF	Antarctic Remote Sensing Facility
ASF	Alaska SAR Facility
AVHRR	Advanced Very High Resolution Radiometer
CDW	Circumpolar Deep Water
CERES	Clouds and Earth's Radiant Energy System
CCRS	Canadian Center for Remote Sensing
CZCS	Coastal Zone Color Scanner
DMSP	Defense Meteorological Satellite Program
DoD	Department of Defense
EOS	Earth Observing System
ERBE	Earth Radiation Budget Experiment
ERS-1	European Remote-Sensing Satellite
ESA	European Space Agency
ESMR	Electronically Scanning Microwave Radiometer
GAC	Global Area Coverage
GEOSAT	Navy's Geodetic Satellite Mission
GLRS	Geoscience Laser Ranging System
GPS	Global Positioning System
GSFC	Goddard Flight Center
HRPT	High Resolution Picture Transmission data
IARPC	Interagency Arctic Research Policy Committee
JERS-1	Japanese ERS-1
JIC	Navy/NOAA Joint Ice Center
JOI	Joint Oceanographic Institutions Incorporated
JPL	Jet Propulsion Laboratory
KRMS	KA band Radiometer Mapping Sensor
LAC	Local Area Coverage
LAWS	Laser Atmospheric Wind Sounder
MODIS	Moderate Resolution Imaging Spectrometer
MSS	Multi-Spectral Scanner
NADC	Naval Air Development Center
NADW	North Atlantic Deep Water
NASA	National Aeronautics and Space Administration
NOAA	National Oceanic and Atmospheric Administration
NOARL	Naval Oceanographic and Atmospheric Research Laboratory
NRL	Naval Research Laboratory

---

NSCAT	NASA wind scatterometer
NSF	National Science Foundation
NSIDC	National Snow and Ice Data Center
NSSDC	National Space Science and Data Center
OCTS	Ocean Color and Temperature Scanner
OLS	Optical Line Scanner
ONR	Office of Naval Research
PR	Polarization Ratio
SAR	Synthetic Aperture Radar
SBUV	Solar Backscatter Ultra Violet
SCAR	Scientific Committee for Antarctic Research
SMMR	Scanning Multichannel Microwave Radiometer
SPOT	French Systeme Probatoire d'Observation de la Terre satellite
SSM/I	Special Sensor Microwave/Imager
TM	Thematic Mapper
TOMS	Total Ozone Mapping Spectrometer
TOPEX/Poseidon	Ocean Topography Experiment
TOVS	Tiros Operational Vertical Sounder
UAF	University of Alaska at Fairbanks
USGS	United States Geological Survey

